UNCLASSIFIED

AD **407 558**

DEFENSE DOCUMENTATION CENTER

FOR

SCIENTIFIC AND TECHNICAL INFORMATION

CAMERON STATION. ALEXANL iA. VIRGINIA
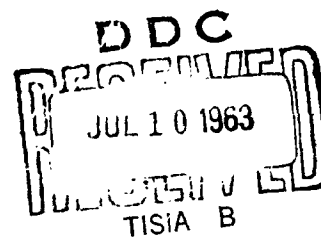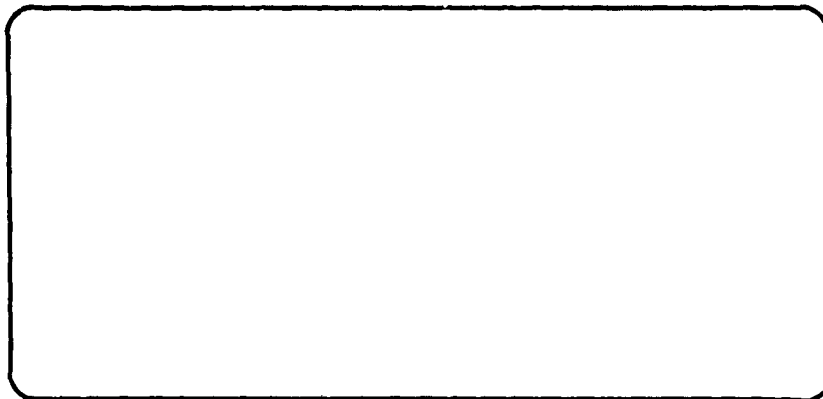
UNCLASSIFIED

407 558

63-4-1

DDC

JUL 1 0 1963

TISIA B

Beech Aircraft Corporation

BOULDER, COLORADO

U. S. A.

AFFTC TR 60-43
VOLUME IV

ESTABLISHING TANK DESIGN CRITERIA
FOR LIQUID HYDROGEN ROCKETS

VOLUME IV - Flight Simulation Test Program

FINAL REPORT
PERIOD ENDING 31 JANUARY 1962

H. L. Breckenridge
D. A. VanGundy

BEECHCRAFT RESEARCH AND DEVELOPMENT, INC.
BOULDER, COLORADO

BEECHCRAFT ENGINEERING REPORT NO. 8768

CONTRACT AF33(616)-5154
SUPPLEMENT S3(59-207)
PROJECT NO. 3084
TASK NO. 30304

June, 1963

AIR FORCE FLIGHT TEST CENTER
AIR RESEARCH AND DEVELOPMENT COMMAND
UNITED STATES AIR FORCE
EDWARDS AIR FORCE BASE, CALIFORNIA

NOTICES

When Government drawings, specifications, or other data are used for any
purpose other than in connection with a definitely related Government pro-
curement operation, the United States Government thereby incurs no respon-
sibility nor any obligation whatsoever; and the fact that the Government
may have formulated, furnished, or in any way supplied the said drawings,
specifications, or other data, is not to be regarded by implication or
otherwise as in any manner licensing the holder or any other person or cor-
poration, or conveying any rights or permission to manufacture, use, or
sell any patented invention that may in any way be related thereto.

FORWARD

This contract was initiated by the Propulsion Laboratory, Wright-Patterson Air Force Base, Ohio, and has been monitored by the Rocket Propulsion Laboratory at the Air Force Flight Test Center, Edwards Air Force Base, California. The work upon which this report is based was accomplished by Beechcraft Research and Development, Inc., Boulder, Colorado, under Air Force Contract AF33(616)5154, Supplement S3(59-207). Mr. J. Branigan at the Rocket Propulsion Laboratory is the Air Force Engineer in charge of the work done under this contract.

This is Volume IV of the final report submitted per Item IV, Part I of the S3(59-207) Supplement to the contract. This report summarizes all work accomplished from July, 1958, to January, 1962.

TABLE OF CONTENTS

TABLE OF CONTENTS (Continued)

TABLE OF CONTENTS (Continued)

LIST OF FIGURES

LIST OF FIGURES

LIST OF FIGURES

LIST OF FIGURES

LIST OF TABLES

INTRODUCTION

This is Volume IV of the final report on work performed under Contract AF33(616)-5154, Supplement 53(59-207), involving a flight simulation test program for liquid hydrogen boost tanks. This program is a continuation of an investigation of propellant tank design problems begun by Beechcraft Research and Development, Inc. in July, 1957.

During the original study program, preliminary design criteria for the tank system of a series of chemical and nuclear rocket vehicles was evolved. It was determined during that program that further research and development work was needed in certain areas in order to firmly establish the desired tank design criteria. The thermal performance of a hydrogen fuel tank during powered flight was determined to be an important tank design parameter and that the relationship between thermal performance and tank design is quite complex.

This flight simulation test program is directed toward the solution of the basic heat transfer problem. A 7,000 gallon liquid hydrogen tank was fabricated from both stainless steel and titanium. This volume considers the fabrication and testing of these tanks.

1.0 7,000-GALLON STAINLESS STEEL TEST TANK SYSTEM

1.1 Reporting Period September 15, 1959, to December 15, 1959

To insure a greater degree of reliability and versatility to the thermal test program, one of the three test tanks will be fabricated out of stainless steel. The following sections describe the progress made during this period on this tank system.

1.1.1 Tank Structural Design

The steel tank is to be built in an identical manner as the titanium tank using existing tools, fixtures, and assembly techniques. The tank is to be fabricated from 304 stainless steel and has been designed to annealed conditions. The preliminary working pressure has been established at 33 psig, however, this pressure may be subject to change pending further structural analysis.

Because the tank is designed with materials which have a lower strength allowable, the skin gages must be larger than the titanium gages that are presently used. The skin thickness of the cylindrical section is now .063 ± .006 inches, and the skin thickness of the spherical section is .050 ± .005. The present major tooling is based on tank I.D. dimensions, thus, the increased thickness of the stainless steel is not expected to create any tooling changes or additional fabrication problems.

1.1.1.1 Preliminary Structural Analysis of the Stainless Steel Tank

The purpose of this preliminary analysis is to establish the nominal material gage requirements for the stainless steel tank. The present analysis will be limited to the two most critical areas on the tank. From the structural analysis of the titanium tank, the two most critical areas exist at:

(a) Circumferential welds of the cylindrical shell, and

(b) Hemisphere splice fitting in the hemispherical shells.

1.1.1.2 Material Selection

The alloy selected for the stainless steel tank is Type 304 in the annealed condition. The selection was based primarily on the good ductility of this alloy at -423°F where the percent elongation is approximately 32%.

1.1.1.3 Approximate Allowable Design Pressure

To obtain a lightweight, airborne, stainless steel tank involves a complete materials study including the use of heat treat and/or cold working techniques. This is beyond the scope of this particular program, therefore, the material will remain in the annealed condition. In this condition, the allowable stress will be quite low with a subsequently large skin gage. For this reason, the

allowable design pressure will be limited to approximately 33 psig, instead of the 43 psig as determined for the titanium tank. The 33 psig allowable design pressure will be greater than any pressure used during thermal runs and the skin gages necessary will not significantly influence heat transfer through the tank skin. A pressure of 33 psig will also allow skin gages that will not necessitate any major tooling change.

1.1.1.4 Design Information

For chosen standard material gages, the calculations for stresses and allowable design pressures in the two critical tank areas will be based on the following design information:

    (1) Material - Type 304 S.S. annealed
    (2) Ultimate stress - 75,000 psi
    (3) Yield stress (minimum specified) - 35,000 psi
    (4) Minimum design factor of safety - 1.25
    (5) Allowable design stress - 35,000 psi
    (6) Poisson's ratio · .25
    (7) Elastic modulus - 29×10^{-6} psi
    (8) Joint efficiency - 90%
    (9) Minimum weld thickness = 100% of minimum sheet thickness
  (10) Inside surfaces flush
  (11) Maximum radial expansion prior to welding circumferential joints of hemispherical or cylindrical shell = .008 inch
  (12) Tank radius - 46.2 inches
  (13) Cylindrical shell gage = .063 + .006 inch
  (14) Hemispherical shell gage = .050 + .005 inch

The standard material gages chosen should make the cylinder circumferential welds more critical than any area of the hemispherical shell. This condition is compatible with the titanium tank design.

1.1.2 Loading and Stress Analysis

The detailed analysis of the cylinder circumferential joints and the hemisphere splice fitting is presented in report FTRDI MR59-2, Appendix C.

The minimum pressures, as limited by pure membrane stresses in welds without discontinuity, are:

<u>In the hemispherical shell</u>

$$p = \frac{2 \sigma t}{r} = \frac{35,000(.050 - .005)(.90)}{46.2} = 61.36 \text{ psi}$$

<u>In the cylindrical shell</u>

$$p = \frac{\sigma t}{r} = \frac{35,000(.063 - .006)(.90)}{46.2} = 38.86 \text{ psi}$$

The analysis of the cylinder circumferential joints indicates a 14.6% reduction in pressure due to a possible induced discontinuity. The discontinuity can be attributed to possible shell thickness differences due to the large skin tolerances and the maximum radial expansion that may occur in sizing of the shell prior to welding.

The 14.6% pressure reduction gives an allowable design pressure (limited by the cylinder circumferential joints) of

$$p = 38.86 - (.146)(38.86) = 33.17 \text{ psi}$$

This pressure can also be referred to as "proof pressure".

The difference between weld and base material modulii is negligible and the large difference between the ultimate and yield stress indicates no problems in demonstrating a 1.25 factor of safety in an ultimate pressure test.

The preliminary analysis of the hemisphere splice fitting indicates that a three-inch taper length is required to distribute stresses from the relatively rigid skirt area into the hemispherical skin. The thickness at the beginning of the taper must be optimized to obtain a balance of stress throughout the taper. These requirements are due largely to the high flexural rigidity of the stainless steel shell as compared to a titanium shell. The high flexural rigidity in effect induces a relatively high bending moment over a much larger distance than was experienced in the titanium tank.

The preliminary analysis consisted of determining a thickness at the beginning of the taper such that the stress at the beginning of the taper and at the weld line do not exceed the allowable material stress of 35,000 psi and (.90 x 35,000 psi), respectively. Figure 1 shows a preliminary plot of allowable design pressure versus thickness at the beginning of the taper. This plot includes the allowable design pressure as limited at the beginning of the taper and at the weld. From Figure 1 a stress balance is obtained with a thickness of approximately .080 inches at the beginning of the taper. Assigning tolerances of ± .005 the allowable design pressure at the weld would be approximately 33.80 psi and at the beginning of the taper, the allowable design pressure would be 34.00 psi. As compared to the allowable design pressure without discontinuity stresses, a reduction of pressure in the hemispherical shell is approximately

$$\frac{61.36 - 34.00}{61.36} = 45\%$$

The cylinder circumferential joints with an allowable design pressure of 33.17 psi are still slightly more critical than the hemisphere splice fitting.

The next smaller standard available material gage that could be used in the hemispherical shell is .038 ± .004 inches. Using this material gage, the hemisphere splice fitting would have limited the tank allowable design pressure.

FIGURE 1
ALLOWABLE DESIGN PRESSURES IN THE HEMISPHERE SPLICE FITTING
VERSUS THICKNESS AT THE BEGINNING OF THE TAPER (STAINLESS STEEL TANK)
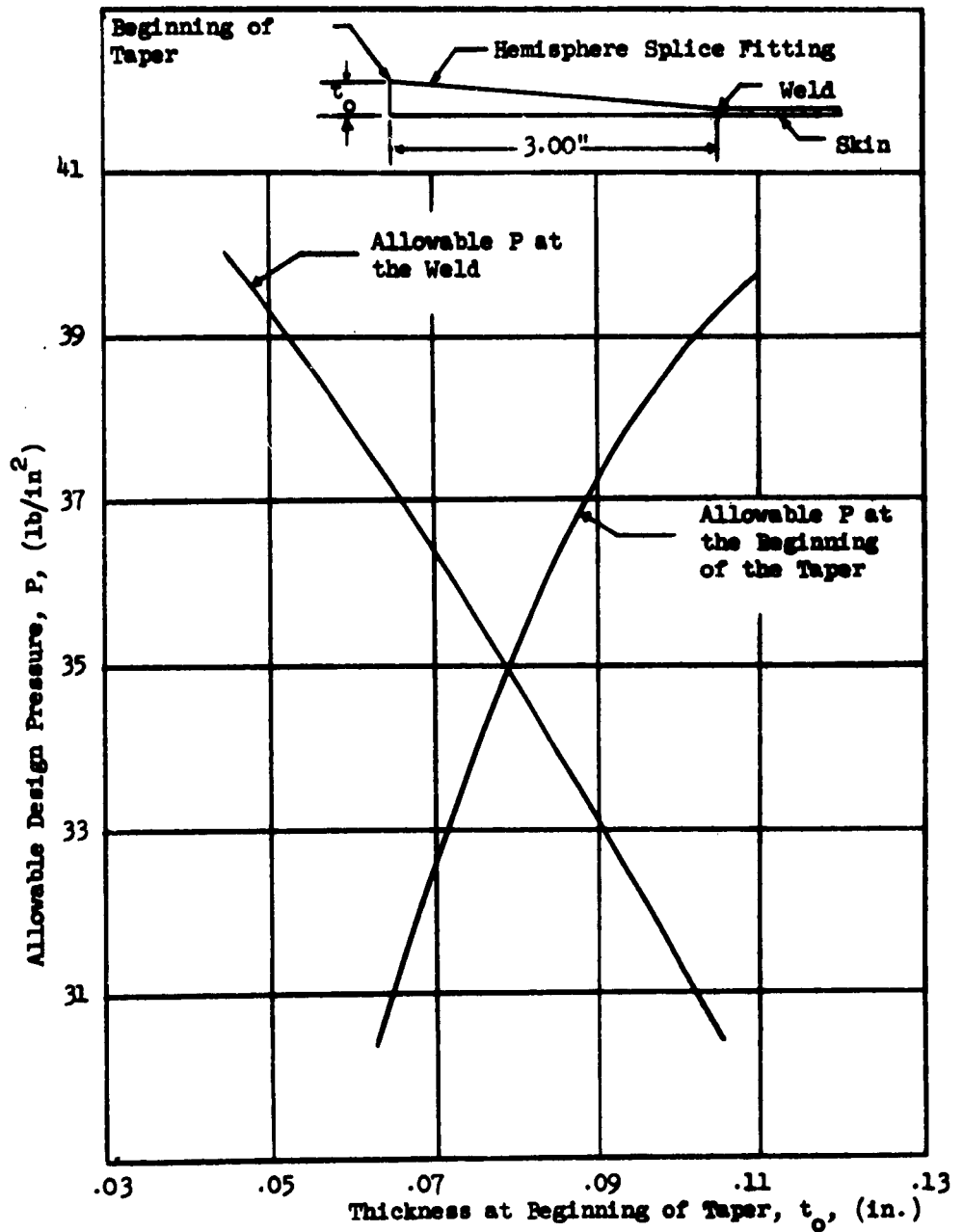
As a preliminary design, the thickness (t_{ss}) of all tapered fittings in the stainless steel tank can be approximately determined by simple proportioning.

$$t_{ss} = t_{ti}\left(\frac{t_{ss\ skin}}{t_{ti\ skin}}\right)$$

Where:

t_{ti} = titanium fitting thickness,

t_{ti}skin = titanium tank skin gage, and

t_{ss}skin = stainless steel tank skin gage.

The knuckle skin gage for the stainless steel tank will be the same as the skin gage in the hemisphere, and the cone skin gage will be the same as the skin gage in the cylinder. The drain fitting skin gage will be approximately .125 inches.

1.2 Reporting Period December 15, 1959, to March 15, 1960

The subsections that follow will describe the work progress that has been made within this reporting period on the 7,000-gallon stainless steel test tank system. The general areas of discussion will cover tank system design, tank fabrication progress, and additional structural analyses.

1.2.1 Tank Structural Design

In order to expedite the fabrication of the stainless steel tank, a number of design concessions have been made. The most notable difference between the two tanks (aside from general material thicknesses) is the elimination of the hemisphere splice fitting in both the upper and lower head assemblies. The requirement for this rather complex fitting was originally dictated by the induced stresses created by differential deflections in this general area of the tank. Increasing the thickness of the hemispherical skins to take these stresses eliminates the requirement for these fittings.

While there is a weight penalty associated with this design analysis, it is considered to be worthwhile in this case since it will facilitate easier and faster fabrication. It is expected that this change will have little effect on the thermal parameters in subsequent thermal tests.

The final configuration of the stainless steel tank shows that the skins, including the cylindrical, hemispherical, and conical sections, are all .063 inch thick. By using these thicknesses, it also will not be necessary to incorporate the transition fitting in the lower head.

1.2.2 Stress Analysis

The structural analysis of the stainless steel tank is essentially the same
as the structural analysis of the titanium tank. The stresses in discontinu-
ity areas of the stainless steel tank were calculated on the digital computer,
utilizing the same programs that were used on computations for the titanium
tank fittings and discontinuity areas.

The input changes of the original computer programs were:

(1) Skin gages and fitting thicknesses
(2) Young's modulus
(3) Poisson's ratio

The results of the computer solutions are presented in Figures 2 through 8.

The design allowable stress for the skins and all fittings is,

$$F = \text{joint efficiency x certified yield stress.}$$

Other design information is given in Section 2.3.2 of Reference .

For the skins and all fittings except the manhole ring, manhole cover ring,
vent ring and instrumentation ring, the certified yield stress is 35,000 psi
and the allowable design stress is,

$$F = .90 \times 35,000 = 31,500 \text{ psi.}$$

For the manhole cover ring, vent ring and instrumentation ring material the
certified yield stress is 30,000 psi and the allowable design stress is,

$$F = .90 \times 30,000 = 27,000 \text{ psi.}$$

By observing the curves of Figures 2 through 8, and calculations given in
Appendix B of this report, the 27,000 psi allowable stress for the fittings
in the head does not limit the tank design pressure, therefore, a certified
30,000 psi was allowed for these fittings.

The allowable tank design pressure is limited by the head skin fixity in the
foam-filled skirt area (Reference Appendix B).

1.2.2.1 Hemisphere-Skirt Transition Area

In the titanium tank, a hemisphere-splice fitting was added in this area.
This type of design was necessary on the titanium tank in order to minimize
head skin weight and, thus, establish a proven structural design criteria
for an airborne tank. The stainless steel tank, however, is not necessarily
designed for an airborne application and the primary purpose of the steel
tank is to provide a secondary tank for thermal runs. After evaluation of
a preliminary analysis of the skirt hemisphere transition area (Reference
Section 2.3.2 of Reference) it was decided that a hemisphere-splice fitting

FIGURE 2 -
VENT AND INSTRUMENTATION RINGS
ALLOWABLE APPLIED MOMENT VERSUS
TANK PRESSURE
(STEEL TANK)
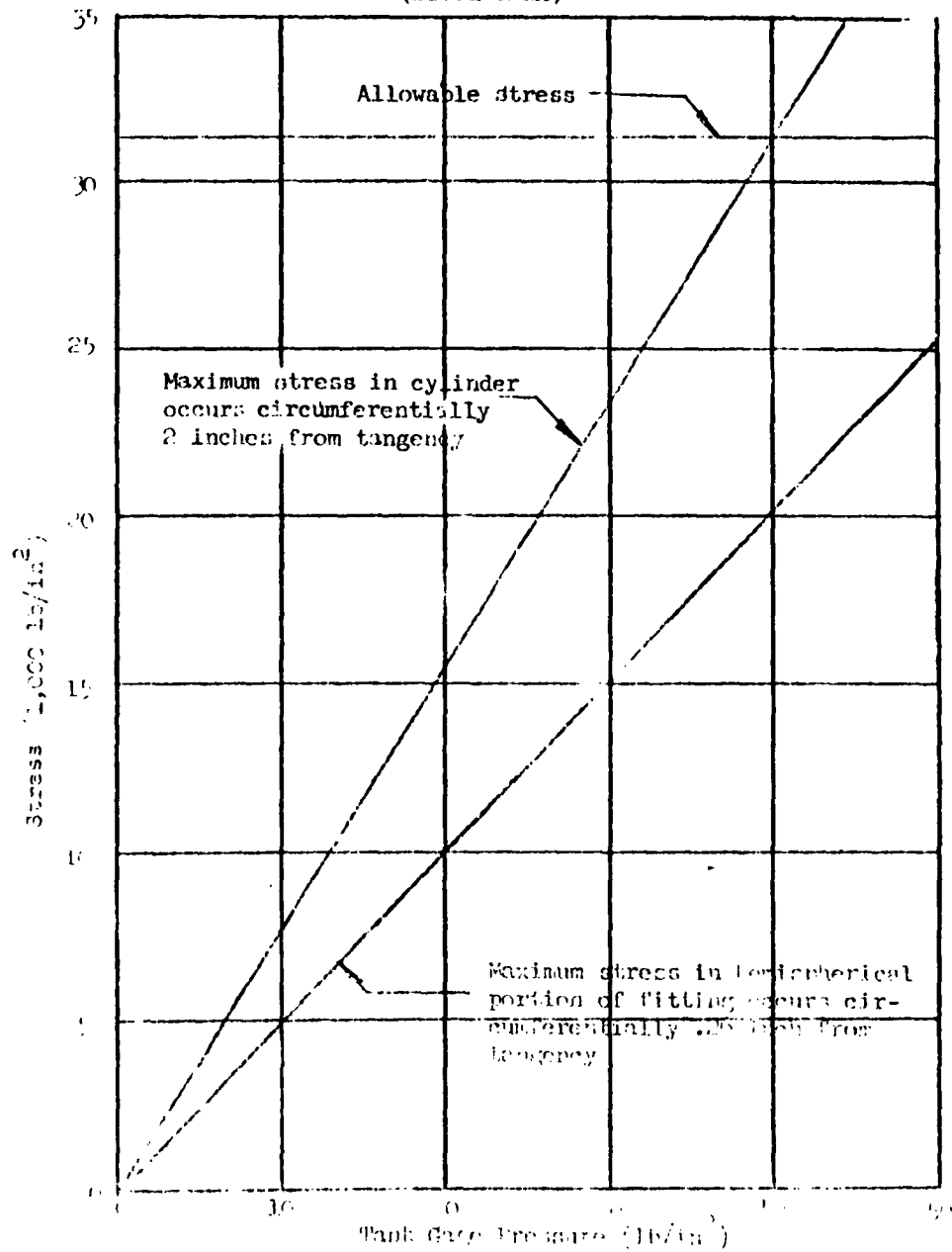
FIGURE 4
MAXIMUM STRESSES IN THE
CYLINDER CIRCUMFERENTIAL WELD
(STEEL TANK)

AFFTC TR 60-43(IV)   -10-
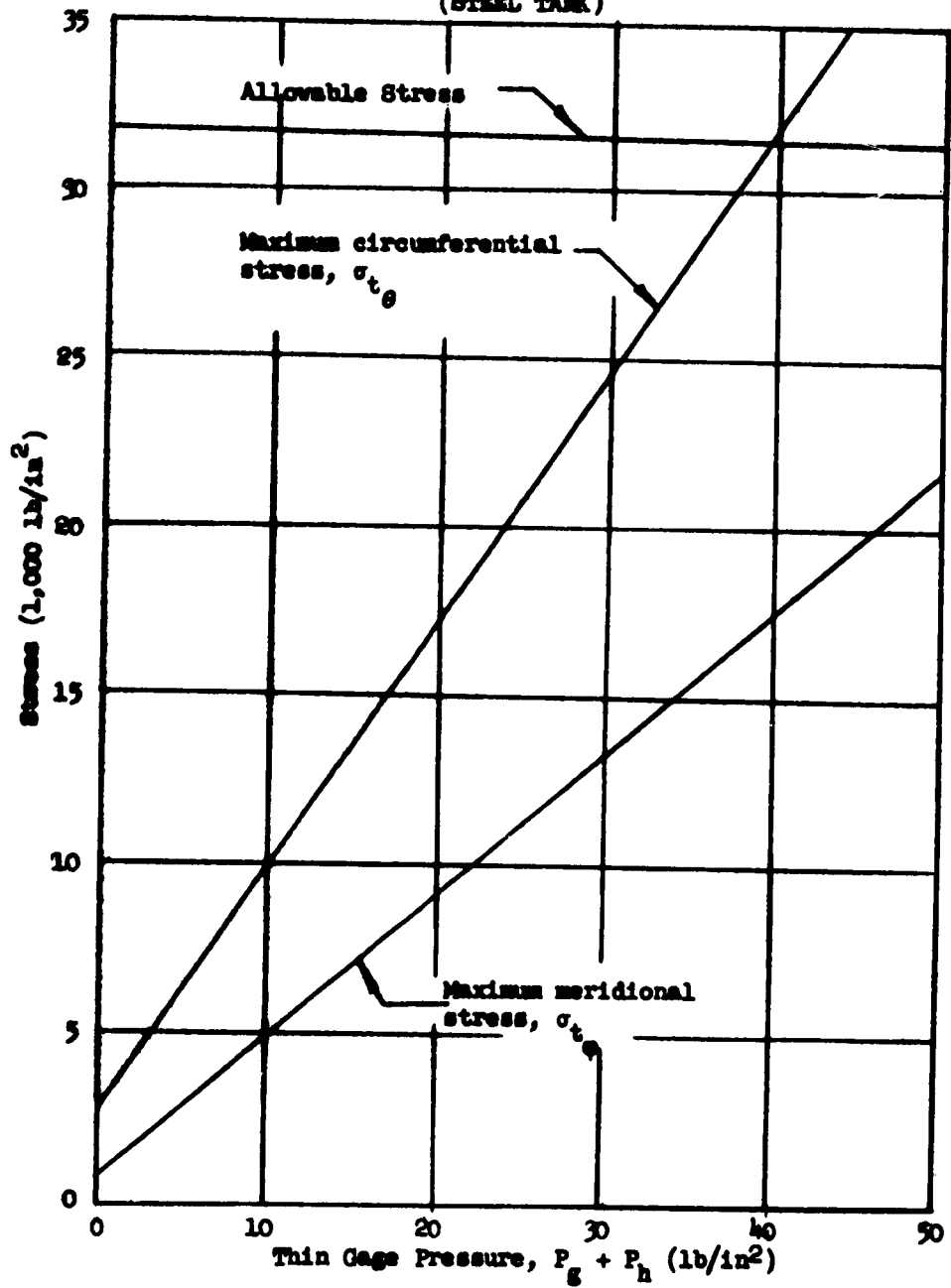
FIGURE 5
STEEL TANK
MAXIMUM STRESSES IN THE MANHOLE COVER AND RING

Maximum Stress in
Manhole Cover Occurs
1" from Juncture

Allowable Stress

Maximum Stress in Manhole
Flange Occurs 2" From Juncture

Stress (1,000 lb/in²)

Tank Gage Pressure, $P_g + P_h$, (lb/in²)
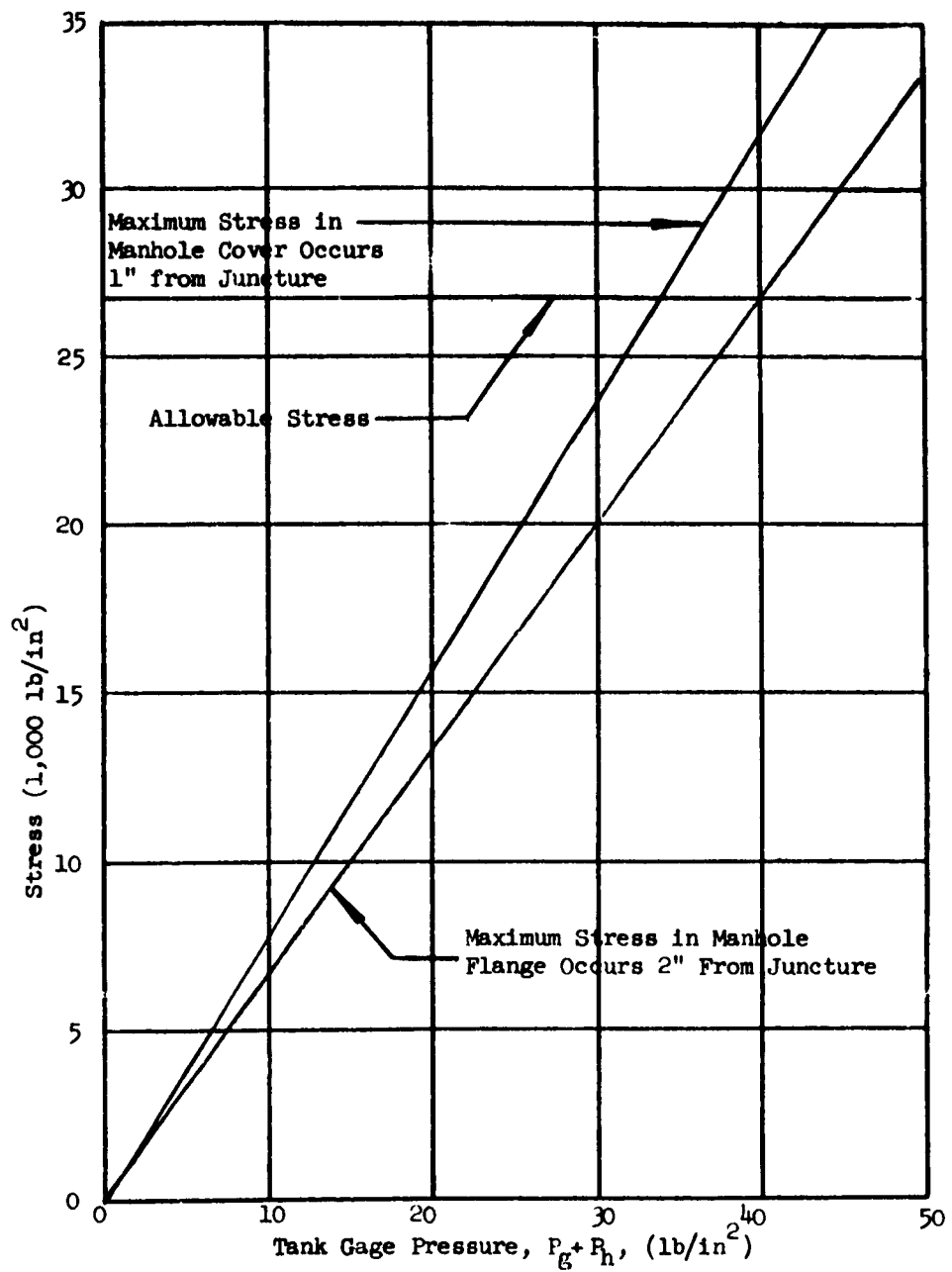
FIGURE   6
CONE STRESS FROM CONE-KNUCKLE DISCONTINUITY
7,000-GALLON STAINLESS STEEL TEST TANK

1.8" below cone-knuckle tangent line

t_c = 0.057

t_k = 0.057

60

50

40

Design Stress (35,000 psi)

30

20

Design Pressure
(43.5 psi)

10

Circumferential Tensile Stress (1,000 psi)

0

0   10   20   30   40   50

Tank Pressure (psi)
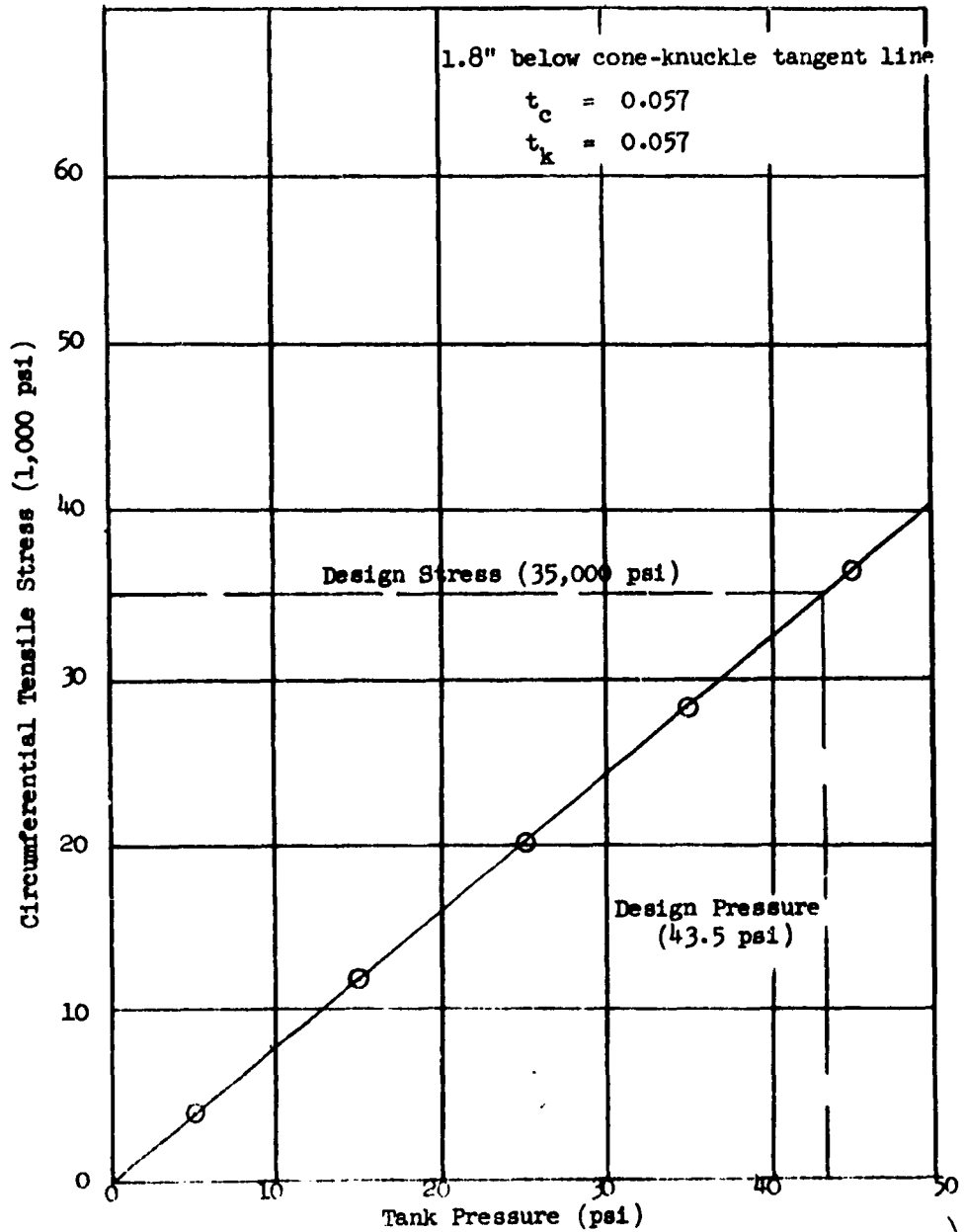
FIGURE   7
KNUCKLE STRESS FROM CONE-KNUCKLE DISCONTINUITY
7,000-GALLON STAINLESS STEEL TEST TANK
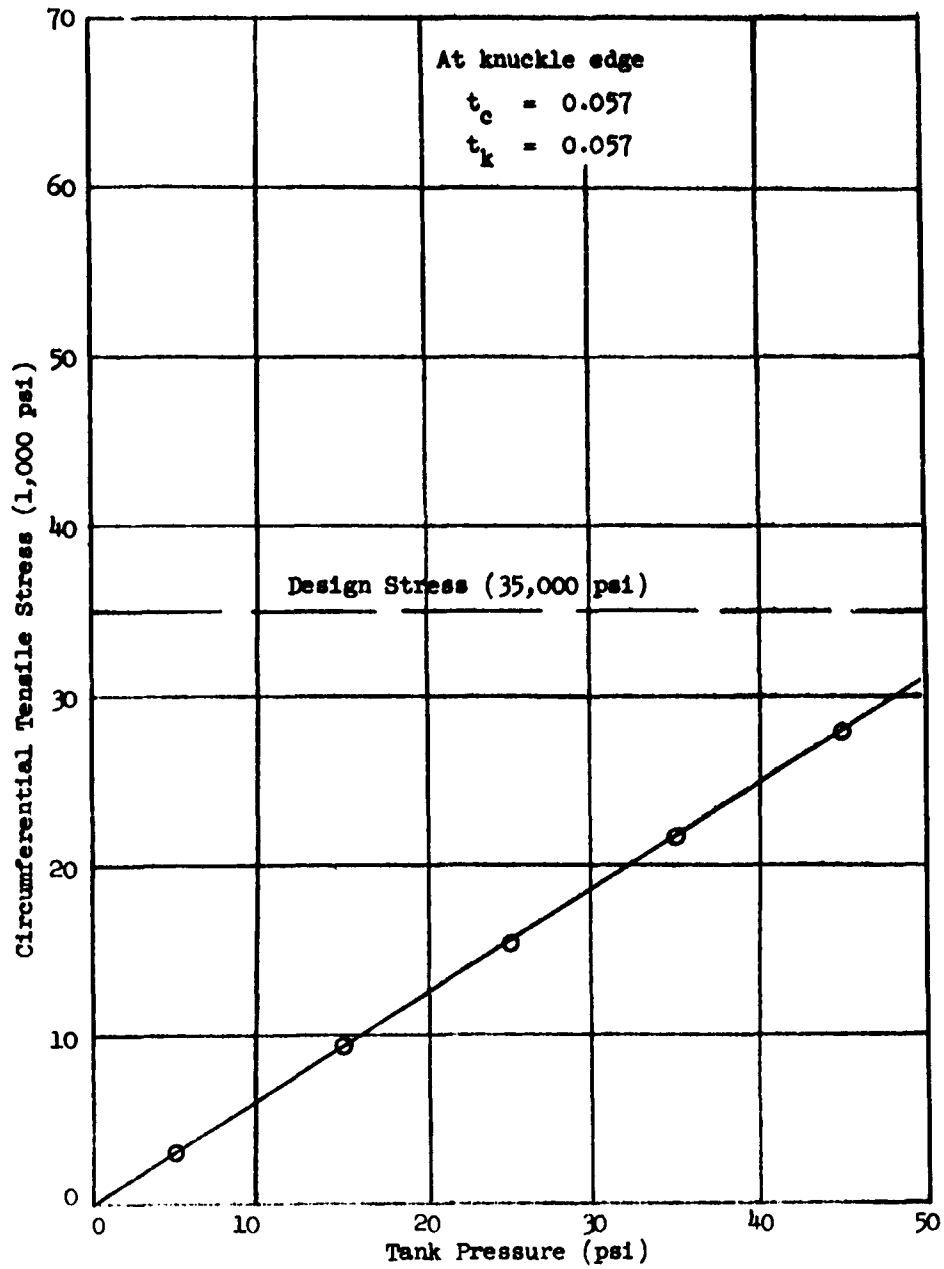
FIGURE 8
CONE STRESS FROM CONE-CIRCULAR ARCH DISCONTINUITY
7,000-GALLON STAINLESS STEEL TANK
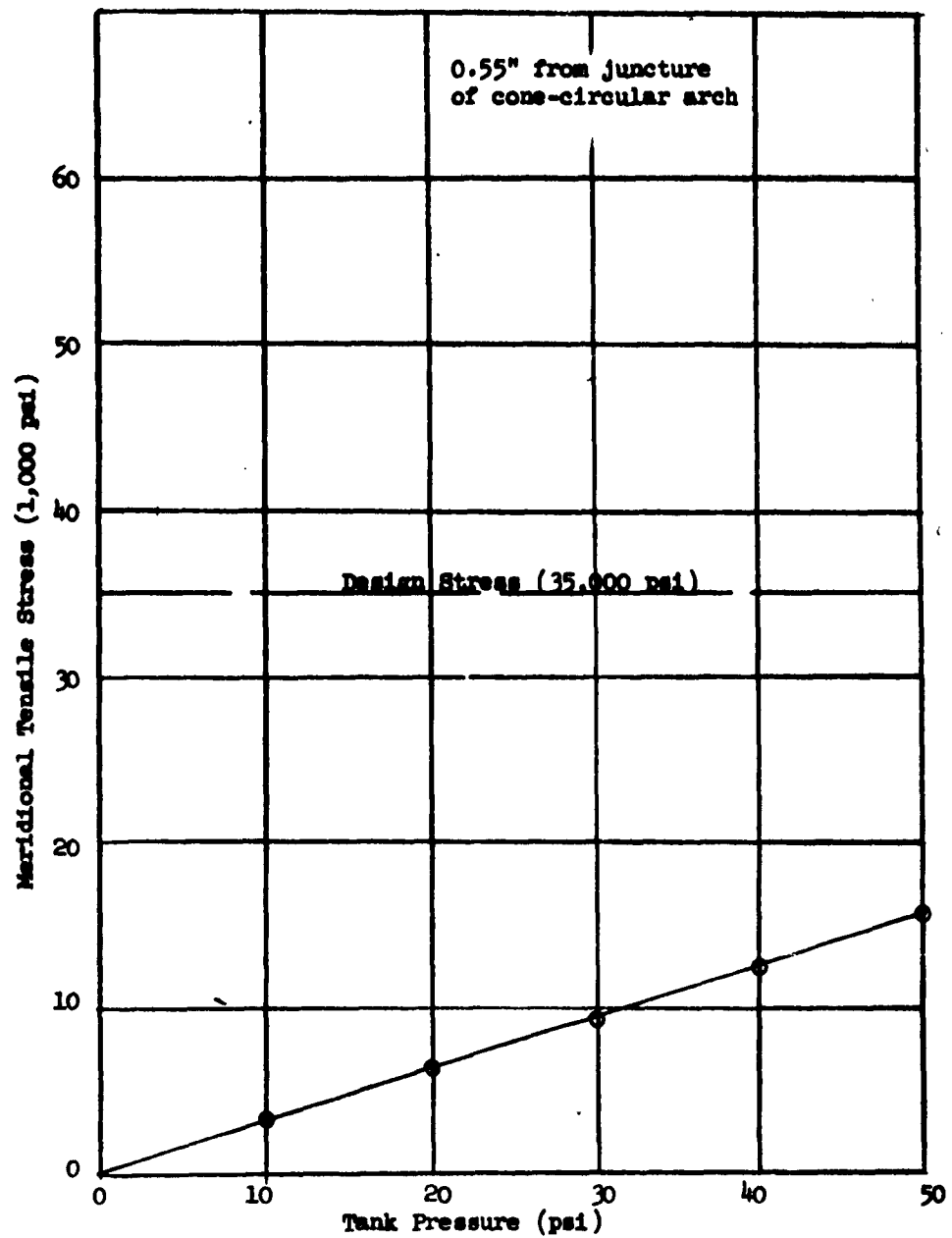
would not adequately dissipate the flexural stresses within the 2.00 inch taper length, and any addition to the taper length would necessitate new tooling. Since weight is not the primary concern on this tank, the fitting was, therefore, eliminated and a head skin thickness of .063 inches nominal was chosen. This thickness is adequate, within its tolerance range, to take out the maximum bending moment induced in the skirt-hemisphere juncture and thus allow adequate tank allowable design pressure. The allowable design pressure, as limited by the juncture, is 32.61 psi which is slightly less than pressures limited by all other tank discontinuity areas. The 32.61 psi will now be considered the allowable tank design pressure unless modifications alter the calculated stresses.

1.3 Reporting Period June 15, 1960, to December 31, 1960

The following subsections will be devoted to describing the work progress during this period on the stainless steel tank system. The general areas of discussion will cover thermal consideration and tank fabrication progress.

1.3.1 Tank Structural Design

The construction of the stainless steel tank using the same tooling was completed and no major design changes were made during this period.

1.3.2 Thermal Considerations

The insulation encapsulation of the stainless steel tank became a major problem in itself. As originally contemplated, the Min-K insulation tiles were to be covered with a cylinder of Mylar, which would allow the insulation to be evacuated.

As conceived, the Mylar jacket was to be fabricated by a vendor into one large cylinder which could then be drawn over the tank and shrink fitted to the insulation. The best grades of Mylar are purported to be free of pin holes, thus allowing the use of the Mylar as one side of a vacuum shell. However, when Mylar is folded such that three loose folds extend from one point, a pin hole almost invariably results. This unique feature of Mylar resulted ultimately in the failure of the Min-K Mylar concept.

The Mylar sleeve could not be slipped over the tank without folding or wrinkling, so it was decided to sleeve the tank and then repair the three-corner leaks. Having accomplished this, the test tank was transported to the thermal test facility for heat shrinking of the Mylar.

Earlier testing on the vacuum bell check-out cylinder using a short cylinder of Mylar indicated that the Mylar was transparent to heat and would not shrink until it was made opaque to heat. Therefore, the test samples were spray painted with a form of carbon black and the shrink test repeated. The Mylar shrank, but without uniformity, causing wrinkles and puckers.

It was then decided that a full-scale attempt should be made to suspend a weighted ring from the bottom of the Mylar cylinder while being shrunk in the vacuum bell. (See Figures 9 through 12) Note that some areas show circumferential shrinkage with gathers of material due to lack of longitudinal shrinkage. Also, in other areas, no shrinkage occurred. It appeared that certain areas were heated and other areas witnessed no heat at all. It has been subsequently determined that the heater control thermocouples attached to the Mylar were not sensing the actual temperature of the Mylar nor were they acting uniformly over the length of the tank wall.

Due to the difficulty in obtaining a vacuum in the insulation space, as well as increased temperature requirements due to LOX-Rp and LOX-LH$_2$ trajectories which would melt the Mylar, it was decided that a new cover should be put on the insulation.

The new covering consisted of wrapping the tank insulation with 1 mil aluminum foil, and then a final wrap of three layers of glass cloth. The foil and glass cloth were wrapped in a spiral fashion. As the foil was wrapped, it was bonded to the Min-K insulation and to itself with General Electric RTV-11 silicone rubber (room temperature vulcanizing). After the foil was installed, the tank was then wrapped with three layers of glass cloth, each layer being impregnated with the RTV-11 silicone rubber. Figure 13 shows a cross section of the tank with the new cover installed. Thermocouples were installed on the aluminum foil prior to being wrapped with the glass cloth. The thermocouples would provide external tank wall temperatures during thermal runs. Although this type of material would results in a heavier cover, the advantages to be gained were worth the extra weight. These advantages were as follows:

(1) More durable outer cover
(2) High temperature allowable (700°F)
(3) Reliable thermocoupling

1.3.3 Tank Fabrication Progress

Design of the insulation encapsulating cover was completed and satisfactory progress was made applying the sidewall insulation. Figures 14 through 17 show the steps in applying the aluminum foil, thermocouples, and glass cloth. The end insulation had suffered damage during the efforts to heat shrink the Mylar cover. Consequently, the damaged foam in the transition space between the skirts and heads had to be removed and repoured. Resealing of the end insulation was then necessary to hold a vacuum.

1.4 Reporting Period May 8, 1961, to July 31, 1961

The following subsections will be devoted to the work progress during this period on the stainless steel tank system. The general areas of discussion will cover thermal considerations and tank fabrication progress.

FIGURE 9
PHOTOGRAPH OF MYLAR-COVERED TANK
BEING LOWERED INTO VACUUM BELL

FIGURE 10
PHOTOGRAPH OF MYLAR-COVERED TANK PRIOR TO HEATING

FIGURE 11
PHOTOGRAPH OF WRINKLING EFFECT ON MYLAR COVER AFTER HEATING
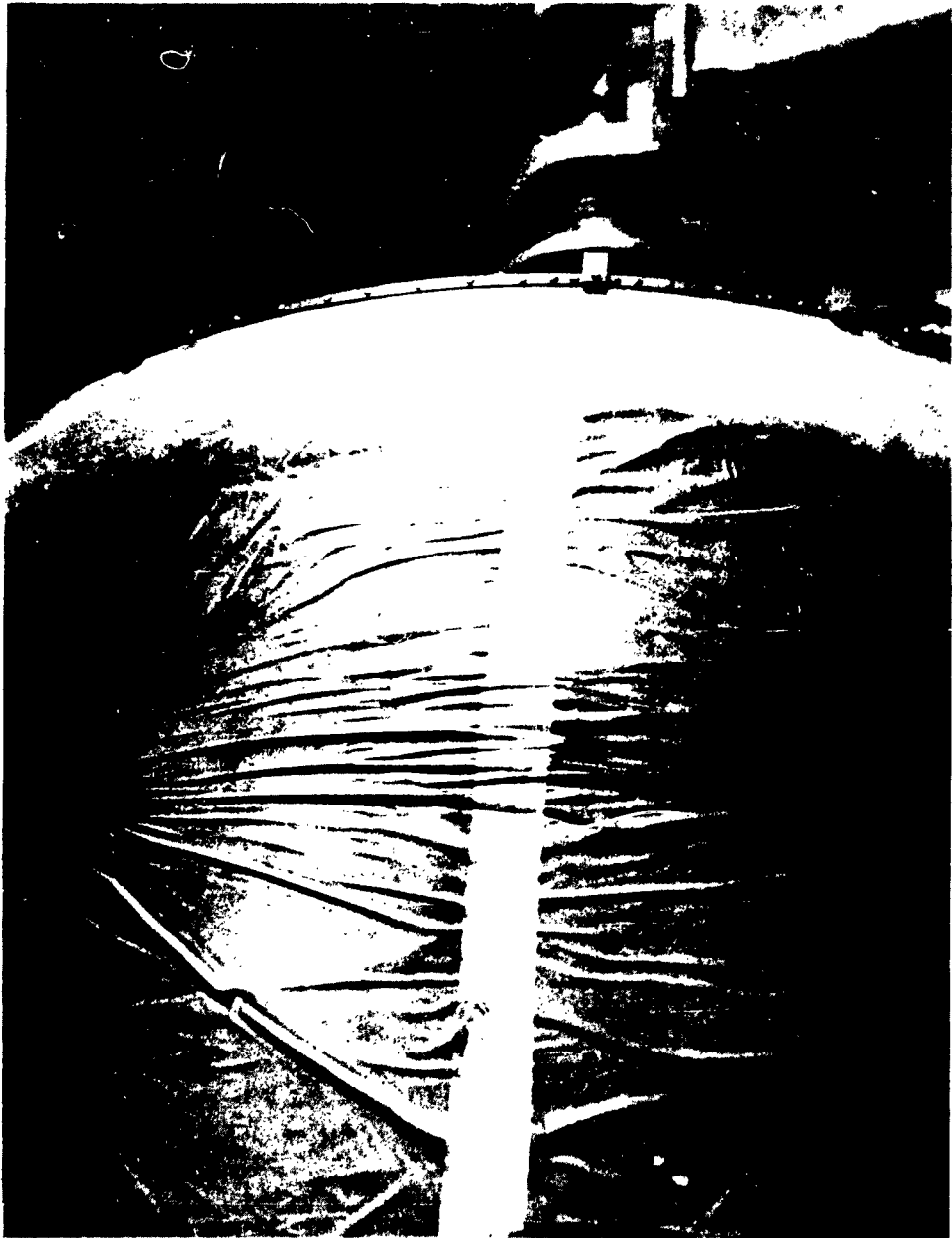
FIGURE 12
PHOTOGRAPH OF WRINKLING EFFECT OF MYLAR COVER AFTER HEATING

FIGURE 1
INSULATION CONCEPT
7,000 GALLON STAINLESS STEEL TEST TANK

RTV-11 Impregnated
Glass Cloth

MIN-K Tiles

Aluminum Foil

Tank Wall

Thermocouple
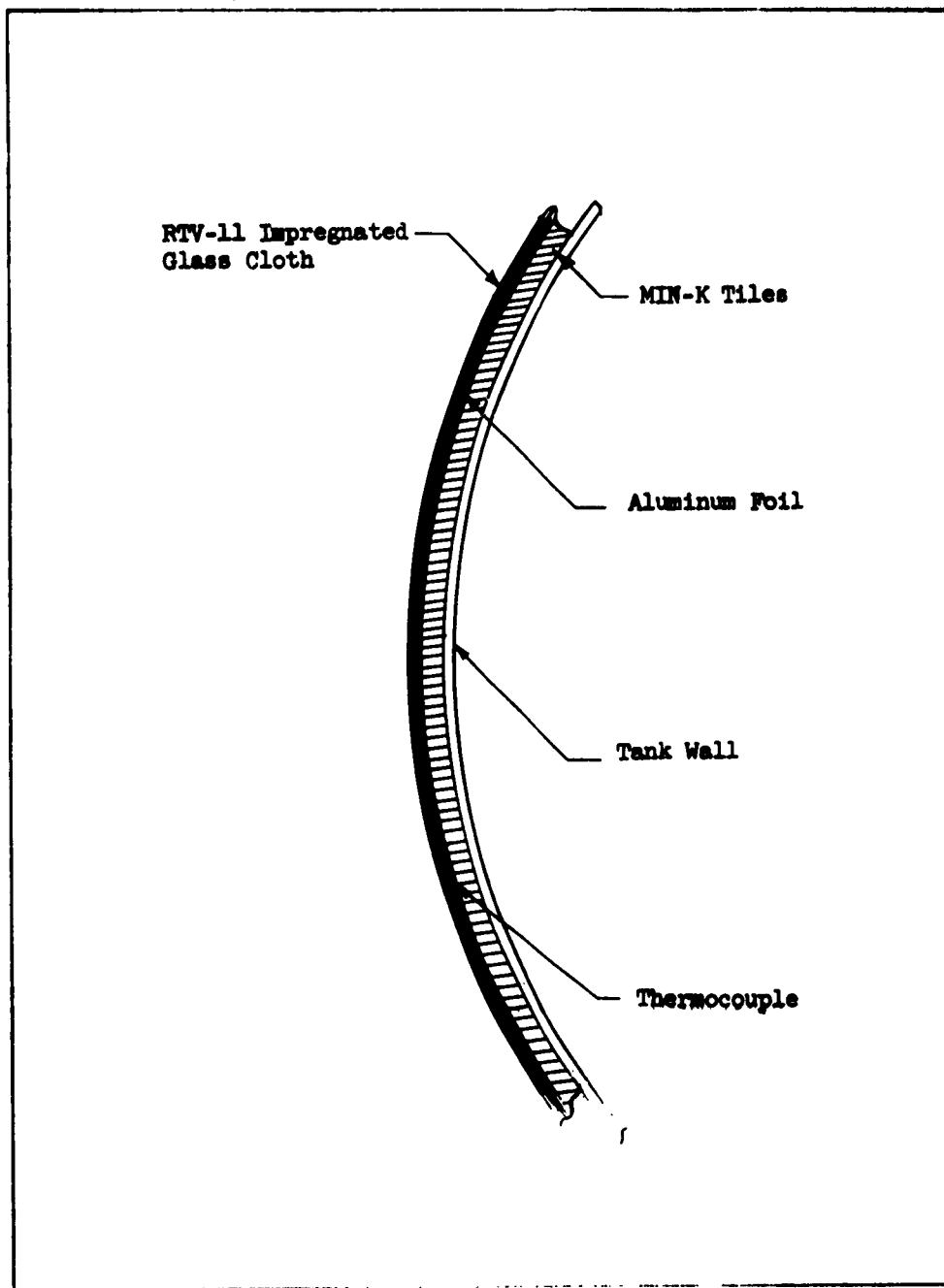
FIGURE 14
PHOTOGRAPH OF ALUMINUM FOIL BEING APPLIED TO SIDEWALL
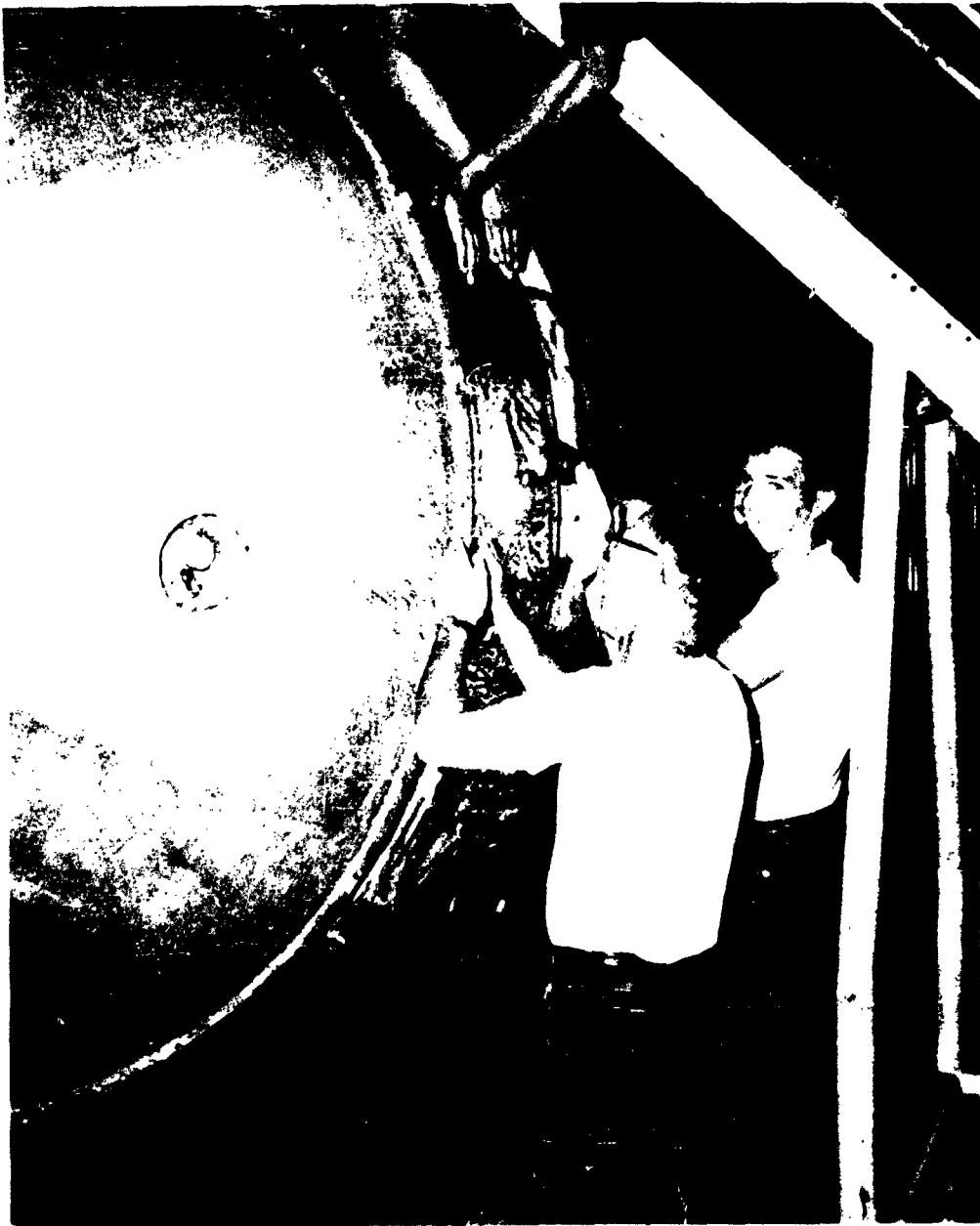
FIGURE 15
PHOTOGRAPH OF FINISHED ALUMINUM FOIL COVERING
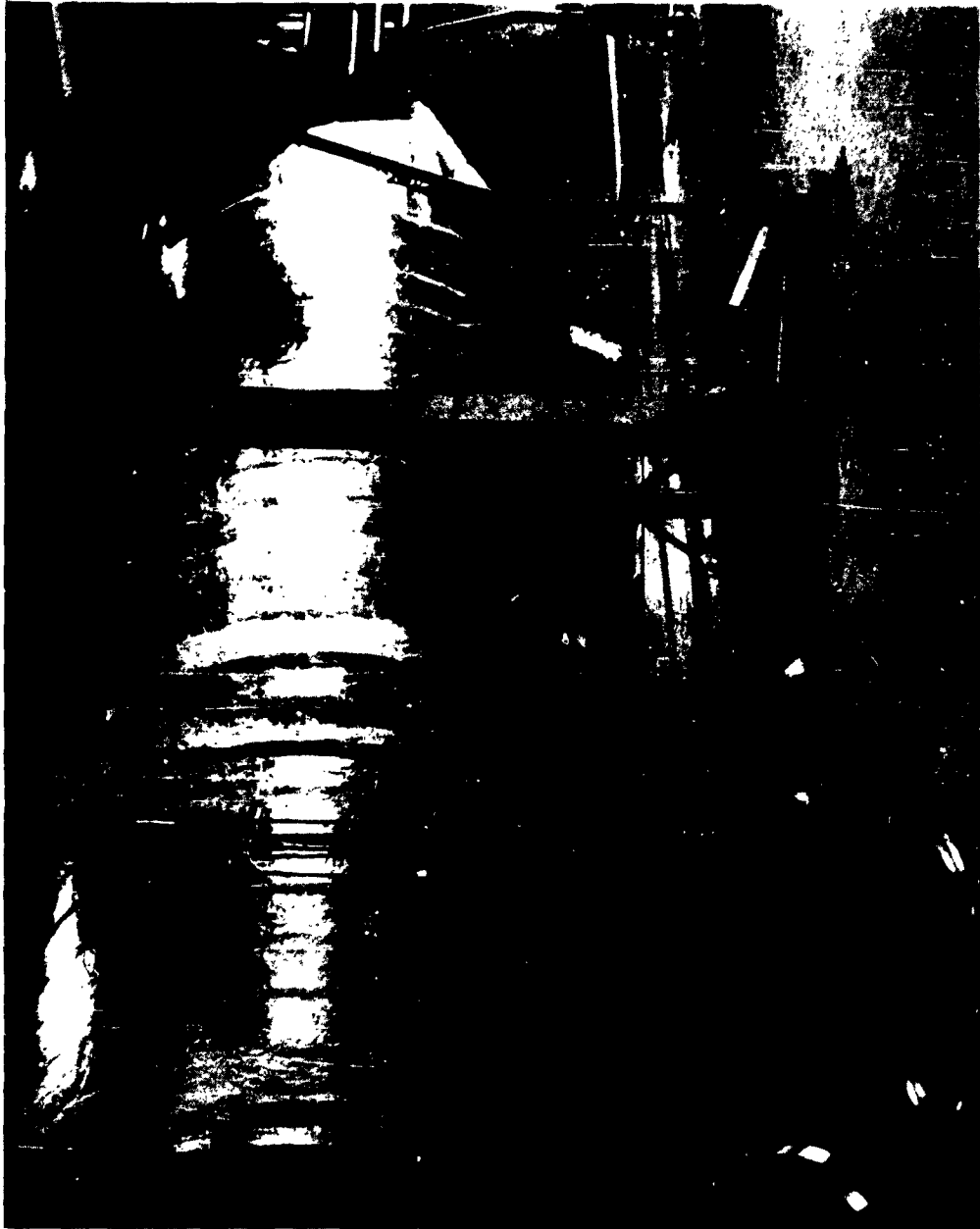
FIGURE 16
PHOTOGRAPH OF INSTALLING TEMPERATURE SENSORS TO SIDEWALL

FIGURE 17
PHOTOGRAPH OF INSTALLING FIBER GLASS CLOTH
IMPREGNATED WITH RTV-11

1.4.1 Thermal Considerations

A new insulation concept was designed during this period. This new concept is as follows:

(1) The tank to be wrapped in a spiral fashion with one (1) mil thick fiber-glas cloth 36 inches wide. Sufficient wraps will be accomplished until an insulation thickness of .10 inches is built up.

(2) The insulation will then be encapsulated in an aluminum foil cover. The aluminum foil will also be wrapped in a spiral fashion for three (3) layers. Each layer of foil will be bonded to the previous layer with General Electric RTV-11 silicone room temperature curing rubber. Prior to wrapping, the foil will be primed with General Electric SS4004 primer for good bonding characteristics. The last wrap will be primed on one side only, so that the finished exterior will be a bright aluminum color. (See Figure 18)

(3) The heads will be insulated with contoured fiberglas segments. The segments will be attached to the heads with Stabond 511 adhesive. After installing the segments, the insulation will be encapsulated with aluminum foil. The aluminum foil is to be applied in great circle strips 12 inches wide with each layer bonded to the previous layer with General Electric RTV-11 silicone rubber. The foil will also be bonded to the skirt angle rings to seal the entire head area. (See Figure 19)

1.4.2 Tank Fabrication Progress

The following subsections will describe the work progress of reconditioning the tank and installation of the new insulating concept.

1.4.2.1 Reconditioning

The following steps were taken to recondition the tank in preparation for installing new insulation:

(1) Strip all old insulation from tank except foam in annulus between skirt and head.
(2) Repair any "cans" or dents remaining in tank cylinder when the tank was collapsed previously.
(3) X-ray examination of all weld seams in damaged areas.
(4) Repair NPSH ring and reinstall.
(5) Leak check entire tank assembly.

1.4.2.2 Insulation

The insulation of the sidewall proceeded without difficulty. By the end of this period the sidewall insulation was completed and initial pumpdown was started. This initial pumpdown indicated that the aluminum foil cover will hold a reasonable vacuum. Further testing in this area was done.

Figures 20 and 21 show the method of applying the fiberglas cloth and aluminum foil cover.

FIGURE 28
CROSS SECTION OF SIDEWALL INSULATION AND COVER

Tank Wall

Fiberglass Cloth
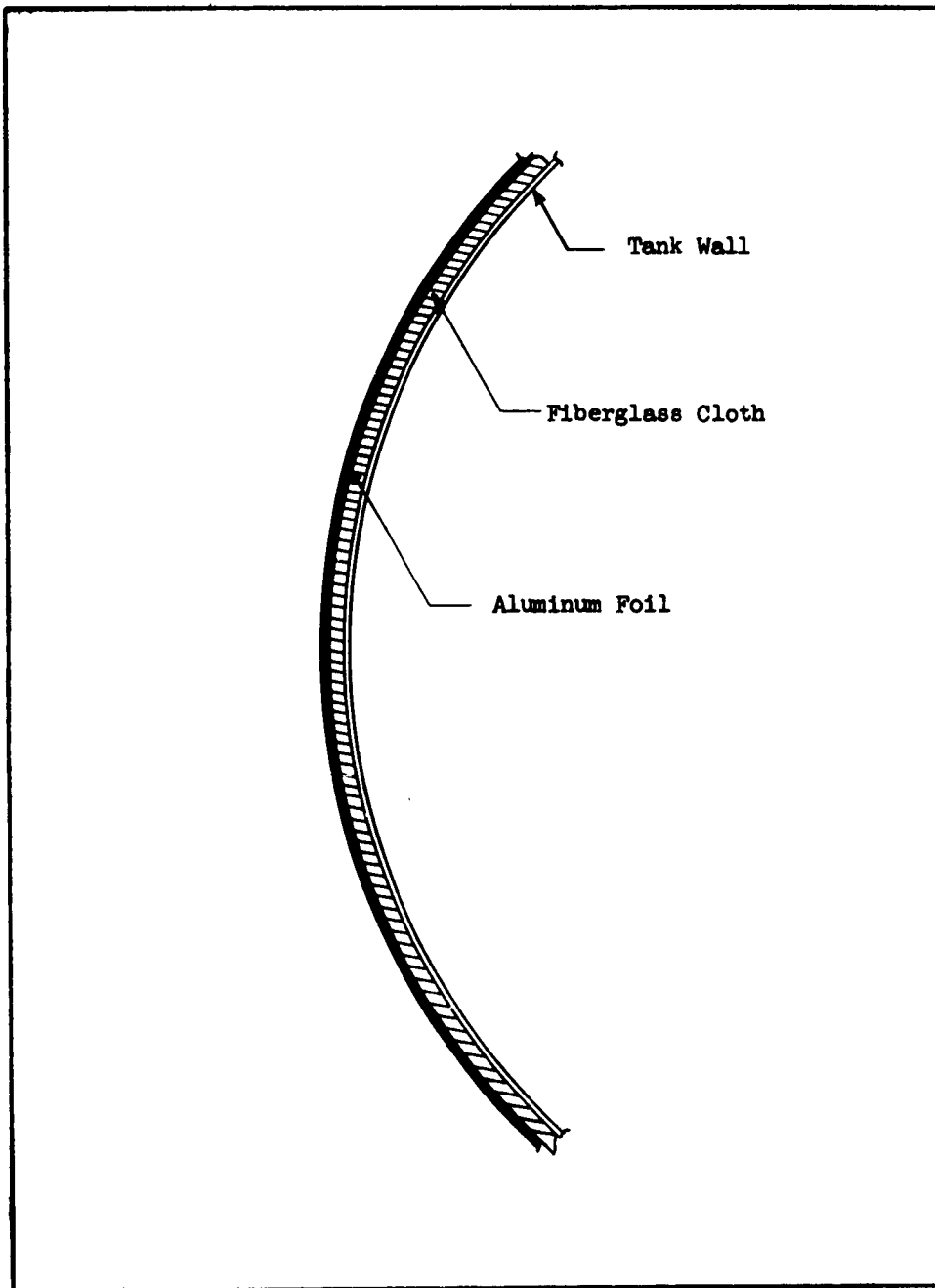
Aluminum Foil

FIGURE 19
CROSS SECTION OF HEAD INSULATION
AND ALUMINUM FOIL COVER

Aluminum Foil

Formed Fiberglass Segment

Tank Wall

Poured-In-Place Urethane Foam
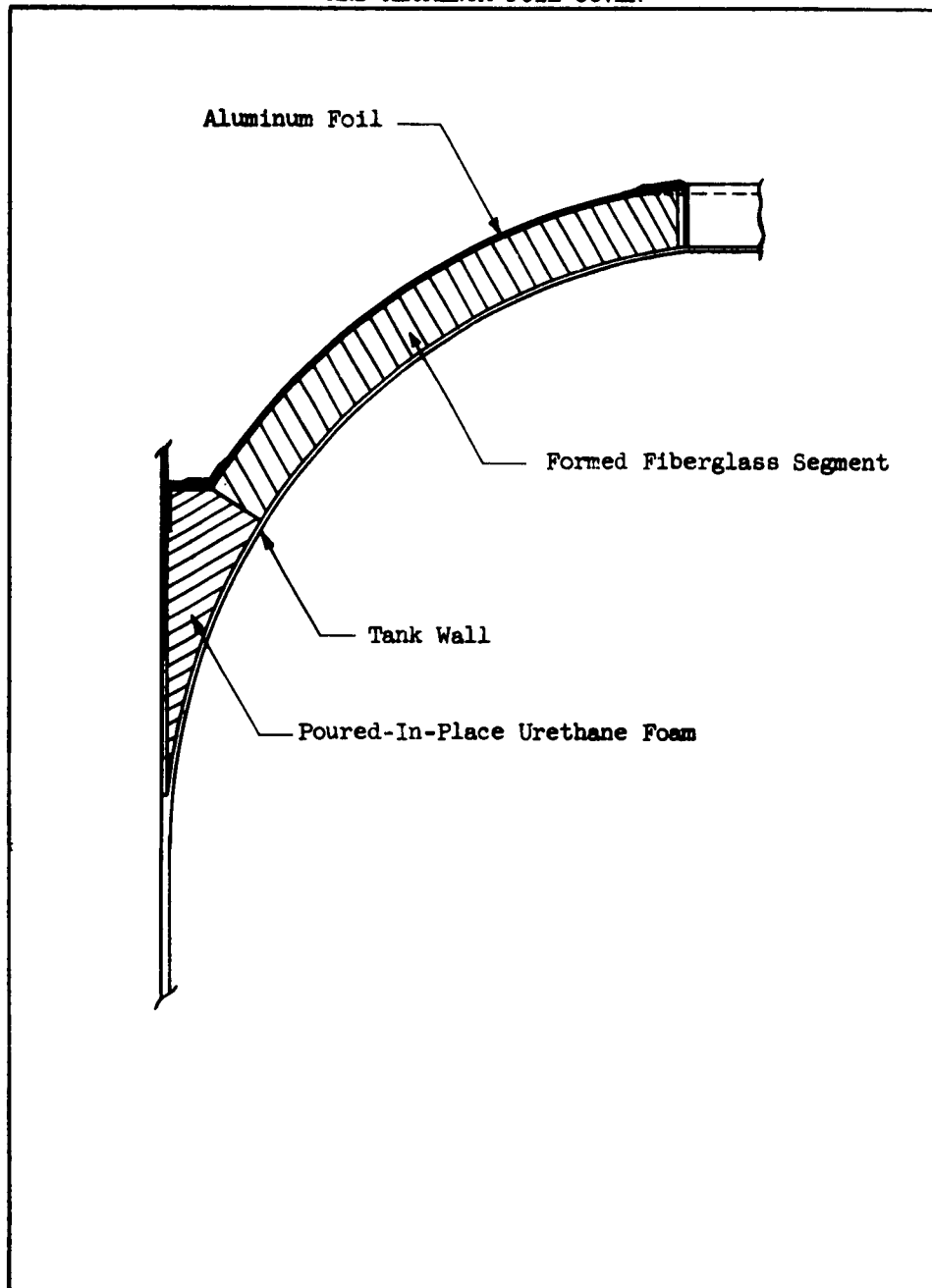
FIGURE 20
PHOTOGRAPH OF APPLYING FIBER GLASS CLOTH INSULATION

FIGURE 21
PHOTOGRAPH OF APPLYING ALUMINUM FOIL COVER

1.5 Reporting Period August 1, 1961, to October 31, 1961

This section will describe the progress made during this period on the fabrication of the stainless steel test tank. The following subsection will be devoted to describing the topic subjects.

1.5.1 Tank Fabrication Progress

The insulation for the heads was composed of nine segments, each preformed to fit the contour of the hemisphere of the forward head and the combination hemisphere and 90° cone of the aft head. After each segment was trimmed to print dimensions, it was attached to the head by means of Stabond 511-A adhesive. After the insulation was installed, three overlapping layers of aluminum foil were bonded to the insulation and itself with General Electric RTV-11 silicone rubber sealer.

This completed the fabrication of the stainless steel tank.

2.0 7,000-GALLON TITANIUM TANK SYSTEM

2.1 Reporting Period June, 1959, to September, 1959

The following sections will discuss the progress made during this period. In order to properly describe the progress made, the tank system reporting will be divided into the following major headings:

Tank Structure, and

Tank Insulation.

2.1.1 Tank Structural Design

2.1.1.1 Tank Skirts

One of the more difficult design problems with the tank has been the skirts and the small annulus between the skirts and the heads (See Figure 23). Earlier designs of this area depicted the tank end insulation extending down to the edge of the skirt stiffening ring. On a flight article, the small annulus below the foam and inside the skirt would be filled with foam and evacuated in conjunction with tank and insulation. This foam would eventually soften or melt due to excessive aerodynamic heating, and the vacuum would be lost. At the time that this happened, however, the tank end insulation would have completed its intended function. For the test article, however, a serious problem would exist in that only one test could be run, at which time the foam would have to be replaced or left as is with the accompanying heat short. Replacement of the foam could be very difficult and time consuming so it was decided to leave this wedge-shaped annulus empty during testing.

Leaving this annulus empty would require that the evacuated foam insulation on the tank ends be sealed off independently of the annulus since the tank skirt is not capable of withstanding a vacuum condition. At the present time, there is no sealant available which will adhere to foam and titanium and maintain a seal at liquid hydrogen temperatures with any degree of dependability.

One method of solving the problem would be to fill the annulus with a high-temperature powder insulation, and to evacuate both insulations (powder and foam) as one common chamber. This system would require that the pressure (vacuum) in the annulus be higher than that which is outside of the tank skirts, in order to prevent collapsing of the skirts. During the test phase, it would mean that this vacuum would have to be vented to atmosphere prior to each test run. This approach is not practical as it would require repeated evacuation of the foam insulation for each test, resulting in a large time delay.

FIGURE 23
DETAILS OF TANK HEAD AND SKIRT AREA

FIGURE 23
DETAILS OF TANK HEAD AND SKIRT AREA
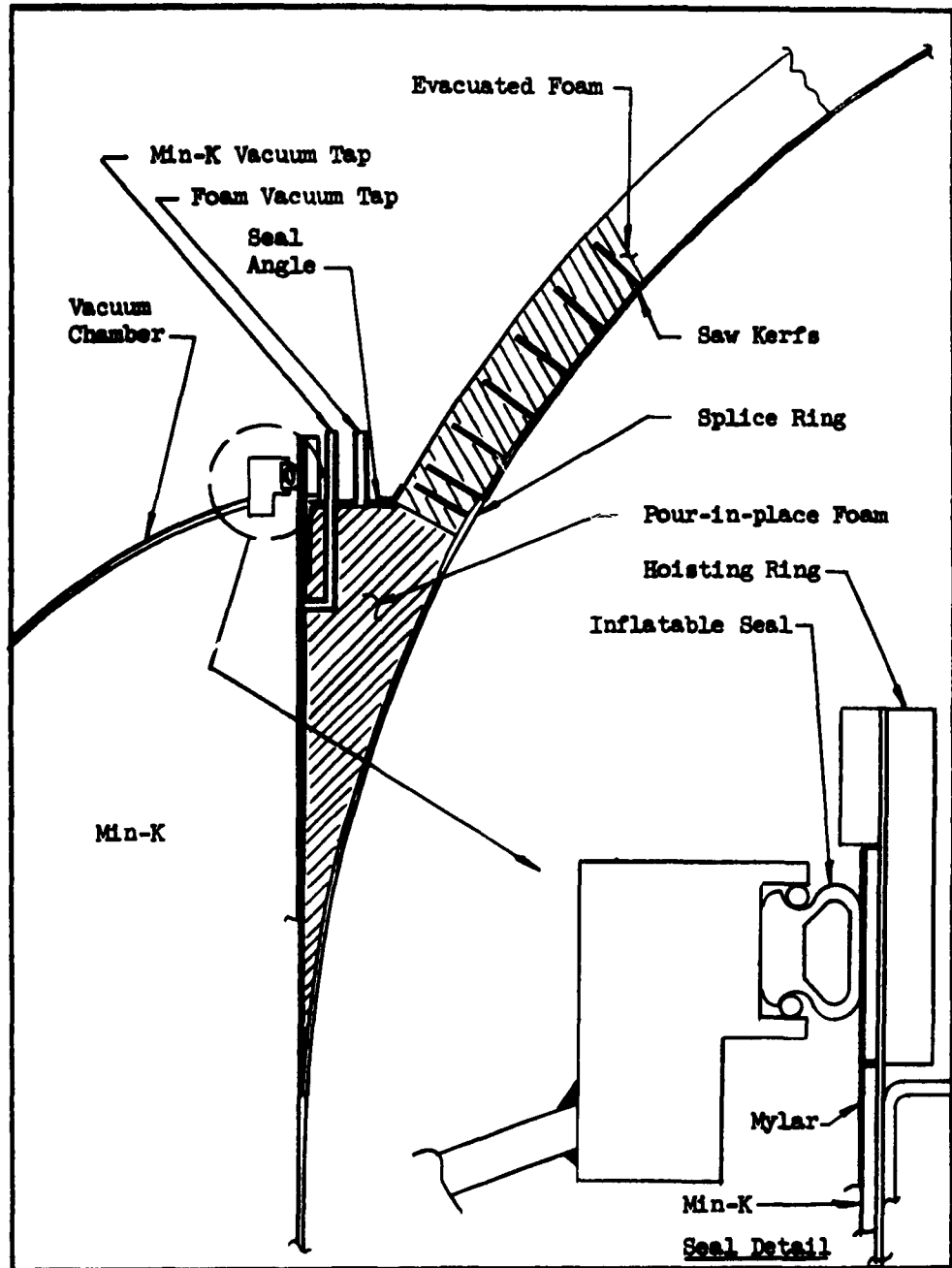
The present design calls for filling the annulus with a poured-in-place plastic foam and extending the external high-temperature insulation so that it will offer protection for the foam. This will prevent the foam from being destroyed due to the simulated aerodynamic heating. By going to this design, a rein-forced splice had to be added to the hemispheres at the junction of the poured-in-place foam and the tank end insulation.

2.1.1.2 Sealing Requirements for Testing

The straps which were added for hoisting capability serve a double purpose. The inner strap is quite thick and wide and provides the necessary moment of inertia to resist the bending loads imposed by the pressure inflatable seals which are attached to the aerodynamic heating fixture and seal against the tank skirts. The aerodynamic heating fixture is a large vacuum chamber which surrounds the test tank, houses the heating elements and provides auxiliary insulation during the filling of the test tank.

2.1.1.3 Material Tolerances

The selection of tolerances for the sheet material has required a study of cost versus weight. The allowable thickness tolerance on the titanium sheet coming from the mill has been reduced with the consequent increase in price. This increase in price is not significant when compared to the savings in weight as can be seen from the following analysis.

Using the N85-100 configuration, as reported in WADC TR 58-273, the ratio of wet weight to dry weight is,

$$536,460 \text{ lb}/145,040 \text{ lbs} = 3.70.$$

The total tank skin area of that configuration is 13,434.3 ft.^{2}. If it can be assumed that a .001" of thickness can be saved on all of the skin, the reduction in weight would be,

$$(.001)(13,434.3)(144)(.161) = 311.46 \text{ lbs.}$$

To save the .001" in skin thickness, the manufacturer will charge a toler-ance premium. A conservative (high) estimate for this tolerance premium is assumed to be $2.00/lb. The total weight of a titanium tank for the N85-100 configuration is 8,449 lbs, based on room temperature tensile allowables, with a resulting tolerance premium of ($2.00/lb.)(8,449 lbs.) = $16.898.

The ratio of wet weight (launch weight) to dry weight (burnout weight) being 3.70, the theoretical weight saved at launch is (3.70)(311.46) = 1,370 lbs.

Assuming that the cost of fuel will be $.50/lb., that structural cost is $50/lb., and that 73% of the total launch weight is fuel, the gross dollar saving of the 1,370 lbs. saved at launch is:

Fuel	1,370(.73)($.50)	= $	500
Structure	1,370(.27)($50)	=	18,500
	Gross Dollar Savings	=	$19,000

Thus, at an expense of $16,898 to gain an extra .001" on the sheet tolerances a net savings of 19,000 - 16,898 = $2,112 is effected.

It should be noted that these savings are gained for only a .001" savings in tolerances. Greater savings may be effected by further reduction in tolerances.

Another important point to be considered is the maximum wall temperature of the tank. As the maximum operating temperature decreases, the design allowables increase, the skin thicknesses decrease and a .001" savings in sheet tolerance represents a larger percentage. Therefore, on the basis of a .001" saving on thickness tolerance for any gage, the net dollar savings is a function of maximum operating temperature. As an illustration, and using the N85-100 configuration with fuel costs at $.50/lb. and fuel weight being 73% of the total tank wet weight, a plot of net savings versus operating temperature for various structural unit costs is shown in Figure 24.

As a result of this study, certain reductions in sheet tolerance for the test tank material were required of the titanium fabricator. The .018" skins in the tank end are ordinarily rolled to a tolerance of $\pm$ .003". A tolerance of plus .002" minus .001" was ordered, providing a net savings of .003". It is believed that the penalty in cost ($2.00/lb. for the specified tolerances) will be more than offset by the savings in launch weight and costs of an actual flight vehicle. The reason for including this design parameter in the present test tank which is not a true flight article is to help determine true weights and costs of tank systems that will be part of future rocket vehicles.

2.1.2 Tank Insulation

The main areas of tank insulation include sidewall insulation and tank end insulation. Each of these areas will be discussed separately in the following sections. In addition, the tank sidewall insulation optimization procedure will be fully described.

2.1.2.1 Tank Sidewall Insulation Optimization

During the past quarter, many computer runs have been made in the thermal analysis of both the N85-100 and C85-100 liquid hydrogen tank systems, the results of which have already been given in WADC TN 59-177, Section 1.2. The first computer calculations were based on using Min-K 1301 for the sidewall insulation and attached to the exterior of the tank skin.

The Min-K 1301 insulation has been used initially in the computer solutions because this particular insulation has high-temperature capabilities, is physically stable over wide temperature gradients, has a reasonable low thermal conductivity (particularly at the higher temperatures), possesses a relatively low density (20 lb./ft.^{3}), and has good compressive strength.

FIGURE 24
NET DOLLAR SAVINGS DUE TO REDUCED SKIN TOLERANCES
VERSUS TANK SKIN MAXIMUM OPERATING TEMPERATURE
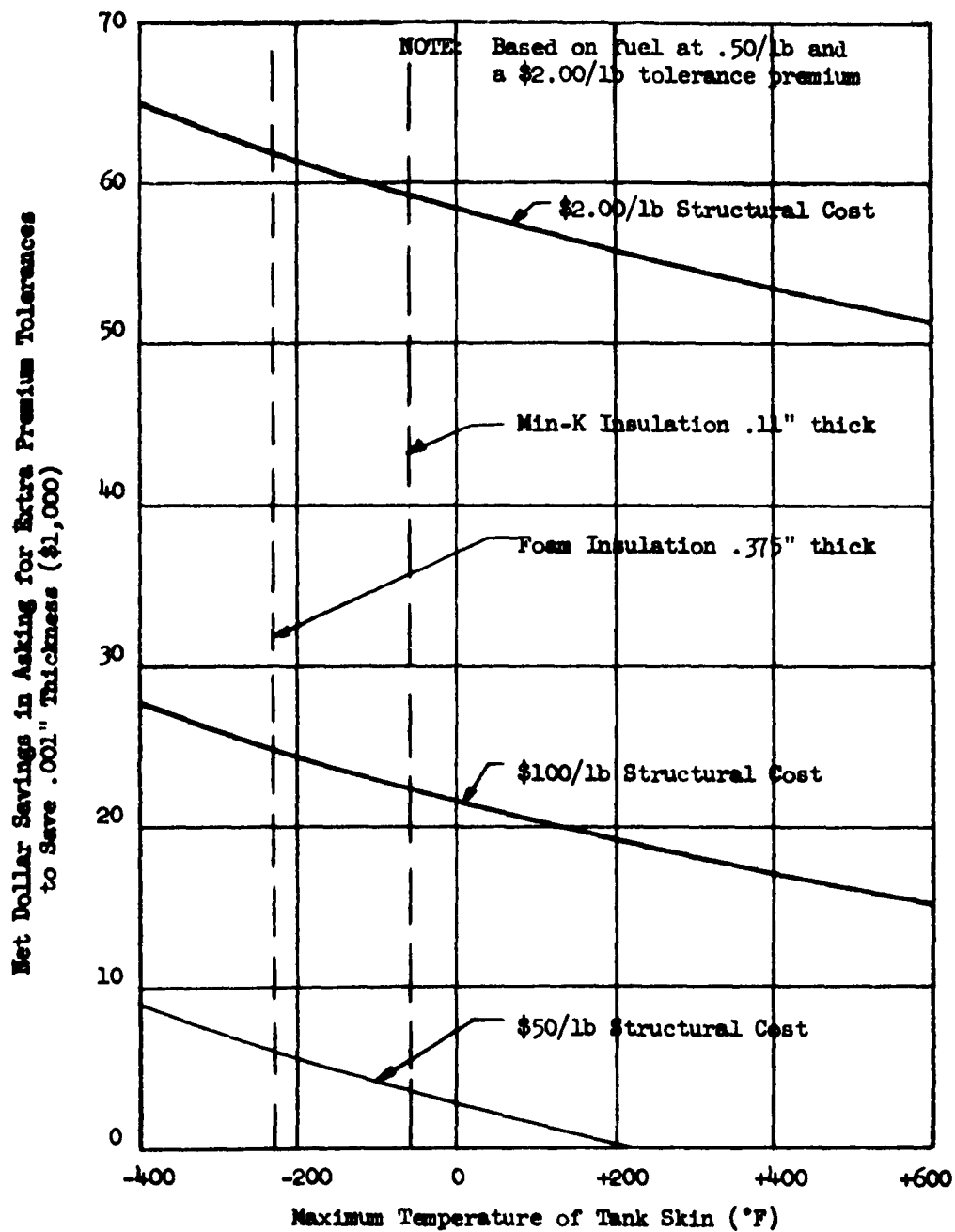
At the time these computer solutions were being solved, only a meager amount of thermal data was available on the Min-K products. The manufacturer (Johns-Manville) of the product did supply some thermal conductivity and specific heat data; however, it was all in the high-temperature region and was not concerned with cryogenic temperatures. In order to supply the computer with the required thermal inputs, it became necessary to extrapolate the existing data to include those temperatures that the insulation was expected to witness during the boost phase of the flight. In addition, since the computer used on the first runs was not at that time set up to handle a variable k or C_p (each as a function of temperature), it was necessary to determine as closely as possible one value each for k and C_p that would represent a mean value over the expected temperature gradient. The finally selected values used in the N85-100 trajectory were $k = .20$ BTU-in/hr-ft.^{2}-°F, $C_p = .17$ BTU/lb.-°F and $p = 22$ lb./ft.^{3} (actual weighing of samples of Min-K 1301 showed this value to be more nearly corrent than the 20 lb/ft.^{3} stated in the product data sheets).

At this point it would be well to state that the prime purpose of these computer solutions is not only to predict the thermal behavior of insulated liquid hydrogen rocket vehicle tanks, but to also assist in optimizing the tank system weight. It should be understood that the tank system weight includes not only the tank structural weight and the insulation weight, but it also includes the weight of any vented vapor and the weight of the residual vapor remaining in the tank at the time of burnout. Therefore, in order to optimize the tank system with respect to minimum weight, an optimum design method was devised whichcould be used to account for all of these weights and help determine the sidewall insulation requirements that would provide the lowest tank system weight. The details of this optimization process will be fully described in the following paragraphs.

The computer solutions of the heat balance equations were obtained for varying thicknesses of a given insulation (Min-K 1301 in this particular N85-100 example). The computer results are translated with the aid of an x-y plotter into a plot of slab temperatures (skin and insulation temperatures) of the various tank stations each as a function of flight time. A typical example of this plot is shown in Figure 25 and is for a .125" thickness of Min-K 1301. Examination of this plot shows that the maximum insulation temperature (U_1) is 565°R, which occurs at the uppermost tank sidewall station (Station 28). This temperature is, of course, well within the operating temperature range of the Min-K insulation, and it gives some indication that other insulations with lower densities and lower limiting temperatures (such as plastic foams) could be used.

The maximum temperature (U_o) of the structural skin (6Al-4V annealed titanium in this case) is seen to be 374°R for Station 28. The lower tank stations, being in contact with the liquid hydrogen for a longer period of time, have even lower maximum temperatures. In order to help reduce tank weight it is believed that designing to these lower temperatures (hence higher strength allowables) is desirable and realistic. To effect a conservative approach and at the same time to simplify the optimization process, the weight of the tank sidewall if based on the assumption that all of the tank sidewall structural material will witness the maximum temperature that occurs at the uppermost tank station (Station 28). In actuality, the lower tank stations could conceivably be designed to lower temperatures and higher stress levels, and would provide lower tank sidewall weights than indicated.

FIGURE 25
TANK WALL TEMPERATURE VERSUS TIME
N85-100, .125" MIN-K, .025" TITANIUM

NUMBERING CODE:

First Number — Tank Station
Second Number — Wall Lamina

28-9
28-1

62-9
62-1

97-9
97-1

133-9
133-1

170-9
170-1

Tank Wall Temperature - °R

Time - Seconds
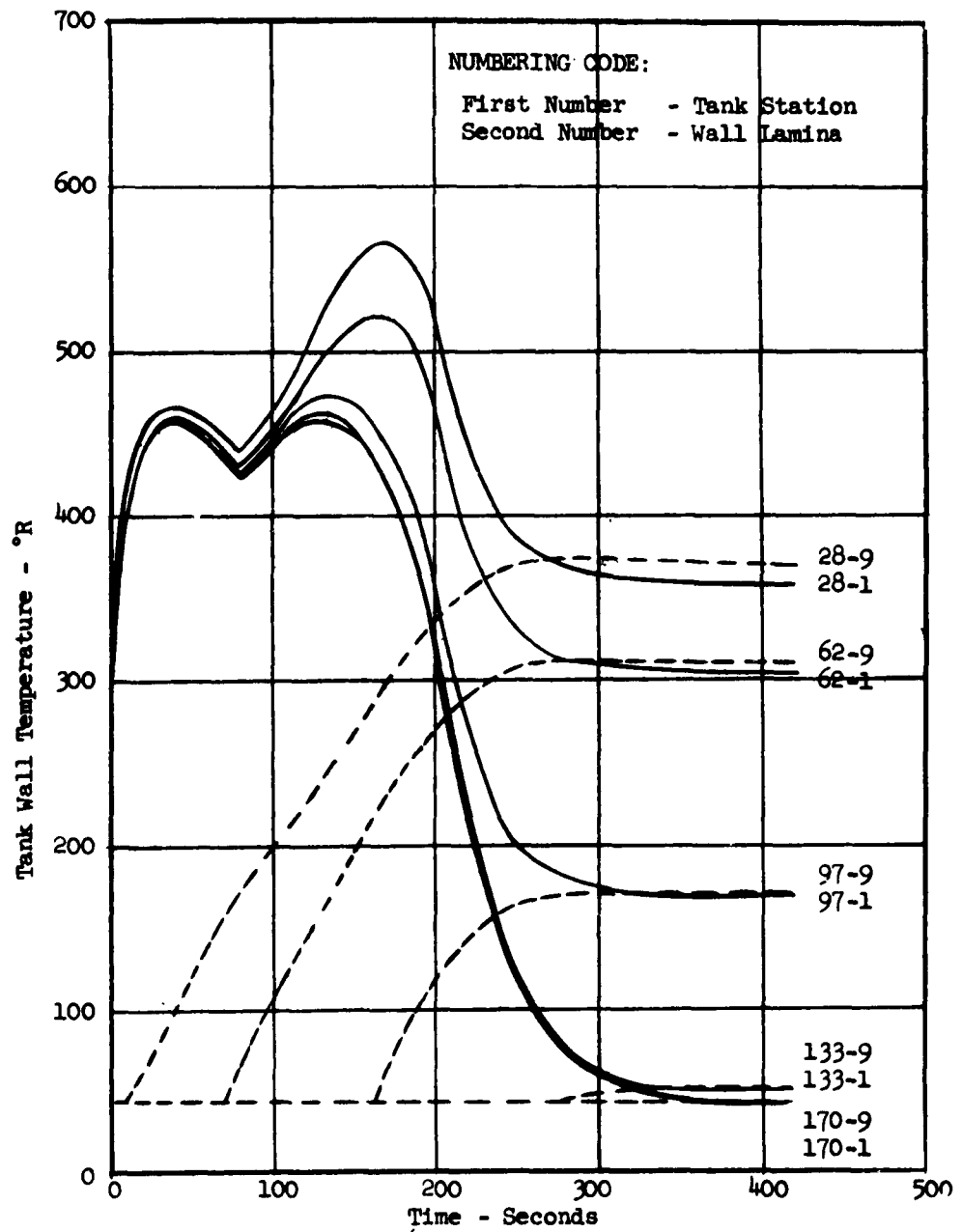
Before the weights of the tank sidewall can be calculated, it is necessary to investigate the role that the added pressurization gas would play in the tank sidewall design. If the propellant use rate is greater than the volume rate of the boil-off gas which is due to aerodynamic heating, it becomes necessary to add pressurization gas into the tank to occupy this volume difference in order to maintain the proper tank operating pressure.

At a first glance, it would appear that the addition of hot gas would be beneficial from a weight standpoint since this gas would be added gas could effect the structural sidewall temperature, changing the allowable stress levels and thus changing tank sidewall weight. Until sufficient tests can be conducted in the heat tower to determine a simplifying, but conservative, assumption has been made. It is assumed that the temperature of the entire tank sidewall will be equal to the added gas temperature. Likewise, for a fair first approximation in determining the optimum sidewall insulation thickness, it has been assumed that the optimum added gas temperature should equal the maximum temperature (U_0) witnessed by the uppermost tank station (Station 28). The latter assumption was made on the basis that under this condition, the influence of the added gas temperature on the tank sidewall would be at a minimum.

The first step in determining the tank sidewall weight as a function of added gas temperature is to define the relationship of tensile strength versus temperature for the structural material under consideration. Figure 26 is a plot of the allowable design stress versus temperature for 6Al-4V annealed titanium alloy. The values shown in this plot are based on average ultimate tensile strengths (References   and   ) divided by a safety factor of 1.3625. These values are a close approximation to values predicated by the present design philosophy of using guaranteed (by the material manufacturer) ultimate tensile strengths divided by a safety factor of only 1.25. Until such time that the material manufacturer will guarantee the ultimate tensile strength at temperatures other than room temperature, the allowable design stress levels will have to be based on compiled ultimate averages divided by the 1.3625 factor.

Based on the allowable tensile stress levels shown in Figure 26, it is possible to calculate the thicknesses and weight of the tank sidewall by applying the suitable critical tank pressures. Figure 27 is a plot of tank sidewall weight (only that portion that is exposed to aerodynamic heating) versus added gas temperature for the N85-100 rocket vehicle configuration.

The weight of the tank sidewall insulation can be easily determined simply by knowing its thickness, area, and density.

The vented vapor weight can be calculated by comparing the propellant use rate with the boil-off rate due to heat flow into the liquid. In all of the single stage or first stage rocket vehicles considered up to this time, the propellant use rate has been the greater, and no vapor is vented. In the case of second- or third-stage tanks where the propellant level is not descending during the aerodynamic heating phase, one would expect vented vapor losses. Preliminary studies on these types of tank systems has shown that even by using the boil-off gas to raise the tank pressure to the proper operating value, venting of some of the vapor cannot be prevented.

The weight of the boil-off gas can be determined by referring to the computer solution where the total heat into the propellant as a function of flight time is plotted on the x-y plotter. This total Q is then divided by the latent heat of vaporization (at saturation temperature and tank operating pressure), the result being the weight of boil-off gas. If none of this is vented, it will become a portion of the residual gas remaining in the tank at burnout or cut-off.

The weight of the added pressurization gas (gas at any temperature) can then be determined by converting the above boil-off gas weight into a volume based on saturated conditions and subtracting this from the total volume of the tank. The weight of this added gas can then be calculated by multiplying this volume difference by the appropriate gas density which is at an arbitrary temperature and at the tank operating pressure.

The remaining weight factor that influences the tank system weight would be the heat exchanger and associated hardware that would be required to provide the added pressurization gas at the specified temperature. To again simplify the optimization process it has been assumed that the rocket engine nozzle will provide sufficient heat exchanger area to convert the required volume of added gas from the liquid propellant itself. It is believed that the difference in size and weight of the associated hardware (valves, fittings, lines, etc.) to accommodate varying flow rates of this added gas would not influence the total system weight to a great degree and would have little or no effect on the optimum conditions. Therefore, for the present time, the heat exchanger weight has been equated to zero.

A tabular form has been established to list each of these influencing weights as a function of added pressurization gas temperature for varying thicknesses of a given insulation. Tables 1 through 5 show these weights as a function of added gas temperature ranging from -400°F to + 200°F with an additional gas temperature which is equal to the maximum skin temperature (U_o) at the uppermost tank sidewall station resulting from the aerodynamic heating. Again, it was believed that the total optimizational weight at this added gas temperature would provide a good first approximation for determining the optimum tank sidewall insulation requirements.

The insulation thicknesses that were analyzed on the computer included .044" (the minimum thickness of Min-K 1301 that would preclude the condensing of air on the exterior surface of the insulation), .125", .250", .500", and 1.00". It was believed that this range would embrace the optimum thickness based on the minimum tank system weight concept, yet would allow investigation of insulation requirements that could possibly be used to circumvent the use of the proposed ground insulation concept.

The plot illustrated in Figure 28 shows the sum total of the combined weights that affect the optimizational tank weight. This optimizational tank weight should not be confused with the total tank system weight. The optimizational tank weight does not include the weights of the upper or lower metallic heads, tank end insulation, skirts, tank fittings, or fuel system components since each of these items is considered independent of the tank sidewall insulation requirements and their entry into the optimization procedure would be of no benefit.

Average ultimate tensile strength
(References 17 and 18)

Guaranteed Ult.

$$\frac{\text{Guar. Ult.}}{1.25} \quad \text{or} \quad \frac{\text{Ave. Ult.}}{1.3625}$$

$$\frac{\text{Ave. Ult.}}{1.3625}$$

Allowable
Design Stress

Temperature (°F)

Tensile Stress (1000 psi)

FIGURE 27

EXPOSED TANK SIDEWALL WEIGHT VS. ADDED PRESSURIZATION GAS TEMPERATURE
(6Al-4V ANNEALED TITANIUM ALLOY)
(N85-100 CONFIGURATION)

Note: This curve is based on all of the tank skin working at the same temp. and assuming a constant taper in all skins.

Exposed Tank Sidewall Weight (1000 lb.)

Add Pressurization Gas Temperature (°F)
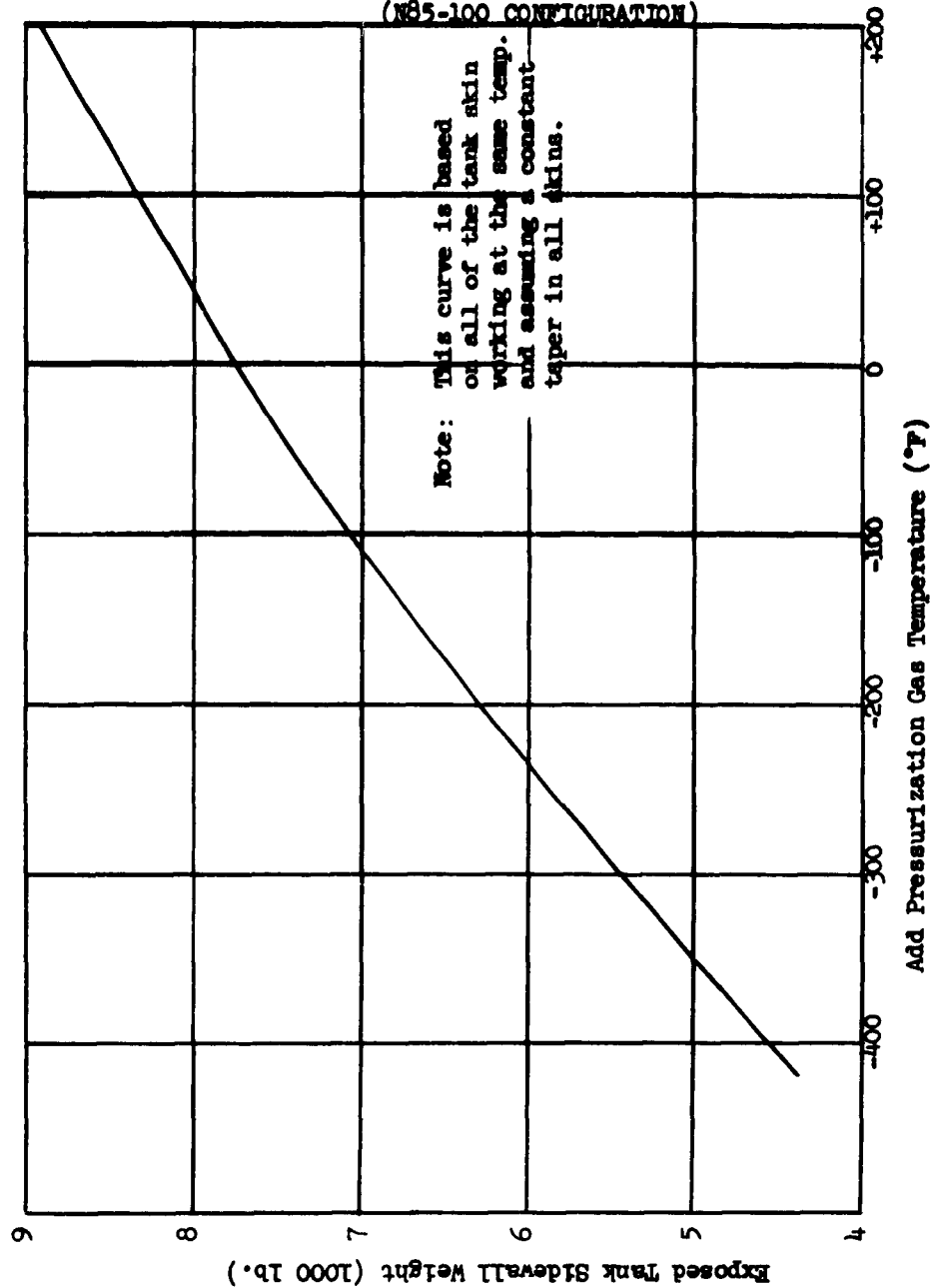
TABLE 1
OPTIMIZATIONAL TANK WEIGHT
FOR N85-100, .044" MIN-K 1301 INSULATION

Configuration N85-100   Insulation Min-K 22 lb/ft³   Thickness .044"

	Added Gas Temperature (°F)							
	-400	-300	-200	-100	0	+100	+200	+95
Exposed Tank Sidewall Weight	4560	5450	6290	7060	7720	8350	8910	8260
Sidewall Insulation Weight	962	962	962	962	962	962	962	962
Vented Gas Weight	0	0	0	0	0	0	0	0
Boil-off Gas Wt. at .100 lb/ft³	3840	3840	3840	3840	3840	3840	3840	3840
Added Pressurization Gas Weight	2843	1070	653	464	363	301	255	308
Heat Exchanger or Gas Bottle Weight	0	0	0	0	0	0	0	0
Optimizational Tank Weight	12,205	11,322	11,745	12,326	12,885	13,453	13,967	13,370

TABLE 2

OPTIMIZATIONAL TANK WEIGHT
FOR N85-100, .125" MIN-K 1301 INSULATION

Configuration N85-100   Insulation Min-K 22 lb/ft³   Thickness .125"

	Added Gas Temperature (°F)							
	-400	-300	-200	-100	0	+100	+200	-86
Exposed Tank Sidewall Weight	4560	5450	6290	7060	7720	8350	8910	7160
Sidewall Insulation Weight	2734	2734	2734	2734	2734	2734	2734	2734
Vented Gas Weight	0	0	0	0	0	0	0	0
Boil-off Gas Wt. at .100 lb/ft³	1717	1717	1717	1717	1717	1717	1717	1717
Added Pressurization Gas Weight	4046	1522	929	661	517	429	363	637
Heat Exchanger or Gas Bottle Weight	0	0	0	0	0	0	0	0
Optimizational Tank Weight	13,057	11,423	11,670	12,172	12,688	13,230	13,724	12,248

TABLE 3
OPTIMIZATIONAL TANK WEIGHT
FOR N85-100, .250" MIN-K 1301 INSULATION

Configuration N85-100	Insulation Min-K 22 lb/ft³	Thickness .250"						
	Added Gas Temperature (°F)							
	-400	-300	-200	-100	0	+100	+200	-182
Exposed Tank Sidewall Weight	4560	5450	6290	7060	7720	8350	8910	6420
Sidewall Insulation Weight	5467	5467	5467	5467	5467	5467	5467	5467
Vented Gas Weight	0	0	0	0	0	0	0	0
Boil-off Gas Wt. at .100 lb/ft³	1027	1027	1027	1027	1027	1027	1027	1027
Added Pressurization Gas Weight	4437	1669	1012	725	567	470	398	940
Heat Exchanger or Gas Bottle Weight	0	0	0	0	0	0	0	0
Optimizational Tank Weight	15,491	13,613	13,796	14,279	14,781	15,314	15,802	13,854

Configuration N85-100 Insulation Min-K 22 lb/ft³ Thickness .500"								
	Added Gas Temperature (°F)							
	-400	-300	-200	-100	0	+100	+200	-250
Exposed Tank Sidewall Weight	4560	5450	6290	7060	7720	8350	8910	5870
Sidewall Insulation Weight	10,934	10,934	10,934	10,934	10,934	10,934	10,934	10,934
Vented Gas Weight	0	0	0	0	0	0	0	0
Boil-off Gas Wt. at .100 lb/ft³	721	721	721	721	721	721	721	721
Added Pressurization Gas Weight	4610	1734	1059	753	989	488	413	124
Heat Exchanger or Gas Bottle Weight	0	0	0	0	0	0	0	0
Optimizational Tank Weight	20,825	18,839	19,004	19,468	19,964	20,493	20,978	18,849

TABLE 5
OPTIMIZATIONAL TANK WEIGHT
FOR N85-100, 1.00" MIN-K 1301 INSULATION

Configuration N85-100   Insulation Min-K 22 lb/ft³   Thickness 1.00"

	Added Gas Temperature (°F)							
	-400	-300	-200	-100	0	+100	+200	-347
Exposed Tank Sidewall Weight	4560	5450	6290	7060	7720	8350	8910	5030
Sidewall Insulation Weight	21,868	21,868	21,868	21,868	21,868	21,868	21,868	21,868
Vented Gas Weight	0	0	0	0	0	0	0	0
Boil-off Gas Wt. at .100 lb/ft³	241	241	241	241	241	241	241	241
Added Pressurization Gas Weight	4882	1837	1121	798	624	517	437	2552
Heat Exchanger or Gas Bottle Weight	0	0	0	0	0	0	0	0
Optimizational Tank Weight	31,551	29,396	29,520	29,967	30,453	30,976	31,456	29,691

FIGURE 28
OPTIMIZATIONAL TANK WEIGHT VERSUS INSULATION THICKNESS
(N85-100, MIN-K 1301)

NOTE: Pressurization gas added at temperature equal to medium skin temperature due to aero heating. $(U_9$

.11 in.

12,210

Insulation Thickness (in)

Optimizational Tank Weight (1000 lb)
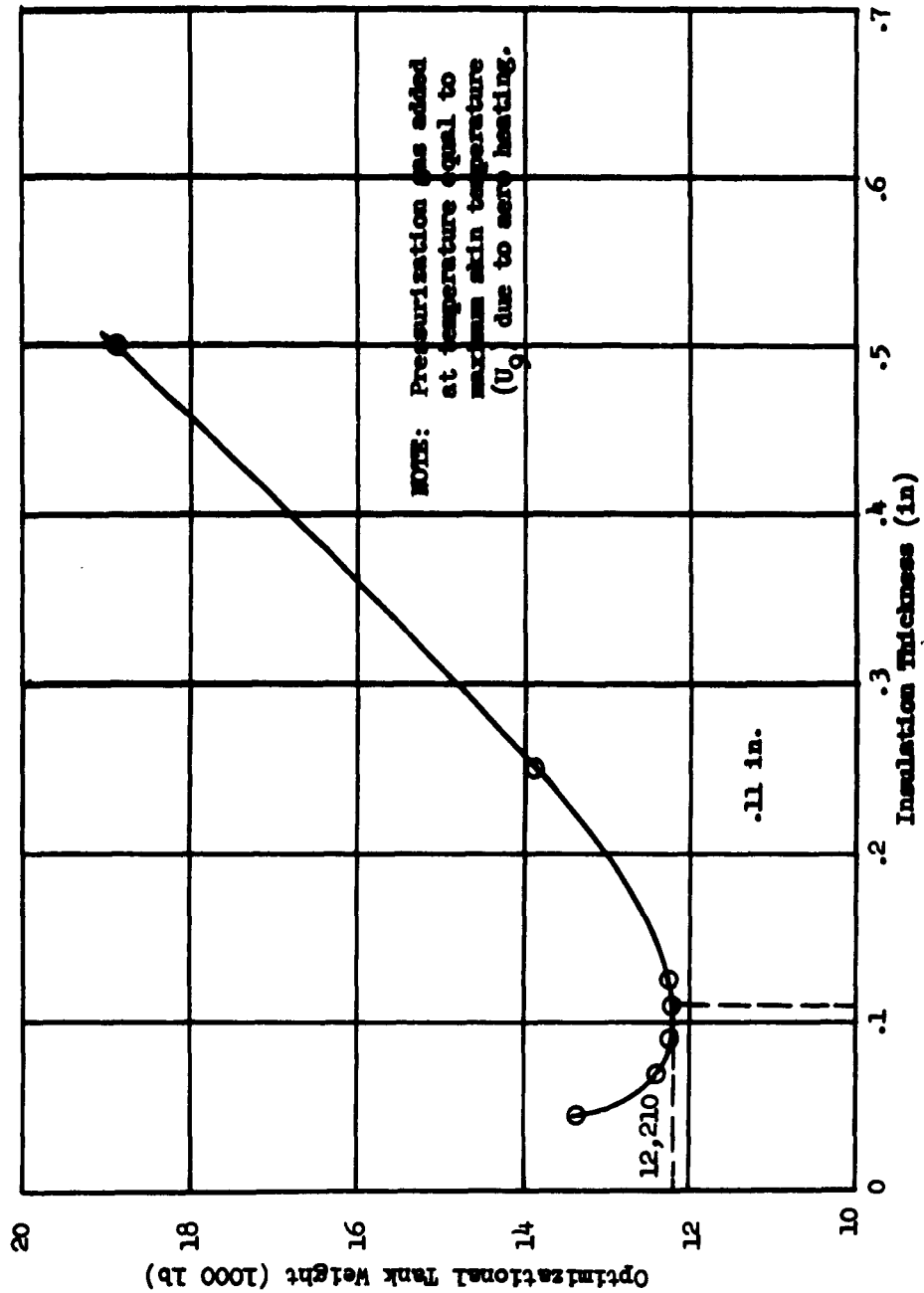
The inflection point of the curve shown in Figure 28 shows that for the N85-100 rocket vehicle configuration, using Min-K 1301 as the tank sidewall insulation, and a "thermal" thickness of .025" 6Al-4V annealed titanium alloy for the structural skin, the optimum insulation thickness is .11 inch. The optimizational tank weight based on this thickness is 12,210 lbs.

Further examination of the tabulated results shows that an additional weight saving could be achieved if the added pressurization gas could be at a lower temperature than that which was equal to the maximum skin temperature (U_9) at the uppermost tank station. By cross-plotting the tabulated oprimizational tank weight against added pressurization gas temperature and with insulation thickness as the parameter, a family of curves as shown in Figure 29 was obtained. The shaded points of each thickness curve indicate the added gas temperature which is equal to the maximum U_9 temperature for that particular thickness of insulation.

A curve drawn through these shaded points in effect duplicates the plot shown on Figure 28. An analysis of Figure 29 indicates that a weight saving could be realized if the added gas were at a temperature of -280°F instead of -66°F as dictated by the first approximation. Likewise, it would appear that the optimum insulation thickness would occur at .07 inch instead of the .11 inch. This weight savings and/or change in optimum insulation thickness would occur only if it could be established that the colder added gas would, in effect, "refrigerate" the metallic skin in the areas where the skin would tend to become warmer than the added gas as a result of aerodynamic heating. Until suitable film transfer coefficients of cold hydrogen vapor to the wall in question can be experimentally determined in the heat tower tests, the optimum insulation thickness for this type of configuration and insulation shall be considered to lay in a range from .07 to .11 inch and the temperature of the added pressurization gas shall occur between -66 and -280°F.

It appears that the added gas temperature has greater influence on the optimization weight than does the insulation thickness. This can be partially explained by the fact that the use of Min-K with its relatively high density and specific heat provides the tank with a thermal barrier which is in itself a formidable heat sink. Later computer solutions, in which a low density plastic foam was used as the sidewall insulation, revealed that this range of optimum conditions is greatly reduced and that the inflection points of the thickness and gas temperature curves occur approximately at the same point (Reference Figures 30, 32, and 33).

In addition to the N85-100 rocket vehicle configuration using Min-K 1301 as the sidewall insulation which is described above, the following combinations were analyzed in a similar manner:

N85-100 with 1.8 lb/ft.^{3} polystyrene plastic foam (Figure 30)
C85-100 (First stage) with Min-K 1301 (Figure 31)
C85-100 (First stage) with 1.8 lb/ft.^{3} polystyrene plastic foam (Figure 32)
C85-100 (First stage) with 4.0 lb/ft.^{3} polyurethane plastic foam (Figure 33)

FIGURE 29
OPTIMIZATIONAL TANK WEIGHT
VERSUS ADDED PRESSURIZATION GAS TEMPERATURE
(N85-100, MIN-K 1301)
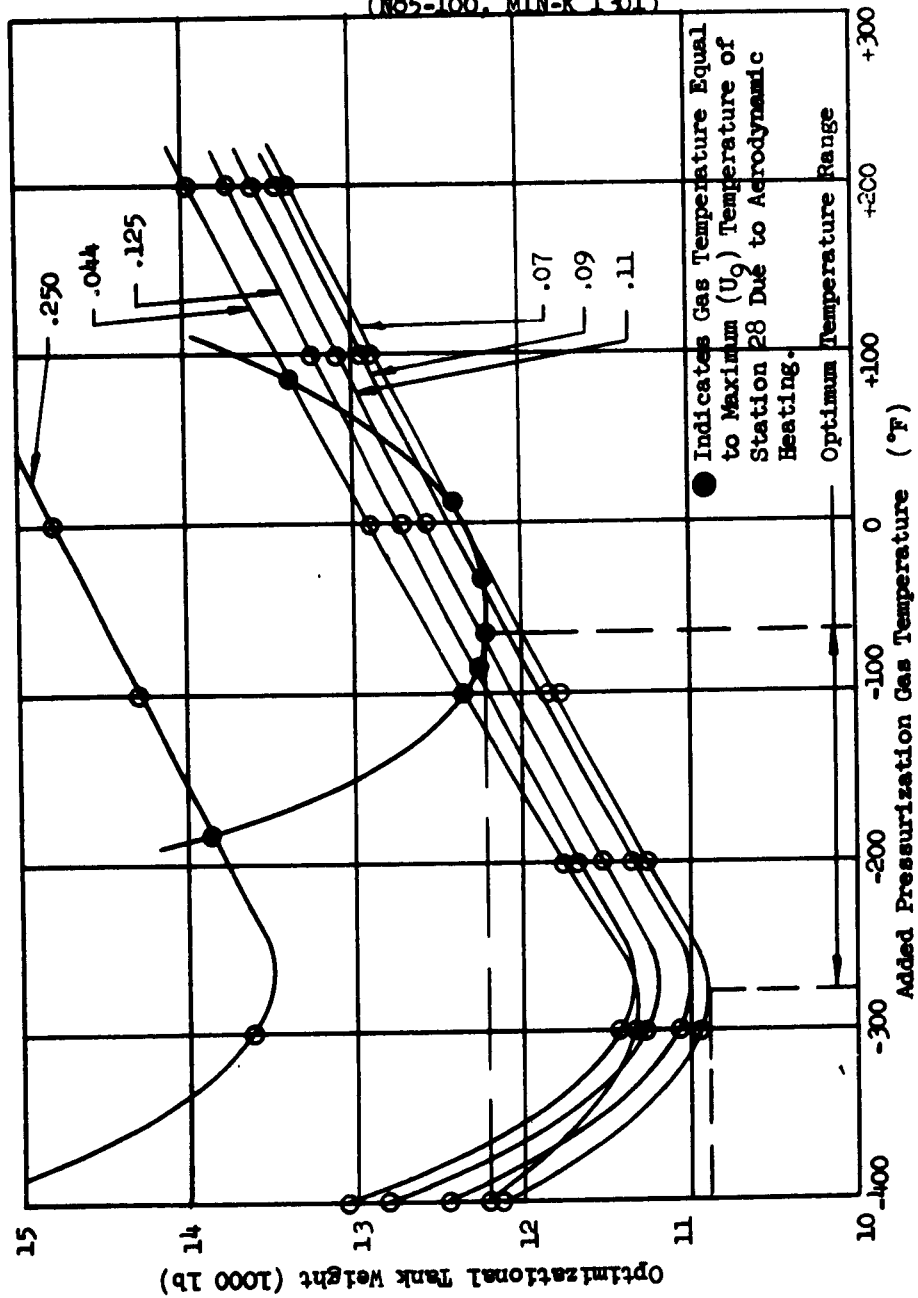
FIGURE 30
OPTIMIZATIONAL TANK WEIGHT
VERSUS ADDED PRESSURIZATION GAS TEMPERATURE
(X85-100, 1.8 lb/ft^3 POLYSTYRENE PLASTIC FOAM)
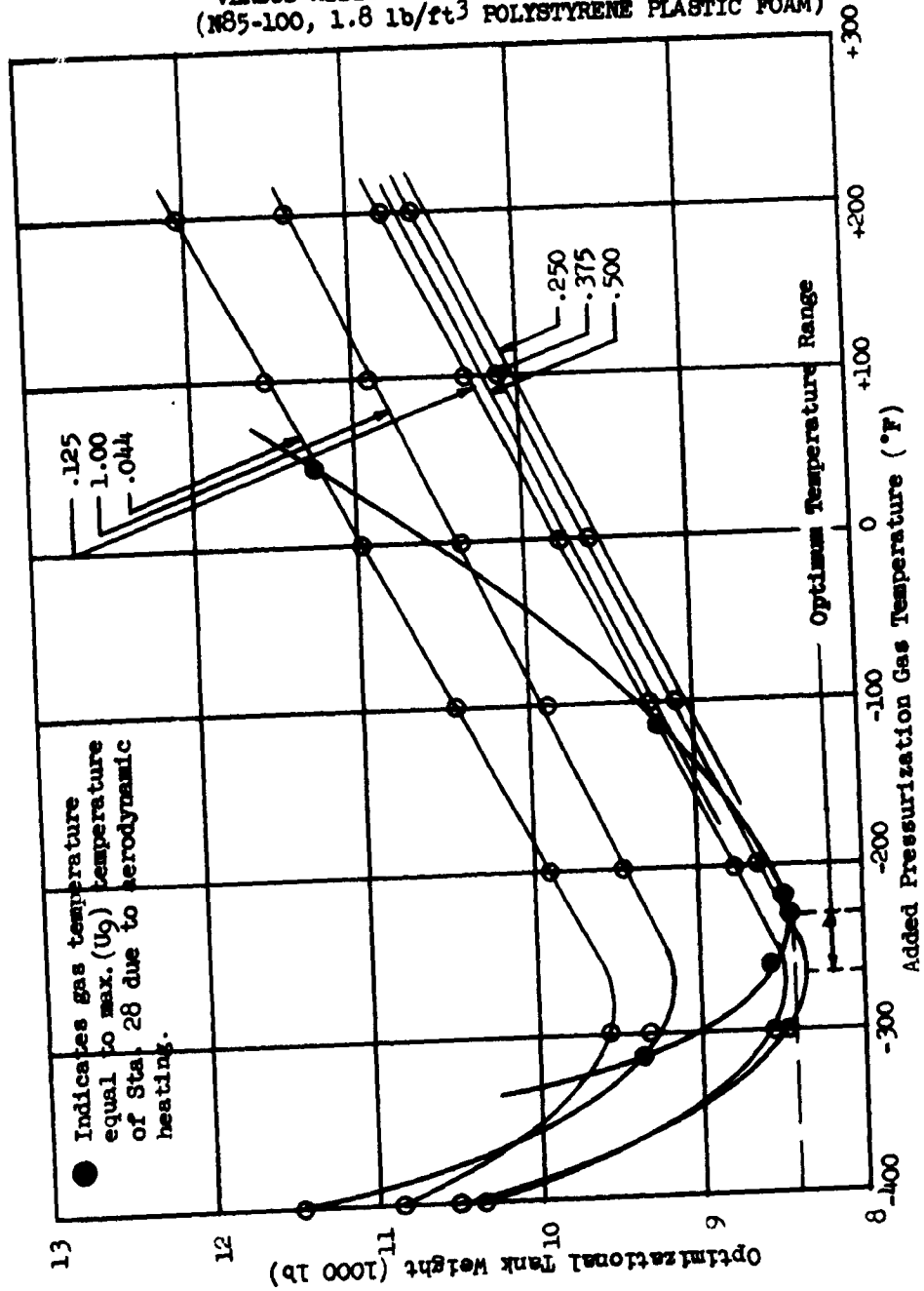
FIGURE 31
OPTIMIZATIONAL TANK WEIGHT
VERSUS ADDED PRESSURIZATION GAS TEMPERATURE
(C85-100, FIRST STAGE, MIN-K 1301)
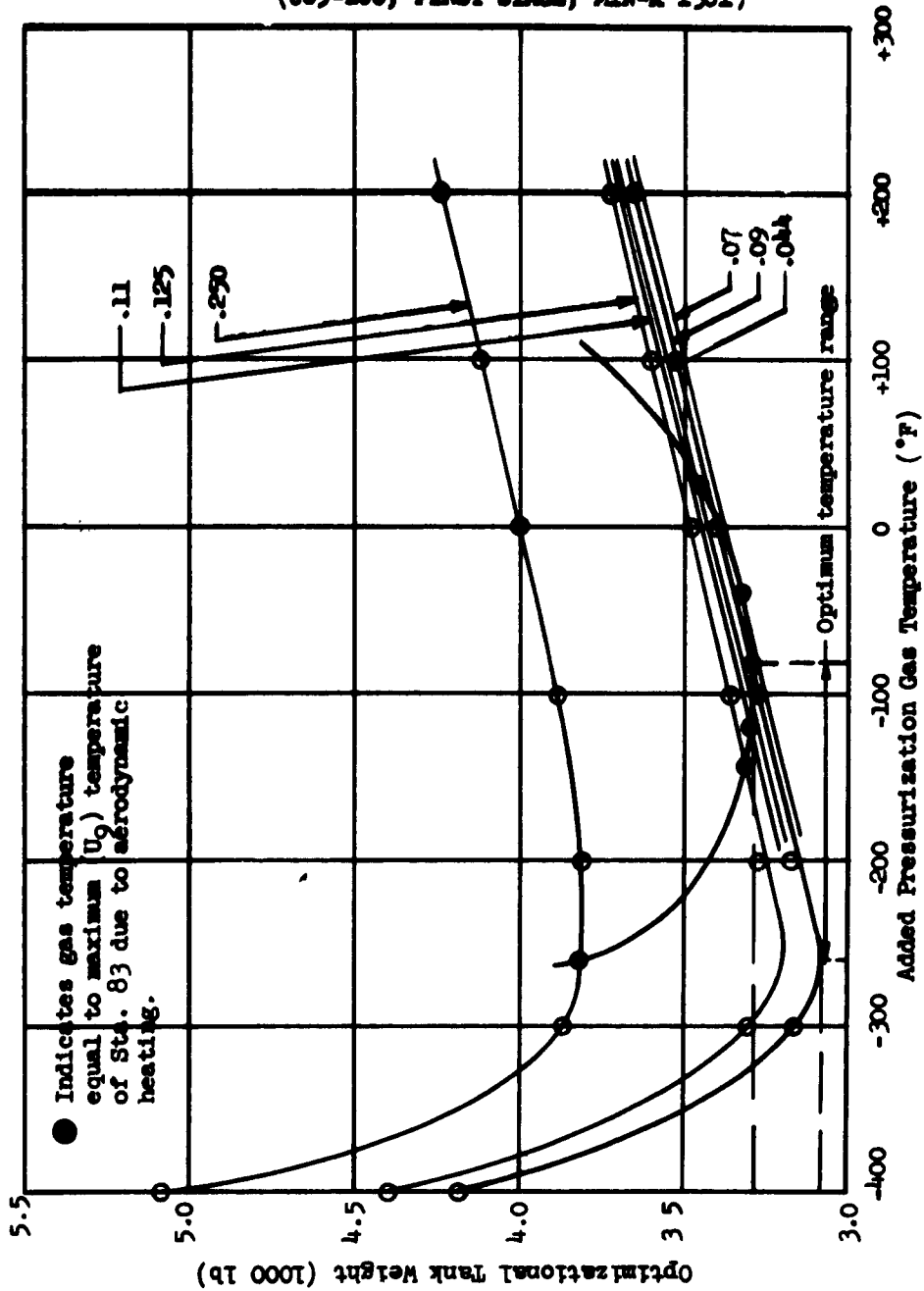
FIGURE 32
OPTIMIZATIONAL TANK WEIGHT
VERSUS ADDED PRESSURIZATION GAS TEMPERATURE
(C85-100, FIRST STAGE, 1.8 lb/ft^3 POLYSTYRENE PLASTIC FOAM)
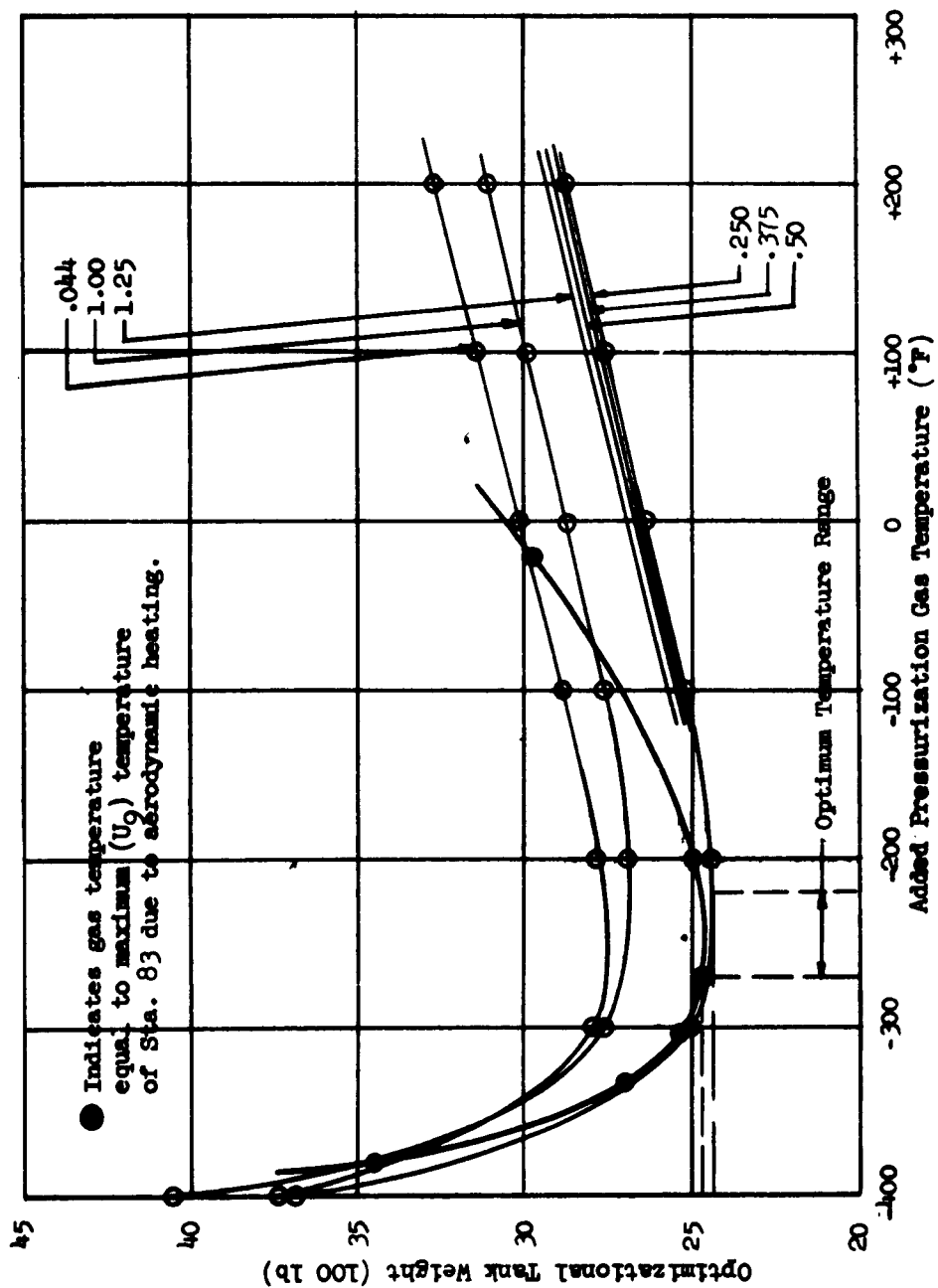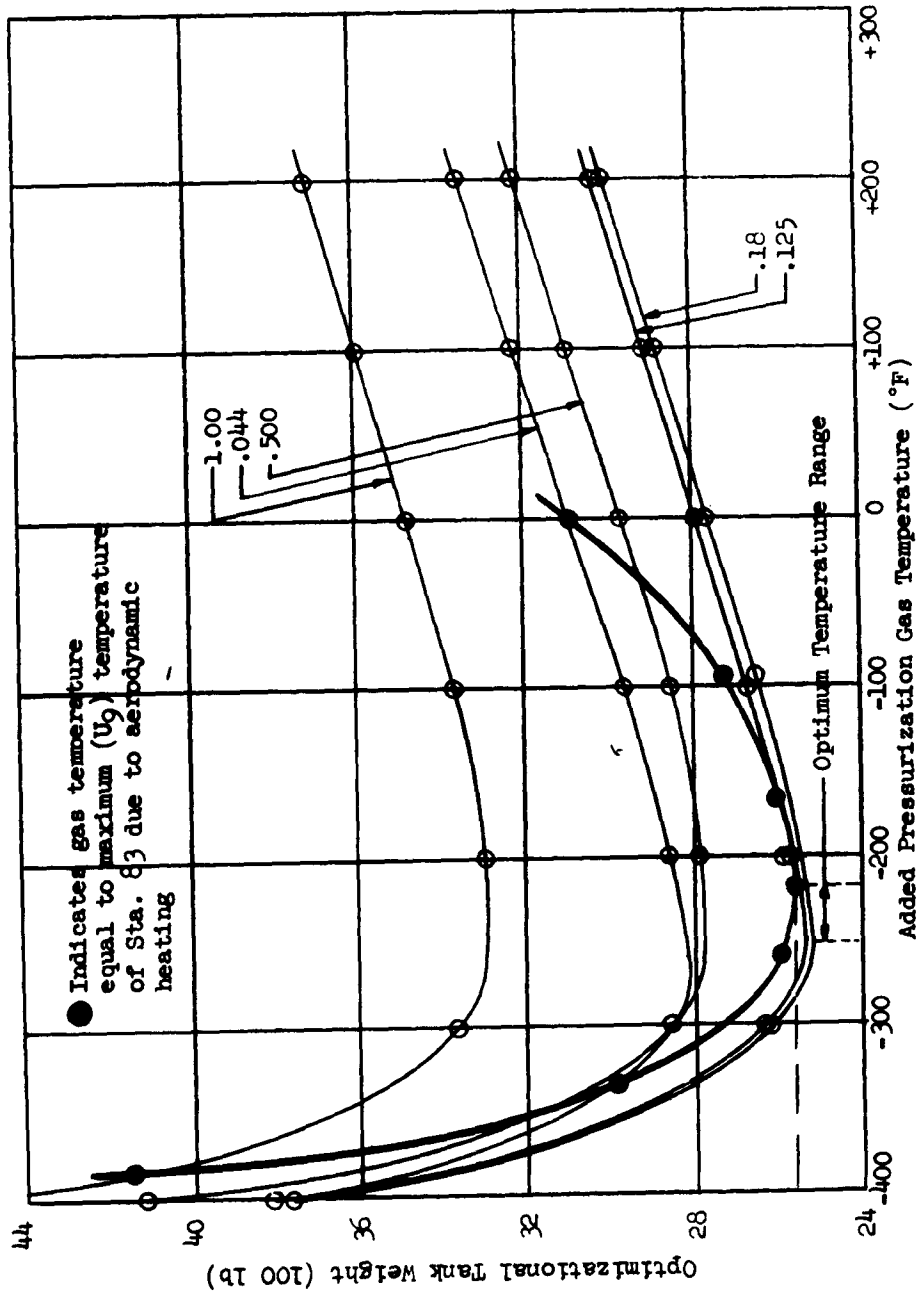
ADDED PRESSURIZATION GAS WEIGHT VERSUS INSULATION THICKNESS
(N85-100, MIN-K 1301)
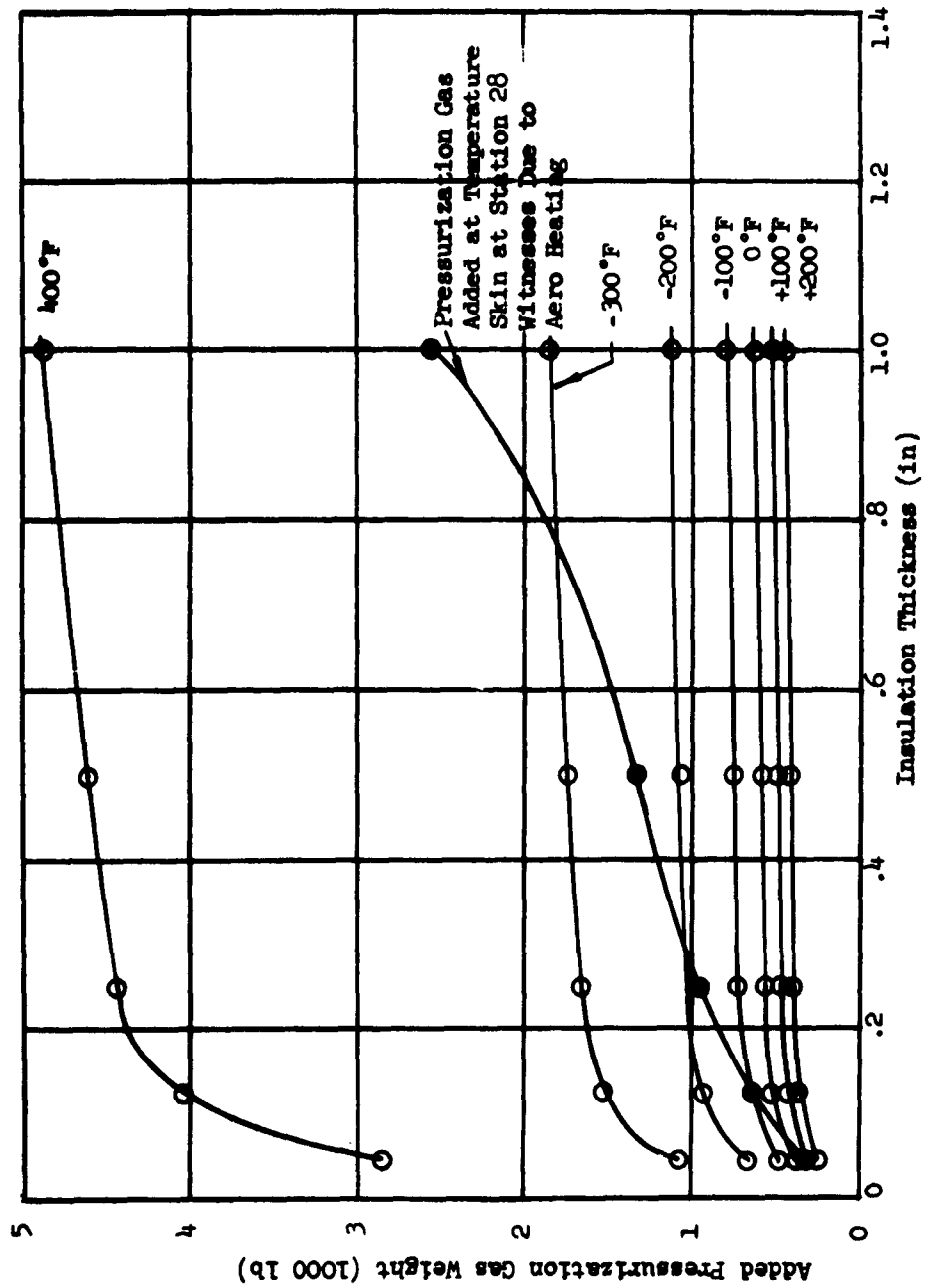
TABLE C
OPTIMIZATIONAL TANK WEIGHT COMPARISON

Configuration	Insulation Type and Mfgr.	Insulation Service Temperature Limit °F	Optimum Insulation Thickness in.	Maximum Insulation Temperature at Optimum Thickness °F	Maximum Insulation Thickness at Service Temperature Limit in.	Total Optimizational Tank Weight lb.
C85-100 First Stage	Min-K 1301 Johns-Manville	1300	.09	215	---	
	1.8 lb/ft³ Polystyrene Plastic Foam - Dow Chem.	170	.250	333 (This exceeds temp limits)	---	Theoretical ...
	"	170	---	---	.04 (This will not preclude liq. air formation)	Est ...
	4.0 lb/ft³ Polyurethane plastic foam. American Latex	360	.18	290	---	6,552
N85-100	Min-K 1301	1300	.11	115	---	12,210
	1.8 lb/ft³ Polystyrene Plastic Foam	170	.375	225 (This exceeds temp. limits)	---	Theoretical 8,414
	"	170	---	---	.15	8,900

FIGURE 34
MAXIMUM INSULATION TEMPERATURE
VERSUS INSULATION THICKNESS

FIGURE 34
MAXIMUM INSULATION TEMPERATURE
VERSUS INSULATION THICKNESS
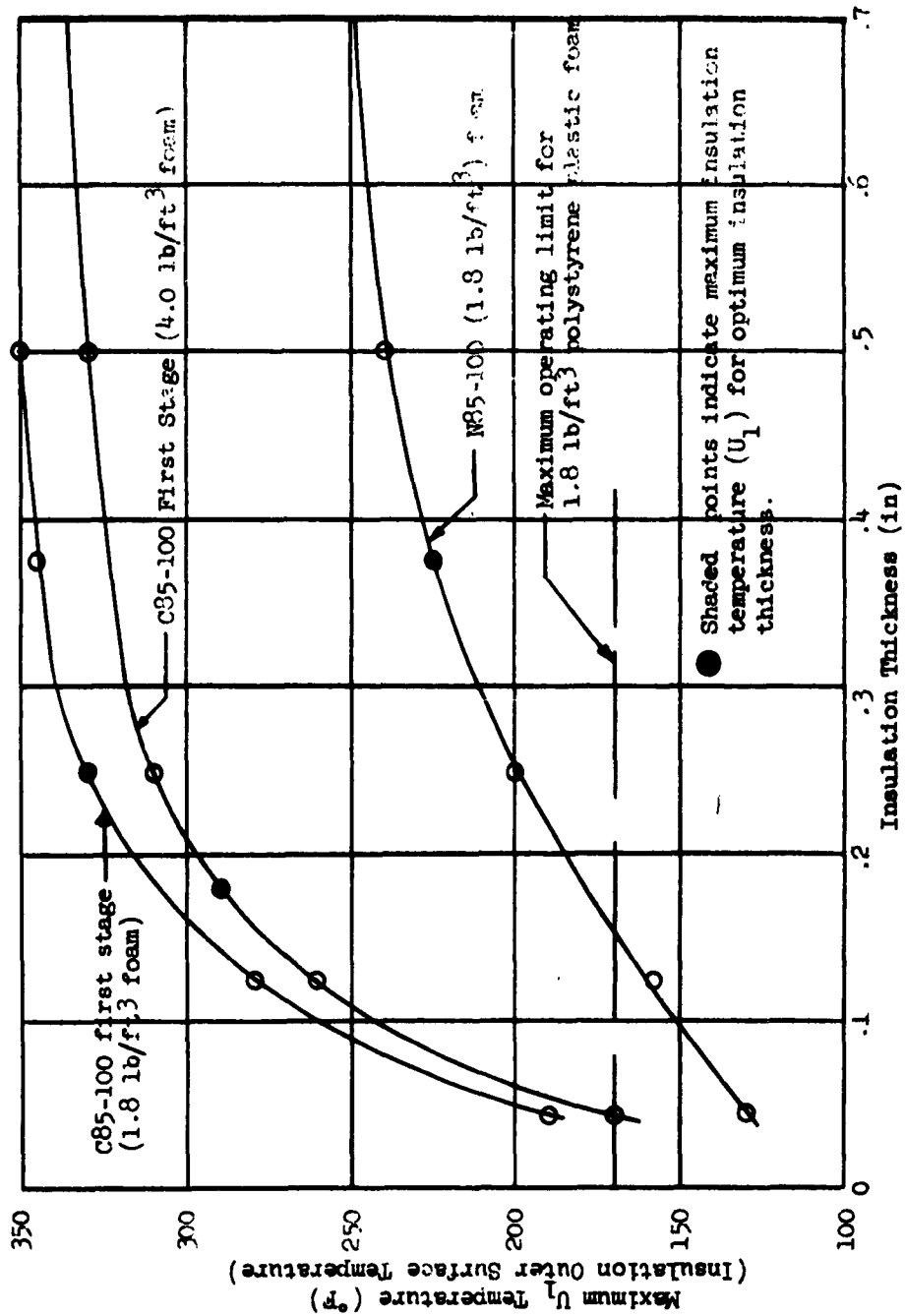
2.1.2.3 Tank End Insulation Design Considerations and Material Selection

As mentioned in earlier progress reports, the primary reason for the tank end insulation is to prevent the formation of ice and frost on the tank ends during the filling, standby, and hold operations.

The method used in determining the optimum insulation for this function has been fully described in WADC Technical Report 58-273. The results in this report have since been brought up to date with new experimental findings and are reported in WADC Technical Report 58-530.

Based on the results in these reports, the tank and insulation to be used on the test tank will be a rigid polyurethane plastic foam with a 2 lb/ft.^{3} density. The specific formulation is called Stafoam C-02, and is made by the Dayton Rubber Company. This foam, when evacuated to an indicated pressure of less than one (1) micron, has an apparent mean thermal conductivity between room temperature and liquid hydrogen temperature of .048 BTU-in/hr-ft.^{2}-°F.

This value has been multiplied by a factor of 1.5 to account for variances in the operating requirements of the insulation and to include any experimental errors that may have been in the original research work. Based on this, the required thickness for the upper tank end is 2.00 inches, while the thickness for the lower end is 1.25 inches.

Preliminary cost studies have been made on various methods of applying the insulation on the tank ends. For a program of this magnitude, where only a few tanks are involved, the high cost of molded segments does not appear to be warranted. A simple, less expensive, method has been devised and is described in the following paragraphs.

The liquid (resin, and catalyst) components will be procured from the manufacturer, mixed in suitable foam-making machinery, and poured into a simple, low-cost open mold. This mold will produce foamed boards of the required thickness and trapizoidal in shape. A total of sixteen (16) such boards will be required for each end of the tank. To gain the flexibility needed to bend these foamed segments to the contour of the tank ends, it is planned to make saw kerfs approximately 1/8" wide and on a 1-1/2" grid pattern into one side of the board. These kerfs will be deep enough to leave approximately a 1/4" web remaining. The boards will then be formed over a plaster mockup of the tank end, and trimmed to the proper gore-shaped pattern.

The individual gores will be positioned on the tank end and spot cemented into the titanium head. When all of the segments are attached in place the entire surface will be sprayed with an encapsulating latex membrane. Suitable vacuum taps will be placed into the foamed ends to facilitate the evacuation process.

The saw kerfs described above will be beneficial in the evacuation of the foam by providing escape paths for the residual gas in the foam cells. Likewise, the saw kerfs will help reduce the problem of differential contraction between the foam and the titanium that will occur with changing temperatures.

The wedge-shaped volume between the tank skirts and the tank ends (Reference Figure 23) will be filled up with a pour-in-place plastic foam. This foam will allow a vacuum to be achieved in this area without danger of collapsing the skirt walls.

The insulation will be procured in a tile form measuring 18 inches by 18 inches and molded to the radius of the test tank. It is intended at this time, that the tiles will be·spot cemented to the titanium sidewall with a suitable low temperature, epoxy type, adhesive. The entire exterior surface of the insulation will then be covered by a Mylar cylinder which will be closed off on either end by cementing the Mylar to the tank skirts. The Mylar covering will prevent cryogenic pumping of condensible gases through the porous Min-K. A suitable vacuum tap extending into the sidewall insulation will be provided to allow evacuation of the Min-K (Reference Figure 23).

The use of vacuum inconjunction with the Min-K is not only desirable from a thermal standpoint, but is also necessary in order to keep the Mylar envelope from "ballooning out" when the atmospheric pressure is reduced.

2.2 Reporting Period June 15, 1960, to December 31, 1960

The following section will discuss the progress made during this period.

2.2.1 Tank Structural Design

All structural stress analysis work has been completed including the computer reruns which are described in paragraph 2.1.2, E.R. 8129.

2.2.2 Tank Fabrication Progress

The fabrication progress of the titanium tank is described in the following section (see Engineering Report 8702 for identification of sections and subassemblies).

2.2.2.1 Hemispherical Heads

The head assemblies had been completed with the exception of welding in the reinforcing splice fittings. Some rework was necessary on the forward head due to cracks in the weld around the manhole cover. The repair of the cracks had been accomplished, and the heads ready for attaching to other subassemblies. It might be noted that some welds in the head had marginal areas as to porosity and thin-out. However, if good quality welds were achieved in the remainder of the assembly, the integrity of the final assembly would be sufficient for the testing purposes intended.

The joining of the 90° cone and hemispherical head section was attempted. However, the tooling proved to be inadequate to hold the material down properly while welding. It was necessary to do minor rework of the tooling in an effort to improve the hold-down features. The efforts to make the circumferential welds joining the subassemblies together was contined. However, the work was plagued with problems resulting from inadequate tooling. As a result, the circumferential welds were of a poor quality and not acceptable, particularly in view of the questionable areas in the heads already mentioned.

2.3 <u>Reporting Period May 8, 1961, to July 31, 1961</u>

The following subsections will be devoted to describing the work progress during this period:

      (a) Tank Structural Design
      (b) Tank Fabrication Progress.

      2.3.1 <u>Tank Structural Design</u>

During this period the upper and lower hemispherical heads were redesigned in an effort to solve the problems as set forth in previous reports in making the circumferential welds joining the subassemblies and also improve the quality of welds joining the head segments. A major change in fabrication of the head segments has been incorporated in the design. This change calls for hot stretch forming of the head segments from .032 titanium material followed by chemical milling to remove the excess material down to .018 where the thicker section is not desirable. The advantages of this process are as follows:

      (1) Provide weld lands around the perimeter of each segment .032 thick by .75 wide. This thicker weld section greatly improved hold-down characteristics and provided a greater heat sink for the actual welding. The use of more heat in the welding process eliminated, for the most part, the problem of porosity encountered previously.

      (2) The reinforcing splice bands that were previously welded into the heads were eliminated. The reinforcement now is an integral part of the segment material, thus eliminating two welds and the corresponding fit-up and trim operations.

      (3) Provide thicker weld lands for attaching the manhole ring, and instrumentation port rings. This essentially eliminated the problem of the skin wrinkling in the weld area as was experienced before.

Figure 35 shows the new concept as it appeared at final assembly. Although a small amount of additional weight was added by this approach, the advantages gained in the fabrication process more than offset the penalty in weight for the particular application. It is believed that the original concept would be feasible for a flight article with adequate tooling.

FIGURE 35
SKETCH OF NEW HEAD CONCEPT

Chem-Milled Areas

Weld Land for Port Fittings

Reinforcing Band

Weld Land
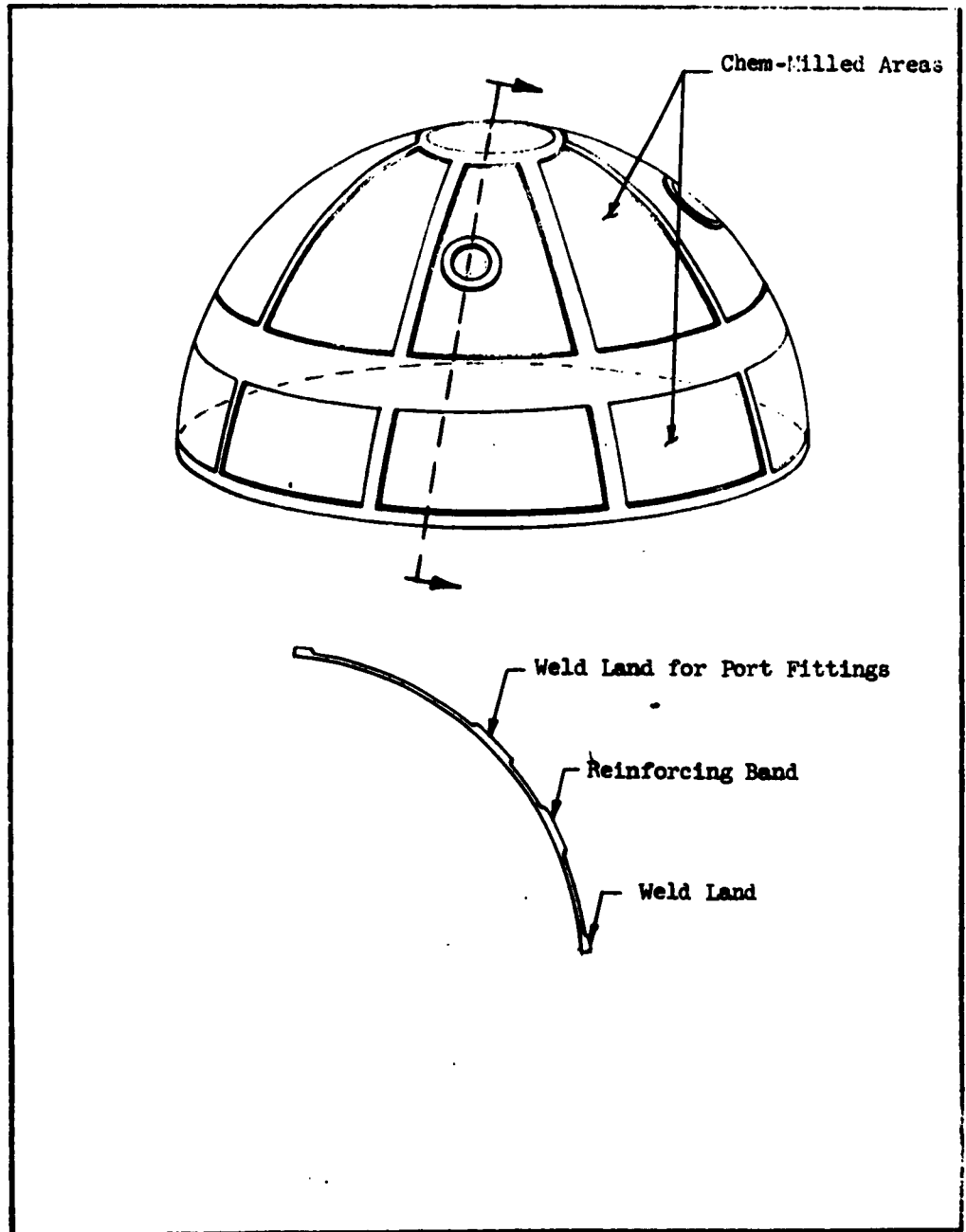
2.3.1.1 Thermal

The insulation concept used on the titanium test tank was the same as the installation that was used on the stainless steel test tank. This concept is described in detail (in paragraph 1.3.2).

2.3.2 Tank Fabrication Progress

The following subsections will be devoted to describing the progress made on the titanium test tank during the period stated above.

2.3.2.1 Cylinder Sections

The cylinder sections were complete except for final trim and closure weld and were still in storage. These sections were in good condition and ready for final assembly.

2.3.2.2 Hemispherical Heads

Some difficulty was encountered initially in forming the head skins. One head skin parted during the stretch operation and was not salvable. Two other skins also parted, but in such a manner that they can be salvaged. Two extra sheets of material were ordered so sufficient material would be on hand in case further difficulties were encountered in forming.

Welding of the head skins into pairs was commenced. Eight skins of the lower head were welded into pairs of four. The weld X-ray examinations showed good quality and the welding in general was excellent. The ninth skin was refabricated because of wrinkles which appeared in the skin.

Sufficient skins were fabricated and received for the upper head. Prior to welding the skins into pairs, the instrumentation and vent port rings were welded into the individual segments.

2.3.2.3 Hemisphere-to-Cylinder Splice Fittings

Both of these fittings were complete. However, they needed to be re-trimmed to match the new design of the heads, this was performed after the heads were completed and final assembly begun.

2.3.2.4 Miscellaneous Parts

The drain assembly was attached to the 90° cone assembly. The drain adapter was completed and ready for bolting in place at final assembly. The manhole ring, instrumentation rings, and vent rings were removed from the old head and retrimmed for installation in the new head. A new manhole cover plate was fabricated by the chemical milling process to eliminate the need of welding the flange and cover skin. This welding of the thin circular cover skin to the attaching flange was extremely difficult and resulted in a poor quality weld. The cover plate was fabricated to contour from a single piece of material.

2.4 Reporting Period August 1, 1961, to October 31, 1961

The following sections will be devoted to describing the work progress during
this period.

2.4.1 Tank Fabrication Progress

Fabrication of the titanium tank had proceeded very satisfactorily. No criti-
cal problems were encountered. This can be attributed to refined tooling and
the knowledge gained through experience in handling thin section titanium and
its welding. The following subsections will describe the status and the pro-
gress made on each tank component.

2.4.1.1 Manhole Cover Plate

The new approach in fabricating the cover plate proved very satisfactory.
The cover plate was completed except for the drilling of the bolt hole pat-
tern. The combination forming and chemical milling operation produced a
very good contoured cover from a single piece of material, thereby elimin-
ating the need for any welding operation. Figure 36 shows the cover plate
as received from the chemical milling operation prior to drilling the bolt
holes.

2.4.1.2 Forward Head Assembly

Fabrication of the forward head was completed. The assembly was 100 percent
X-ray examined and the welding is of excellent quality. The weld seams are
flat, of uniform width, and have a bright metallic color with no evidence of
discoloration, even in the area adjacent to the hold-downs. All evidence
points to adequate, complete argon coverage, thereby eliminating hydrogen
contamination. Figure 37 shows a close-up of the type of weld seam obtained
compared with Figure 38 and 39. The absence of porosity and color shading
of weld area is evidence of advancement of the welding techniques gained
from experience.

Figure 40 shows the flush installation of one of the two port rings in the
forward head. Figures 41 through 43 show the forward head less manhole,
setup for the manhole ring installation, and the completed forward head.

2.4.1.3 Aft Hemisphere Head Section

Fabrication of this section is complete. The weld seams were all 100 per-
cent X-ray examined and found to be excellent. The weld quality was the
same as described above. The aft hemisphere section was ready for final
trim and assembly to 90° cone section. (See Figure 44).

FIGURE 36
PHOTOGRAPH OF MANHOLE COVER PLATE

FIGURE 37

TYPICAL CHEM-MILLED AREA WITH
LAND WELD SEAM
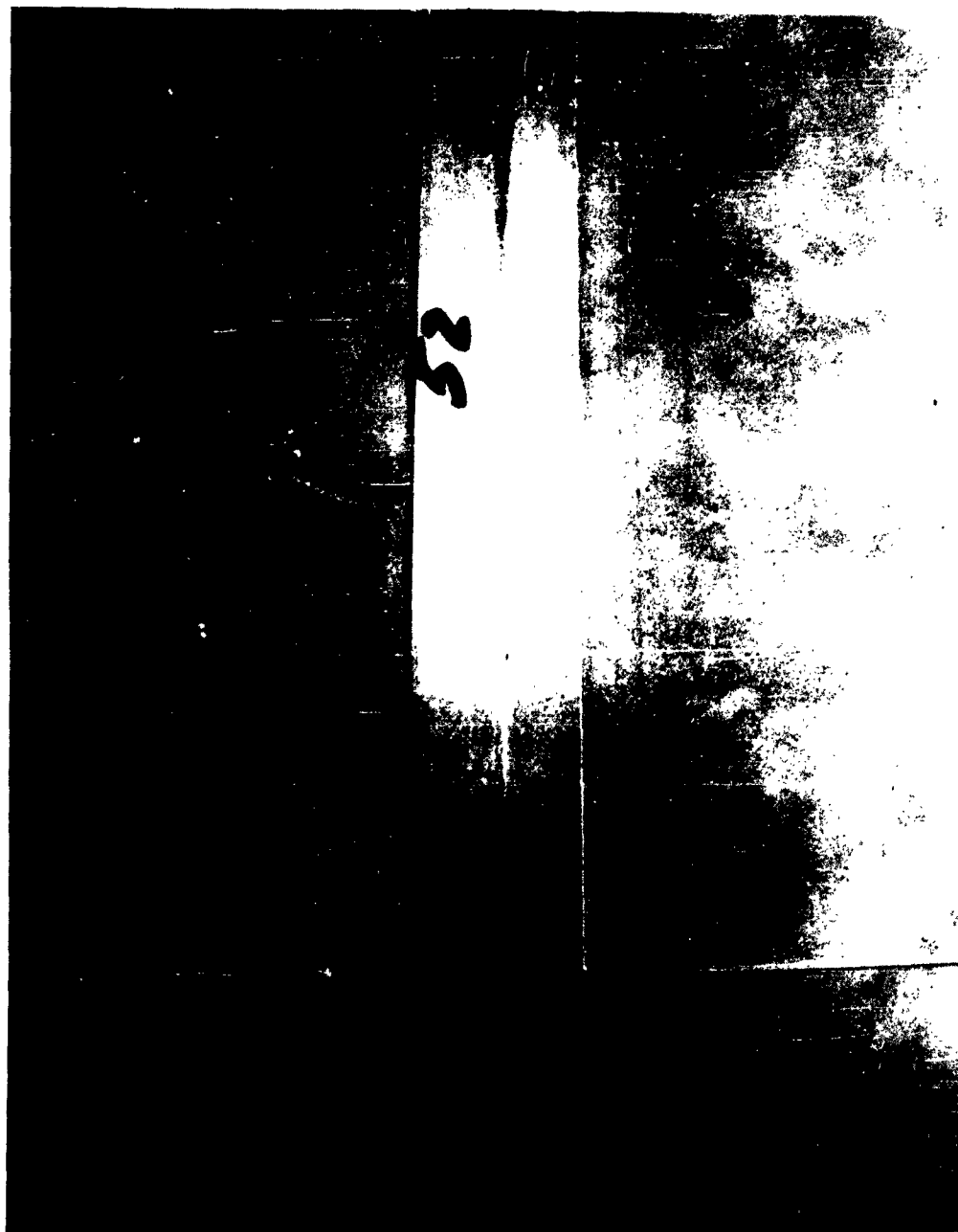
FIGURE 38
PHOTOGRAPH OF X-RAY FILM SHOWING POOR
QUALITY OF WELD OBTAINED DURING INITIAL DEVELOPMENT

FIGURE 39
PHOTOGRAPH OF X-RAY FILM SHOWING GOOD QUALITY
WELD IN COMPLETED TANK

FIGURE 40
PHOTOGRAPH OF FLUSH PORT RING INSTALLATION
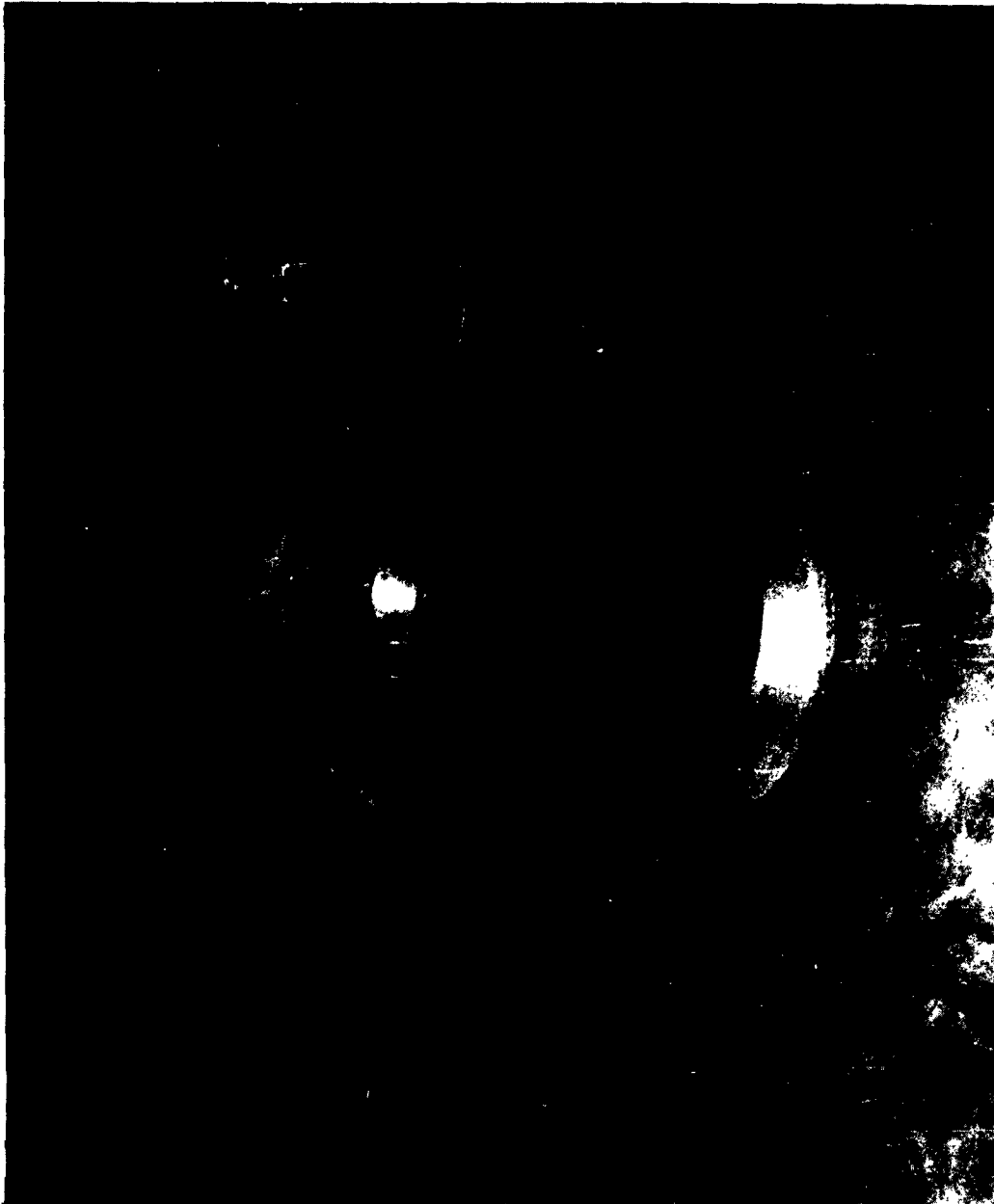
FIGURE 41
PHOTOGRAPH OF FORWARD HEAD ASSEMBLY LESS MANHOLE RING
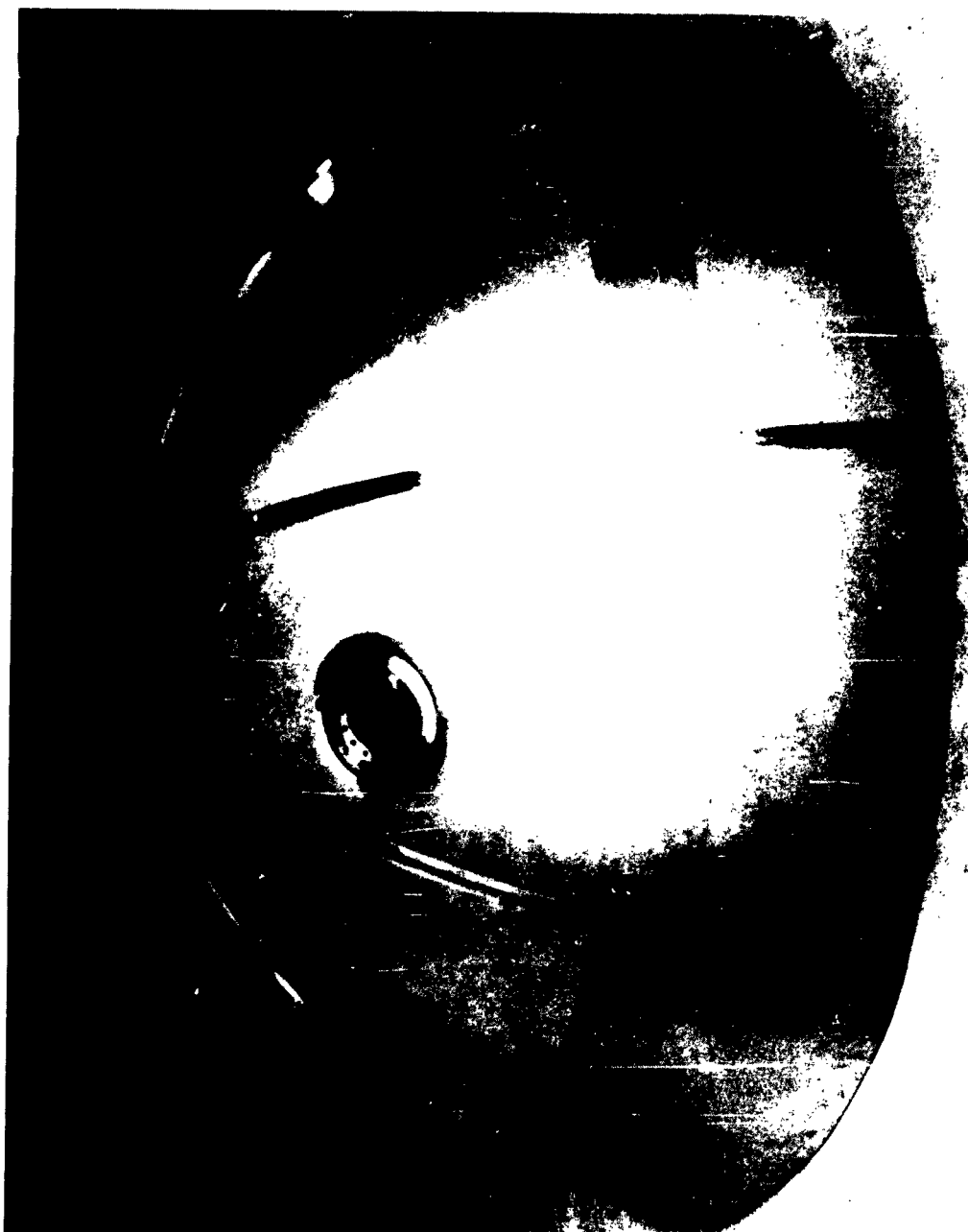
FIGURE 42
PHOTOGRAPH OF SETUP FOR WELDING MANHOLE RING
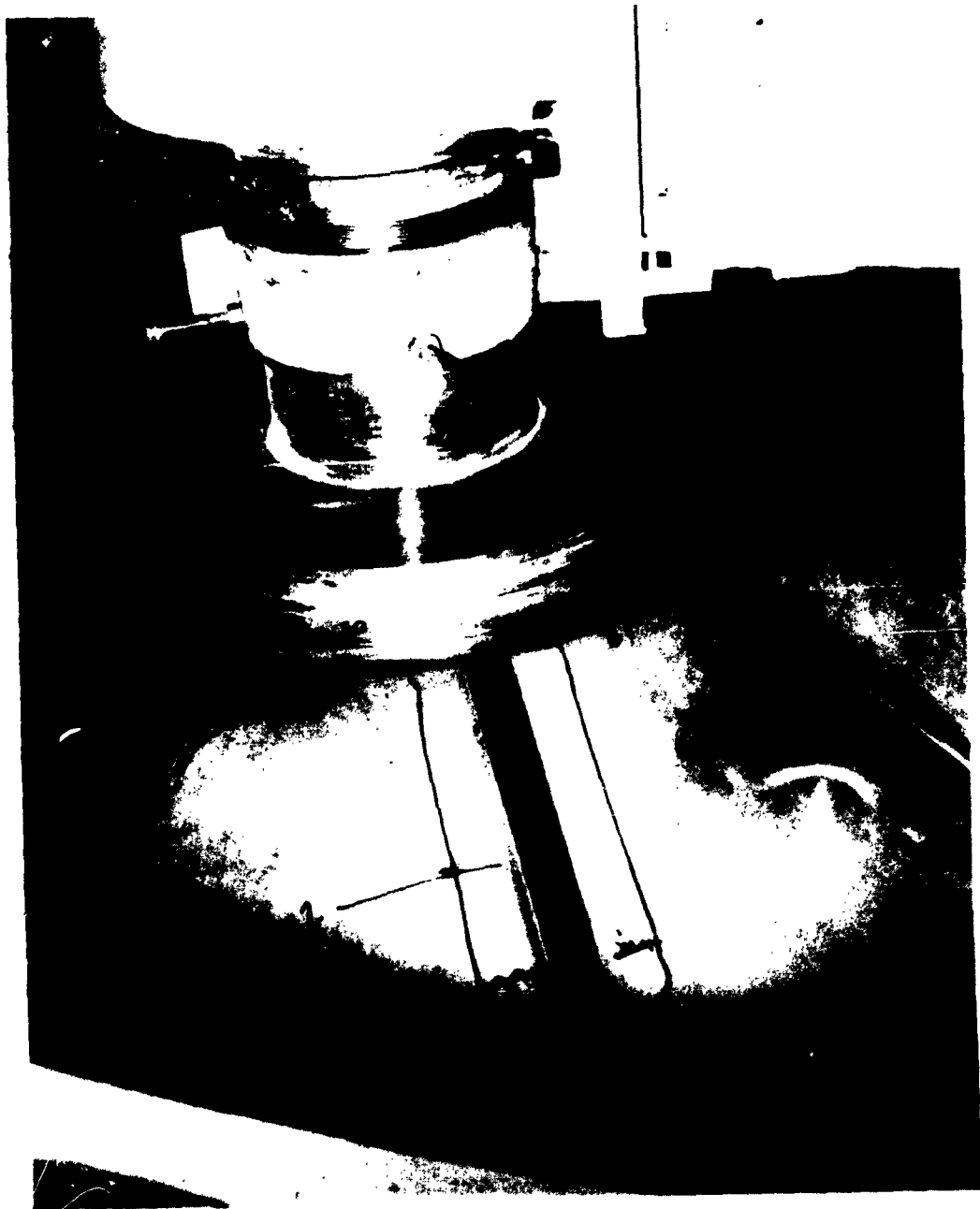
2.4.1.4 90° Cone Section

During this period, the cone was examined again for defects and found to be good. It was now ready for final trim and assembly to aft hemisphere section. Figure 45 shows the 90° cone complete except for final trim.

2.4.1.5 Tank Assembly

Final assembly of the titanium test tank was started during this period and proceeded in a satisfactory manner. The sequence of assembly was as follows:

(a) Joining the aft hemisphere head section to the 90° cone section was performed using the vertical pit welder. To insure a good weld, some refining was necessary to the tooling fixture and hold-downs. Careful attention was given the fit-up operation until a perfect fit between the work and tool was accomplished. This attention to detail resulted in an excellent weld without encountering any difficulties. X-ray examination of the joint revealed no bad areas and the seam was accepted as good. (See Figure 46)

(b) Next step was joining the forward head assembly to the transition splice band. This was accomplished on the horizontal lathe welder. Two operations were accomplished on the lathe. First, the sections were trimmed to print dimensions and then the weld joint was made. Both these operations were performed and the assembly was ready for the skirt. X-ray of the seam was not made until the skirt was attached to that both seams could be shot at the same time. (See Figures 47 and 48)

(c) After welding the head and splice band, the skirt was added. The skirt was fitted to a shoulder machined into the splice band. Careful attention was given to the fit of these two parts. This resulted in a good seam with no wrinkling or "cans" being pulled into the skirt cylinder. After the skirt was attached, the two welds were 100 percent X-rayed. Visual examination of the welds indicated good quality.

(d) The final operation performed to produce a completed half tank was to join the forward head assembly and forward cylinder section. Figure 49 shows the welding of the cylinder section to the forward head assembly. Figures 50 and 51 show the forward half of the titanium tank complete except for the final cylinder trim prior to joining the two tank halves.

2.5 Reporting Period November 1, 1961, to January 31, 1962

The following section will be devoted to describing the work progress during this period.

2.5.1 Tank Fabrication Progress

During this period, assembly of the aft half of the tank was begun. The sequence of assembly was as follows:

FIGURE 44
PHOTOGRAPH OF COMPLETED AFT HEMISPHERICAL ASSEMBLY
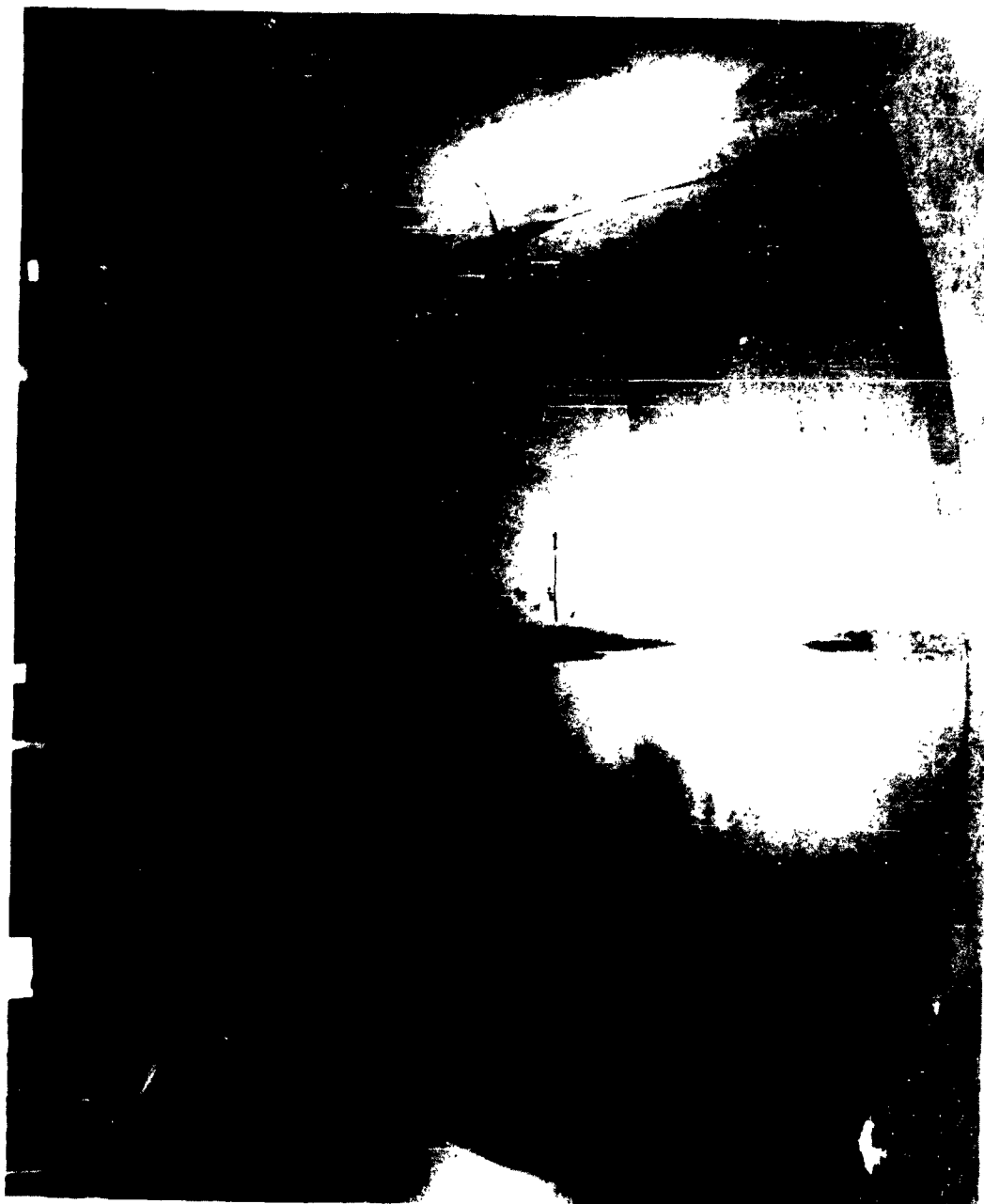
PHOTOGRAPH OF COMPLETED AFT CONICAL ASSEMBLY
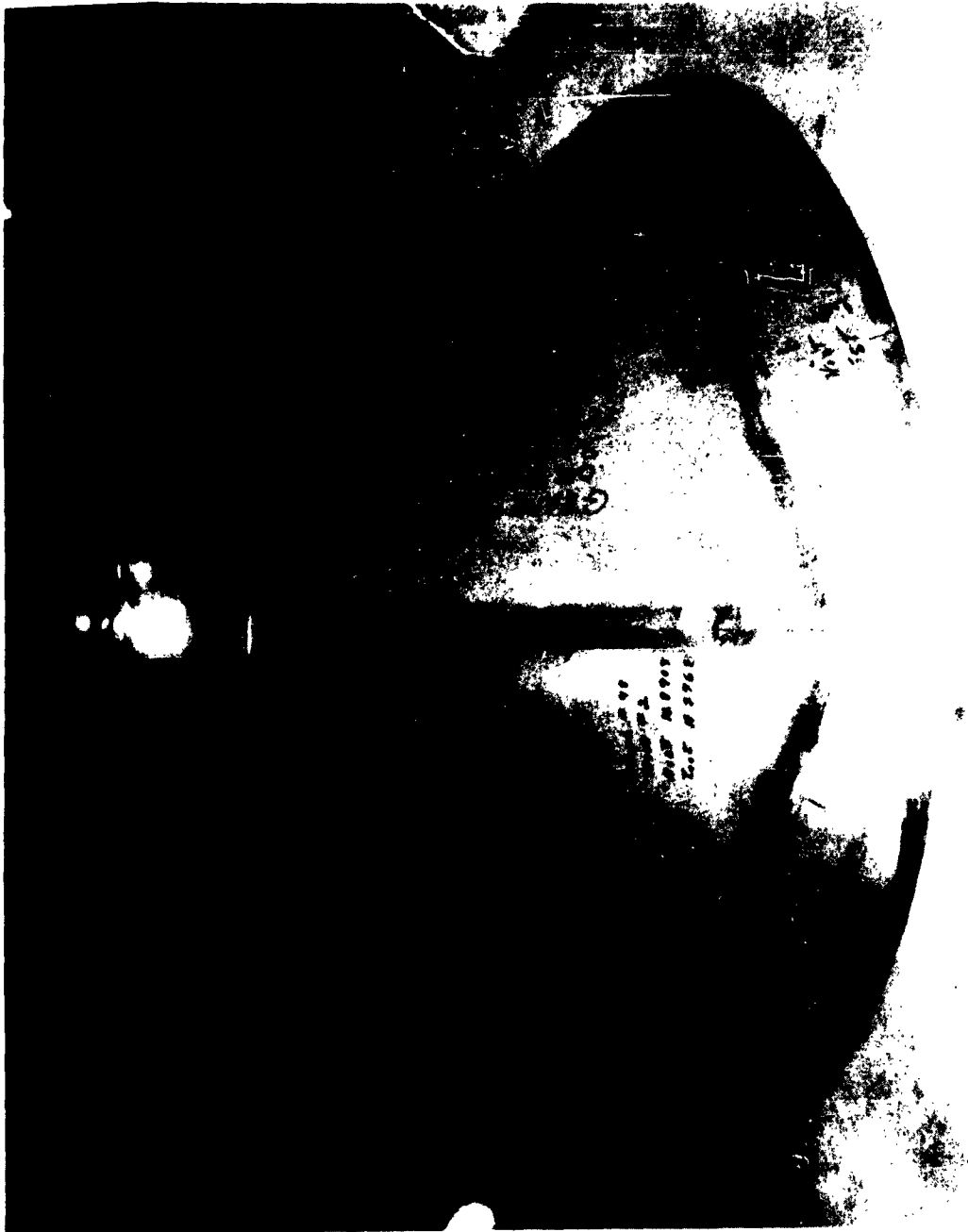
FIGURE 46
PHOTOGRAPH OF COMPLETED AFT HEAD ASSEMBLY

FIGURE 47
MATING OF A SKIRT ASSEMBLY TO A HEMISPHERICAL HEAD ASSEMBLY FOR
A 6A1-4V TITANIUM LIQUID HYDROGEN TANK

FIGURE 48
PHOTOGRAPH OF WELDING OPERATION JOINING
SPLICE BAND TO FORWARD HEAD
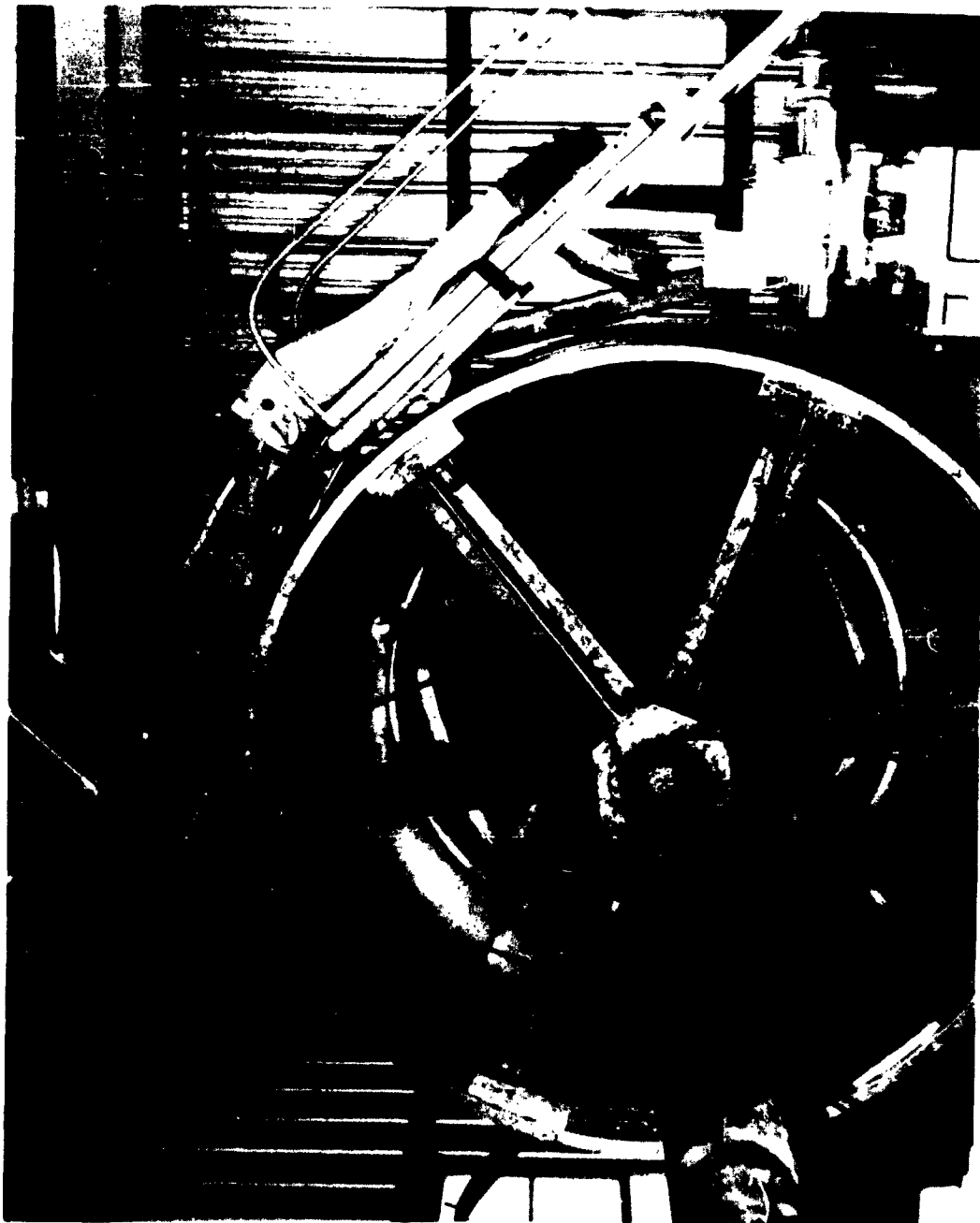
FIGURE 49
PHOTOGRAPH OF WELDING OPERATION JOINING
CYLINDER SECTION TO FORWARD HEAD

FIGURE 50
PHOTOGRAPH OF COMPLETED FORWARD HALF TANK

FIGURE 51
PHOTOGRAPH OF INTERIOR OF COMPLETED FORWARD HALF TANK
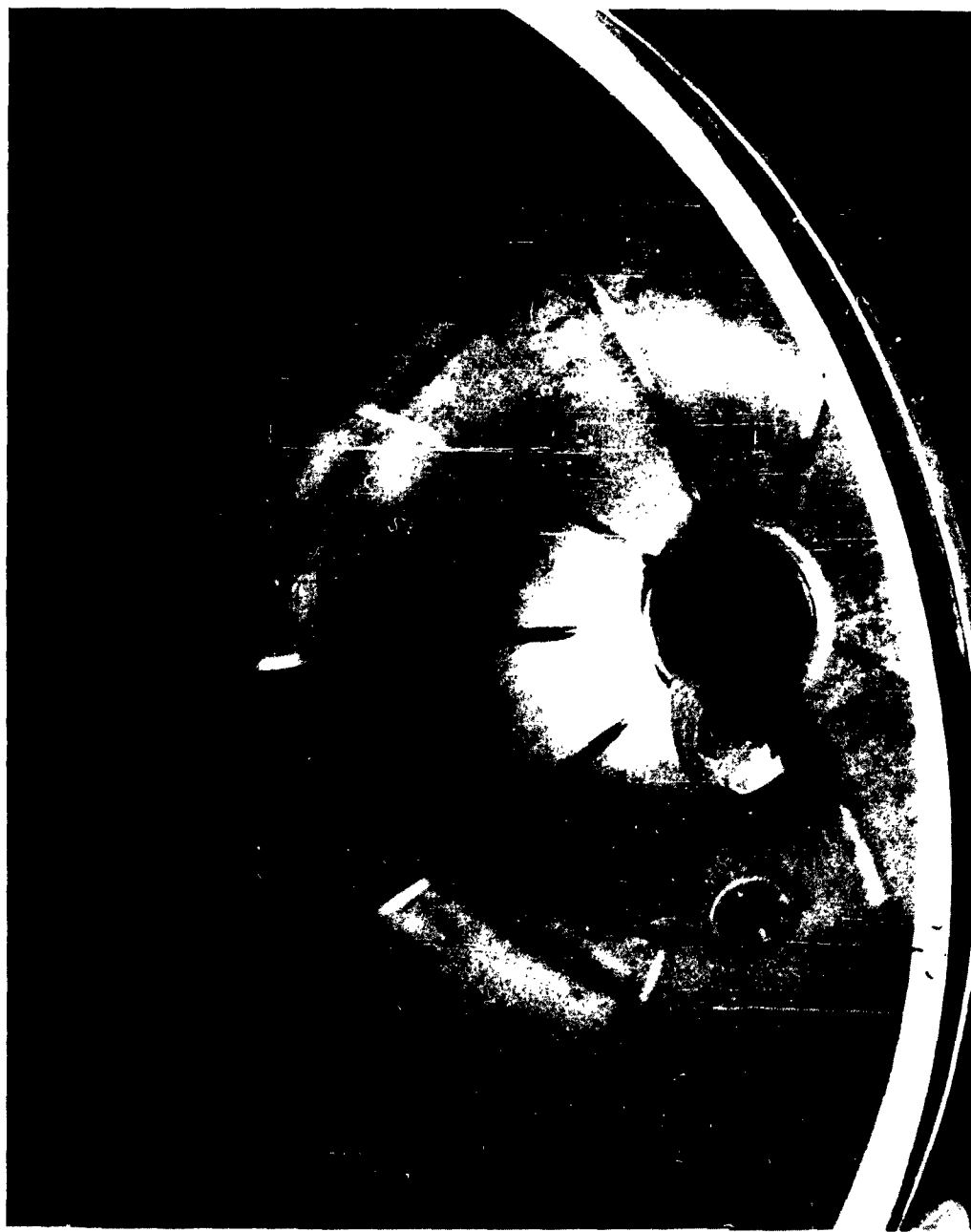
(a) The completed aft head assembly was mounted on the horizontal lathe and trimmed. The transition band that joins the head to cylinder was then trimmed to match the head and fitted together for welding. With careful attention given to the fitting operation, the welding proceeded without difficulty resulting in a satisfactory joint.

(b) After completing the splice band and head weld, the aft skirt was fitted to the shoulder machined into the splice band. The weld was made without difficulty, completing the aft head assembly. (See Figures 52 and 53)

(c) After completing the head assembly, the aft cylinder section was trimmed to fit the diameter of the aft head and the closure weld was made. The cylinder section was then mounted on the lathe and trimmed to match the aft head. The weld was made without difficulty and the aft half of the tank was completed except for final trim to match the forward half. All welds in the tank half were 100% X-ray examined and of good quality. (See Figures 54 and 55)

(d) The final weld joining the two tank halves was made on the horizontal lathe and X-ray examination showed the weld was of excellent quality. This completed the titanium tank except for addition of an internal vent line which was added after hydrostatic testing of the tank. Figure 56 shows the completed tank mounted on the lathe.

2.5.1.1 Tank Insulation

Insulation of the titanium tank was begun. Formed segments of fiberglas were trimmed and fitted to the forward and aft heads. The segments were attached to the head with Sta-Bond 511-A adhesive. Thermal stand-offs were installed on the manhole, instrumentation port, and vent port. Retainer angles which attach the insulation segments to the skirt and poured foam area were installed. Figure 57 shows a cross-section of the head area indicating the work done to date.

FIGURE 52
PHOTOGRAPH OF WELDING SKIRT TO AFT HEAD ASSEMBLY

FIGURE 53
PHOTOGRAPH OF COMPLETED AFT HEAD ASSEMBLY
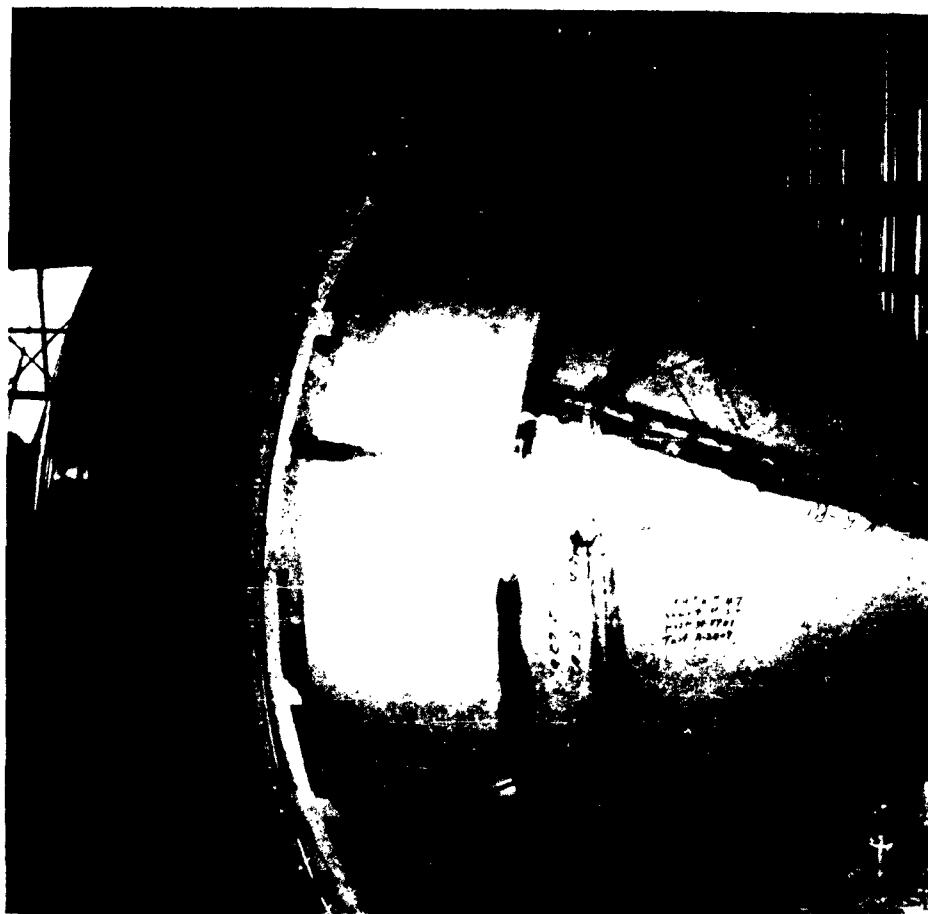
FIGURE 98
PHOTOGRAPH OF WELDING OPERATION JOINING
CYLINDER SECTION TO FORWARD HEAD

FIGURE 55
PHOTOGRAPH OF COMPLETED AFT HALF OF TANK

FIGURE 50
PHOTOGRAPH SHOWING COMPLETED TITANIUM TANK

FIGURE 57
CROSS SECTION OF HEAD AREA
SHOWING FIBERGLASS INSULATION SEGMENT IN PLACE

Formed Fiberglass Segment

Thermal Stand-Off

Retainer Angle

Head Skin

Poured-In-Place Foam
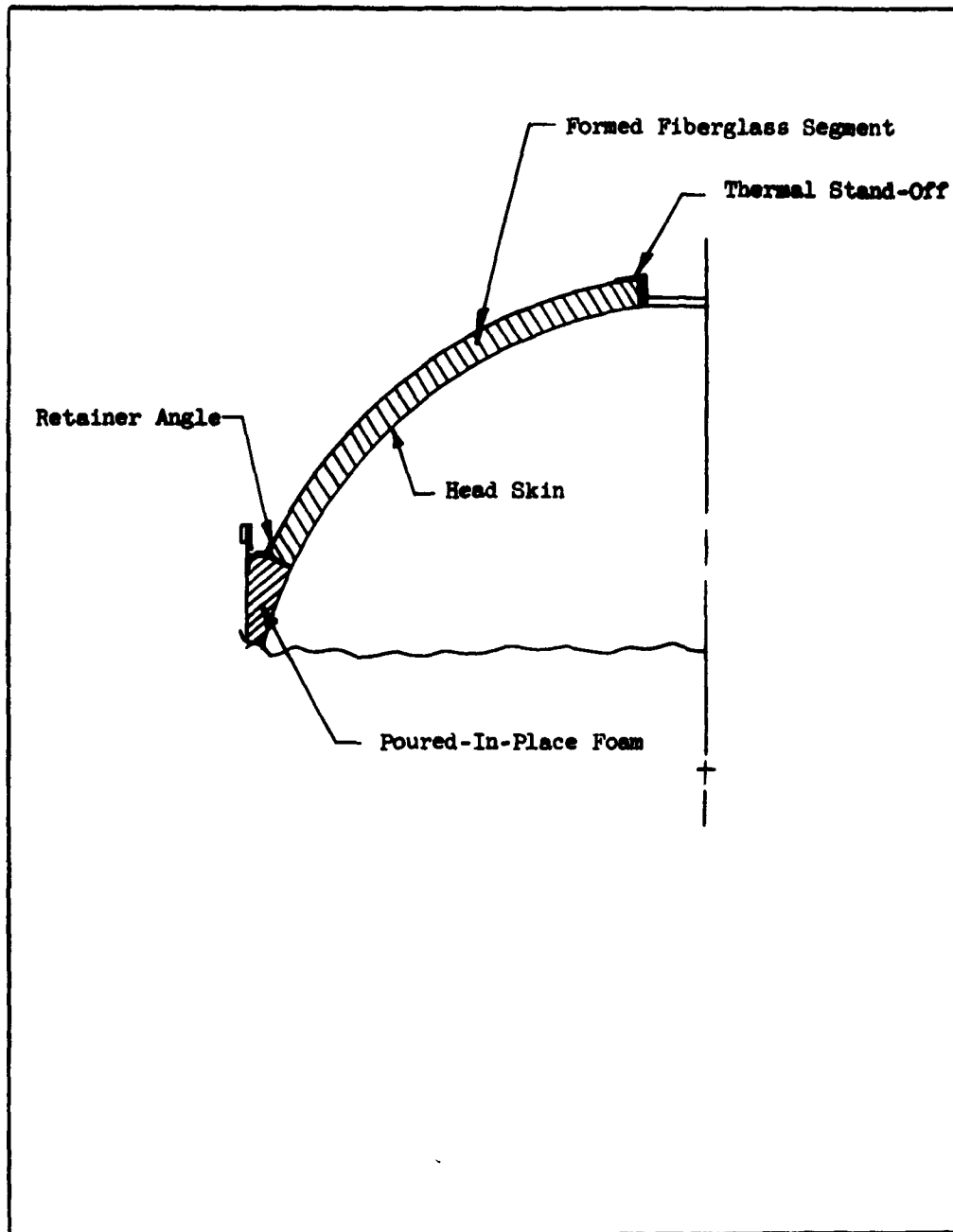
3.0 THERMAL TEST FACILITY

3.1 Reporting Period June 15, 1960, to December 31, 1960

The following subsections will describe the progress during this period in testing the stainless steel test tank.

3.1.1 Instrumentation and Data Acquisition

During the second week of August, 1960, heat tower personnel completed coordinating the tank instrumentation and plumbing with that of the heat tower facility. The completed hook-up consisted of the following:

(1) Installation of NPSH ring and connecting tank drain to facility plumbing for fill and drain operations.

(2) Connecting tank vent assembly to facility vent plumbing.

(3) Installation of internal umbrella assembly containing temperature sensors for recording liquid and vapor temperatures of various stations across the tank from top to bottom.

(4) Installation of rakes to tank wall at two elevations to measure liquid temperature at tank wall and at small increments out from the tank wall. (Tank wall surface temperature sensors, both internal and external, were installed prior to placing the tank in the heat tower facility.)

The distribution and location of the internal and external temperature probes are shown in Figure 58. To provide orientation of these probes, the tank was divided into 26 12-inch vertical zones. Zone no. 1 was located at the top of the tank and the remaining zones numbered consecutively to the bottom of the tank. The center line of the instrumentation port was used for angular orientation.

3.1.2 Thermal Test Preparations

During Spetember, 1960, two limited quantity LH_2 fill tests were accomplished. On September 6, 1960, the tank was filled with 1,100 gallons of LH_2 and drained. The purpose of these two runs was to check out the tank drain assembly. Both runs were successful with no difficulties experienced.

Four days after the above runs were made, the test tank was found to be in a collapsed condition. Investigations were started to determine the reason for the collapse. The following conclusions were drawn after careful study.

(1) The tank did not collapse or suffer any damage during the LH_2 run of September 9, 1960.

(2) The most likely reason for the tank collapsing was being tightly closed off overnight. The ambient temperature that particular night experienced a considerable drop, sufficient to have caused enough negative pressure to collapse the tank.

FIGURE 58
TEMPERATURE PROBE DISTRIBUTION
7,000 GALLON TEST TANK
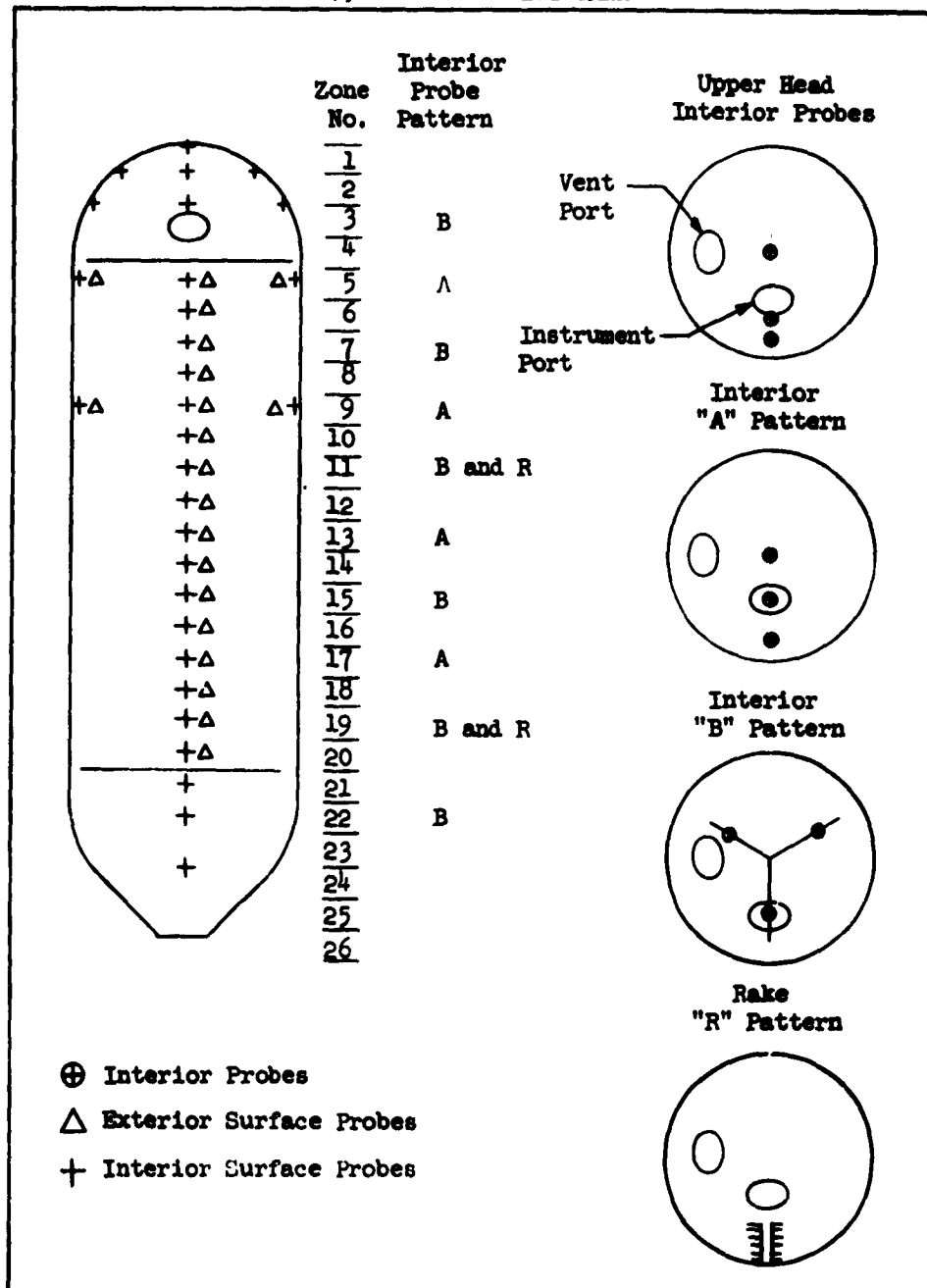
Steps were taken immediately to insure that a collapse for the reason set forth would not happen again.

This difficulty delayed the start of the thermal test runs. The tank was pressurized and most of the cans in the tank popped out to the extent that the tank itself was considered usable. Repairs had to be made to internal instrumentation and some heat lamps in the vacuum bell had to be replaced.

The first LH_2 fill test was attempted on October 6, 1960. When the tank level indicated 750 gallons had been transferred, a leak developed in the drain assembly and resulted in a small fire.

On October 27, 1960, a limited liquid hydrogen run, utilizing 1,720 gallons of LH_2 was made to check the welded drain assembly. No leakage occurred, but during the warm-up period after the tank was emptied, the cone insulation was damaged due to air pumping. After tank warm-up, the insulation was repaired. During the next fill, the insulation was to be continuously evacuated to protect the insulation from damage.

Several LH_2 test runs were made on November 9, 1960, to check out the drain assembly, NPSH assembly, vortexing, quality meter and tank insulation. The amount of fluid used in these runs was 3,300 gallons of LH_2. Two problem areas developed during these runs. The NPSH assembly was found to have a leak inside the tank where the torus ring connects. Since this assembly was now welded into the tank and could not be removed, no repairs could be made. Therefore, on any subsequent test runs, NPSH data could not be taken.

Two other series of test runs were made in November, 1960, for purposes of checking out the system prior to a fill test with heat being applied to the exterior. These test runs were as follows:

    (1)   On November 16, 1960, six flow control tests were conducted, utilizing from 4,250 to 5,150 gallons of LH_2 in each run.

    (2)   On November 22, 1960, six more flow control tests were run. During these runs, the tank pressurization system was used for the first time with good results. These runs utilized from 3,000 to 6,000 gallons of LH_2 in each run.

3.2   <u>Reporting Period May 8, 1961, to July 31, 1961</u>

Reactivation of the thermal test facility was started at the commencement of the contract. The following subsections will be devoted to a description of the work progress during this period:

    (a) Mechanical
    (b) Instrumentation and Electrical

3.2.1 Mechanical

During this period, all flow systems were checked for deterioration and operation. All necessary repairs and maintenance had been performed and the systems were ready for final check with liquid nitrogen when the test tank was installed.

3.2.2 Instrumentation and Electrical

Two major problems existed in the data acquisition systems. These were as follows:

(1) During previous test runs, a temperature sensing device would occasionally develop an open circuit which would cause the data acquisition amplifier to "see" an excessively high voltage, thus overdriving the amplifier to the point where no data could be recorded for that point or any of the remaining points on the commutator since the amplifier could not recover fast enough.

(2) Accurate sensing of the surface temperature of a tank wall. This includes the proper sensing device and method of attachment.

The solution to problem no. 1 was believed to be in the amplifier. A new amplifier specifically designed for rapid recovery was obtained and installed and the results are very satisfactory.

3.3 Reporting Period August 1, 1961, to October 31, 1961

3.3.1 Facility Modification and Maintenance

During this period of readying the thermal facility to resume testing, several items of modification and maintenance were accomplished. These items are described in the following paragraphs:

(a) A nitrogen spray system containing four nozzles equally spaced around the bottom area of the test tank was installed. This system was plumbed into the stationary LN_2 dewar and instrumented for remote control. This system is for the purpose of fire prevention on the ground work level and for purging the lower area prior to an LH_2 run. During previous testing, two fires had been experienced. Fortunately, they were small and could be handled by hand equipment. However, fire of a more serious nature would have required a system as described above.

(b) A vent extinguishing system was installed on the vent stack. During venting operations in the past, some 12 ignitions have taken place. The above-mentioned extinguishing system has proven to be very effective. Also, in conjunction with the vent system, the H_2 warning system probe was moved downstream from the vent valve to measure more accurately the H_2 content in the vent system without being influenced by the tank contents.

(c) The stationary LH$_2$ storage dewars and allied equipment required several modifications. This included repair welding and replacement of a vent assembly bellows. Damage to the dewars was caused by liquid air forming on the vent lines and running down on the outer shells of the dewars, causing severe thermal shock. This was corrected by fabricating and installing metal drains and baffles to collect the liquid air and remove it to a harmless area.

(d) From time to time, the facility has experienced power failures due to normal operation of the utility company. During these times, unattended vacuum pumps, having stopped, will cause oil to be drawn into the space being evacuated. Since these pumps have to operate at times unattended, they were modified to fail safe by the addition of control systems to prevent this oil contamination of the vacuum space.

(e) During previous test runs, the flow control system which automatically controls the LH$_2$ flow during testing proved to be inadequate. The trouble was found to be in the transducer which demonstrated a response time of 18 to 20 seconds, which proved to be too slow for adequate data. This transducer was recommended as suitable and should have performed satisfactorily. However, under actual test conditions, it failed. This posed a problem in gathering data and delayed resumption of testing during efforts to find a solution.

An attempt to rebuild the system was made by obtaining a 0 to 1 psid variable reluctance transducer to be used in conjunction with a 5 amplifier system to produce a differential signal to the flow controller. This system proved to be reasonably satisfactory except that it required considerable time and LH$_2$ to calibrate for any one flow rate. Approximately six fill and drains were required to establish a set of values that could be dialed into the system to set a predetermined rate. Since the various tests required flow rates ranging from 950 gpm to 1950 gpm, it would be a time-consuming effort to calibrate for variable flow rates plus the large amount of LH$_2$ required. Therefore, so as not to delay testing any further, the calibration process was discontinued and the flow rate would be set by a predetermined position of the flow control valve and the actual flow of the test determined by measurement.

(f) Major modification of the heat rate control computers was found to be necessary during previous test runs. The quality of Q/A and T$_s$ data was not as it should be. By the addition of scaling resistors, this problem was overcome and close, accurate control was obtained plus increasing the capability to a temperature range of 300°F to 800°F.

(g) The liquid quality measuring system was rebuilt from a resonant voltage rise system to a frequency to DC voltage conversion system. This change became apparent during actual testing. The quality of the resolution and linearity had to be improved for good data

results. Testing of this new system proved to be disappointing. To facilitate the testing program, the system was taken out of the data acquisition circuitry and proceeded without this system.

3.3.2 Mechanical

The stainless steel test tank was installed in the vacuum bell and internal instrumentation added during August, 1961. External instrumentation was completed by the middle of September and both systems checked out with the facility data acquisition circuitry.

To prevent the possible formation of liquid air on the tank wall, the insulation was evacuated and then purged with CO_2. This procedure was followed through several cycles to replace as much of the air remaining in the insulation as possible with CO_2. This procedure was followed periodically up to the time thermal testing began.

The stainless steel tank was then connected to the facility plumbing system and checked for leaks with LN_2. The tank and facility were then declared operational and ready for preliminary LH_2 fill and drain tests for final check before testing began.

It was discovered that a storage dewar no. 2 had several pin holes in the bellows which required a major repair effort in cutting out the bellows assembly and installing a complete new assembly.

All systems were then rechecked and the facility was operational for preliminary LH_2 fill and drain for final check and calibration prior to trajectory runs.

During the latter part of October, 1961, several LH_2 fill and drain runs were accomplished. Also, the tank was pressurized during one run to check the pressurization system and also the structural integrity of the tank.

3.4 Temperature Sensing Program

The problems pertaining to accurate temperature measurements and response time were outlined in 3.2.2. Programs to investigate the solution to these problems were started and this section will describe the results of these investigations. The programs and their results will be described under the following subtitles:

(a) Surface Temperature Measurement
(b) Response Characteristics of Resistance Thermometers

3.4.1 Surface Temperature Measurement

The problem of surface temperature measurement involves the type of sensor used and the method of attachment to the surface for which the temperature is required. To aid in solving this problem, an industry survey was made by two Beech engineers to ascertain what success, if any, has been achieved in this field. The results of this trip are presented in Appendix A. This

problem seemed to be prevalent throughout industry with no concrete solution being found. However, some of the ideas presented were promising and were included in a test program to determine the best procedure to follow.

The test program that was conducted is presented in Appendix B. As a result of the tests performed, the test method was determined to be a thermocouple with the leads welded to an aluminum foil tape. This type thermocouple has high thermal response, low thermal mass, and will take the expected temperature range.

3.4.2 Response Characteristics of Resistance Thermometers

Platinum resistance probes were being used to measure temperatures inside the tanks to provide a measure of response rates. This section describes the test methods used and the results of the tests in establishing the response time of platinum resistance thermometers during the transition from liquid H_2 to gaseous H_2. The thermometers used were Ruge thermometers with an ice point of 200 ohms. The same type thermometers were used to measure the temperatures at various points in the liquid and the gas temperature immediately above the liquid as the level falls during LH_2 thermal test runs in the stainless steel test tank.

The following subparagraphs will describe the equipment used, test procedure, results, and conclusions.

3.4.2.1 Test Equipment

The test setup was composed of a six-inch I.D. x 18-inch deep open-mouth steel dewar. For temperature comparisons, two rakes were prepared that could be installed in the dewar in a stationary manner. One rake contained four Ruge platinum resistance thermometers placed in a vertical line two inches apart, the other rake contained four copper constantan thermocouples attached in the same manner. Two arms were prepared that were movable up and down in the dewar. One arm had a Ruge platinum resistance thermometer mounted and the other arm had two copper constantan thermocouples mounted.

3.4.2.2 Calibration

Each thermometer completed the fourth leg of the Wheatstone bridge as shown in Figure 59. The output from the bridge was coupled to an oscillograph recorder.

All the PR thermometers were immersed in either LN_2 or LH_2, and the Wheatstone bridge was balanced for zero output. The thermometers were then disconnected from the bridge and a decade resistance box was inserted in their place in the Wheatstone bridge. Different values of resistance were dialed on the decade resistance box until a ten-step calibration was obtained between 1 and 100 ohms for LH_2 and 38 to 150 ohms for LN_2. Each case represented the following temperature ranges:

$$-425°F \text{ to } -200°F \text{ for } LH_2$$
$$-325°F \text{ to } -100°F \text{ for } LN_2.$$

FIGURE 59
SCHEMATIC OF THERMOMETER
HOOK-UP IN RESPONSE TIME TEST
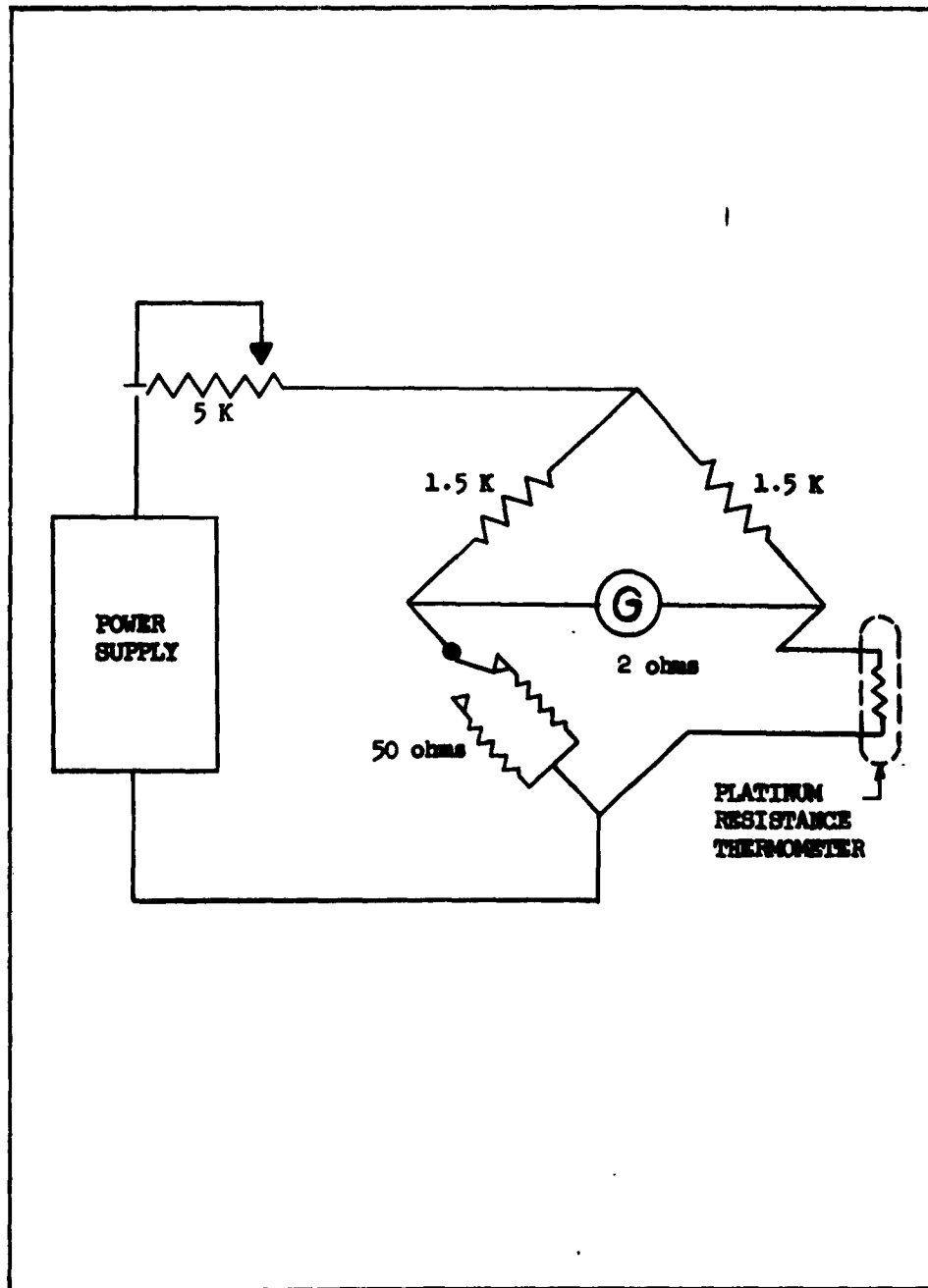
3.4.2.3 Test Procedure

I. Test No. 1

After calibration was completed, the LN_2 was drained from the open mouth dewar until the level was between stationary test probes 2 and 3, reference Figure 60. The movable test probe was positioned opposite stationary probe no. 2 immersed in LN_2 until equilibrium was obtained. The following steps were then followed to complete the test:

(1) Test probe no. 1 was removed from the liquid and positioned opposite stationary probe no. 3 in the gas area and held for one minute.

(2) Probe no. 1 was reimmersed in the liquid opposite no. 2 probe until equilibrium was obtained.

(3) Probe no. 1 was removed from the liquid and positioned opposite stationary probe no. 4 in the gas area and held for one minute.

(4) Probe no. 1 was reimmersed in liquid until equilibrium was obtained.

(5) Probe no. 1 was removed from the liquid and positioned opposite stationary probe no. 5 in the gas area and held for one minute.

II. Test No. 2

The setup and procedure were the same as Test No. 1, except LH_2 was used instead of LN_2.

III. Test No. 3

The setup and procedure were the same as Test No. 2, except the open-mouth dewar was made a closed system (Reference Figure 60).

IV. Test No. 4

The setup and procedure were same as Test No. 3, except copper constantan thermocouples were used in place of platinum resistance thermometers and the movable arm with two thermocouples attached was used.

3.4.2.4 Discussion

The data recorded in the above tests was temperature versus time. This data is presented in Figures 61 through 72 in the form of curves reflecting the performance of platinum resistance thermometers and copper constantan thermocouples.

In Test No. 1 (LN_2 as the fluid) the response times going from liquid to gas were of the order of minutes, with probably 5-10 minutes required for complete stabilization. It is interesting to note the lack of gradient on the movable probe plot of the first run (Figure 61), then the initial gradient on runs 2 and 3 (Figures 62 and 63) which tend to level off with appreciable ΔT's between the movable and stationary probes.
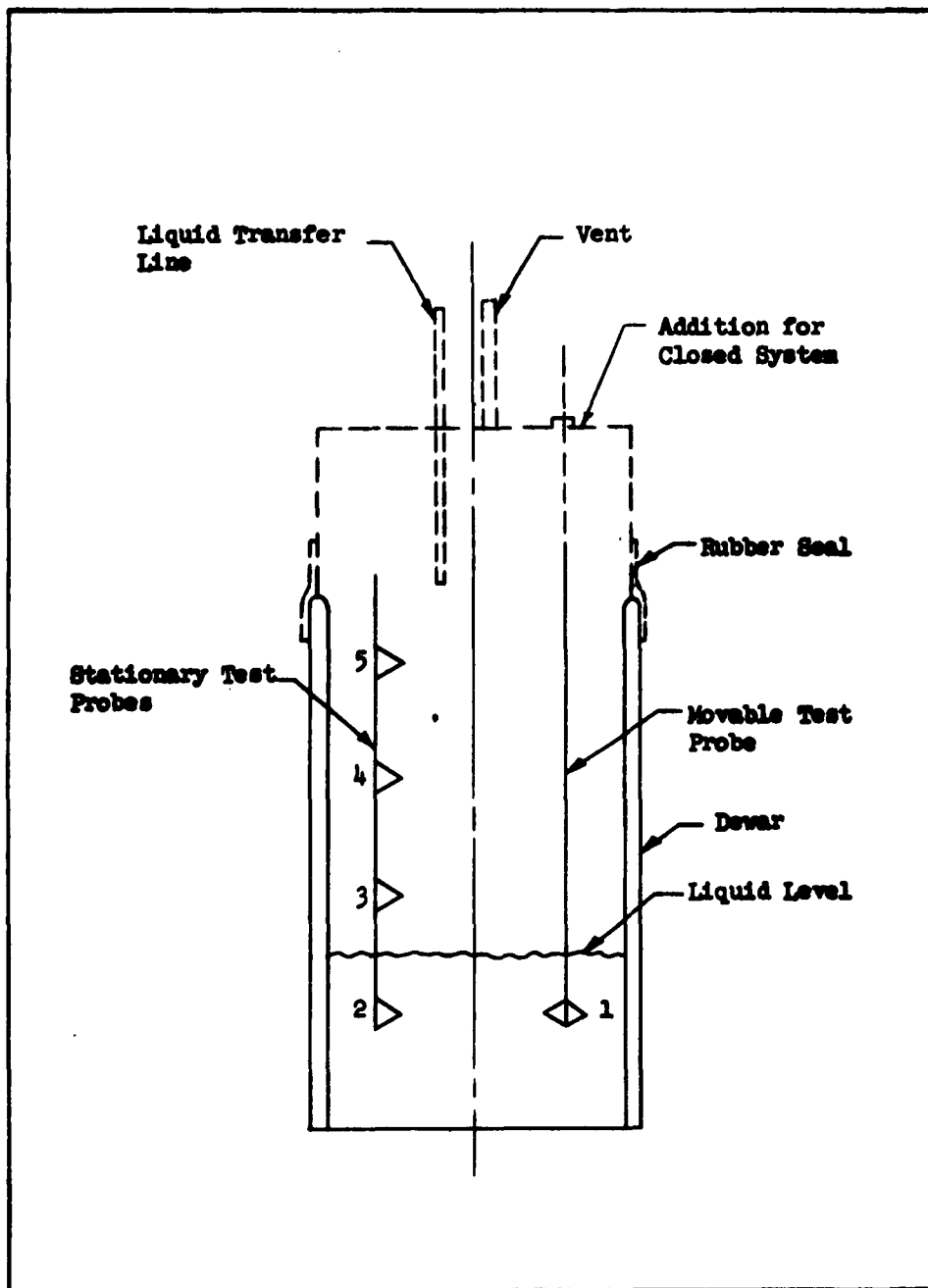
FIGURE 61
RESPONSE TEST NO. 1
RUGE PLATINUM RESISTANCE THERMOMETER
ICE POINT 200 Ohms

△ PRT 3 Stationary in GN₂ Approximately 1" Above Liquid Level

⊙ PRT 1 Moved from LN₂ to PRT 3 Position

TIME/SECONDS

TEMP °F

△ PRT 4 Stationary in GH$_2$ Approximately 3" Above Liquid Level

⊙ PRT 1 Moved from LH$_2$ to PRT 4 Position

TIME/SECONDS

TEMP °F

-100

-200

-300

10

20

30

40

50

60
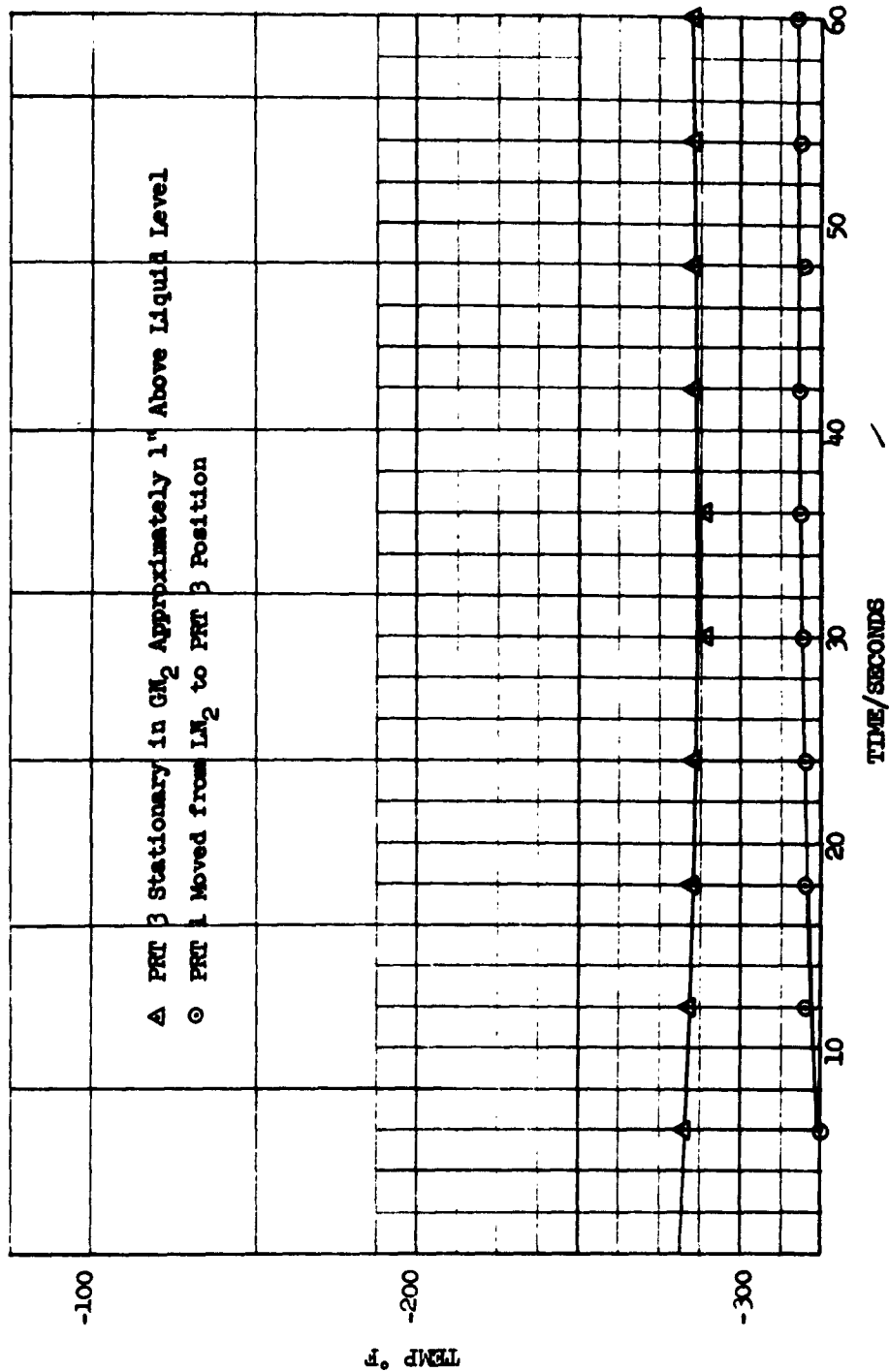
FIGURE 62
RESPONSE TEST 1
RUGE PLATINUM RESISTANCE THERMOMETER
ICE POINT 200 Ohms

△ PRT 5 Stationary in GN₂ Approximately 5" Above Liquid Level
⊙ PRT 1 Moved From LH₂ to PRT 5 Position

TEMP °F

TIME/SECONDS
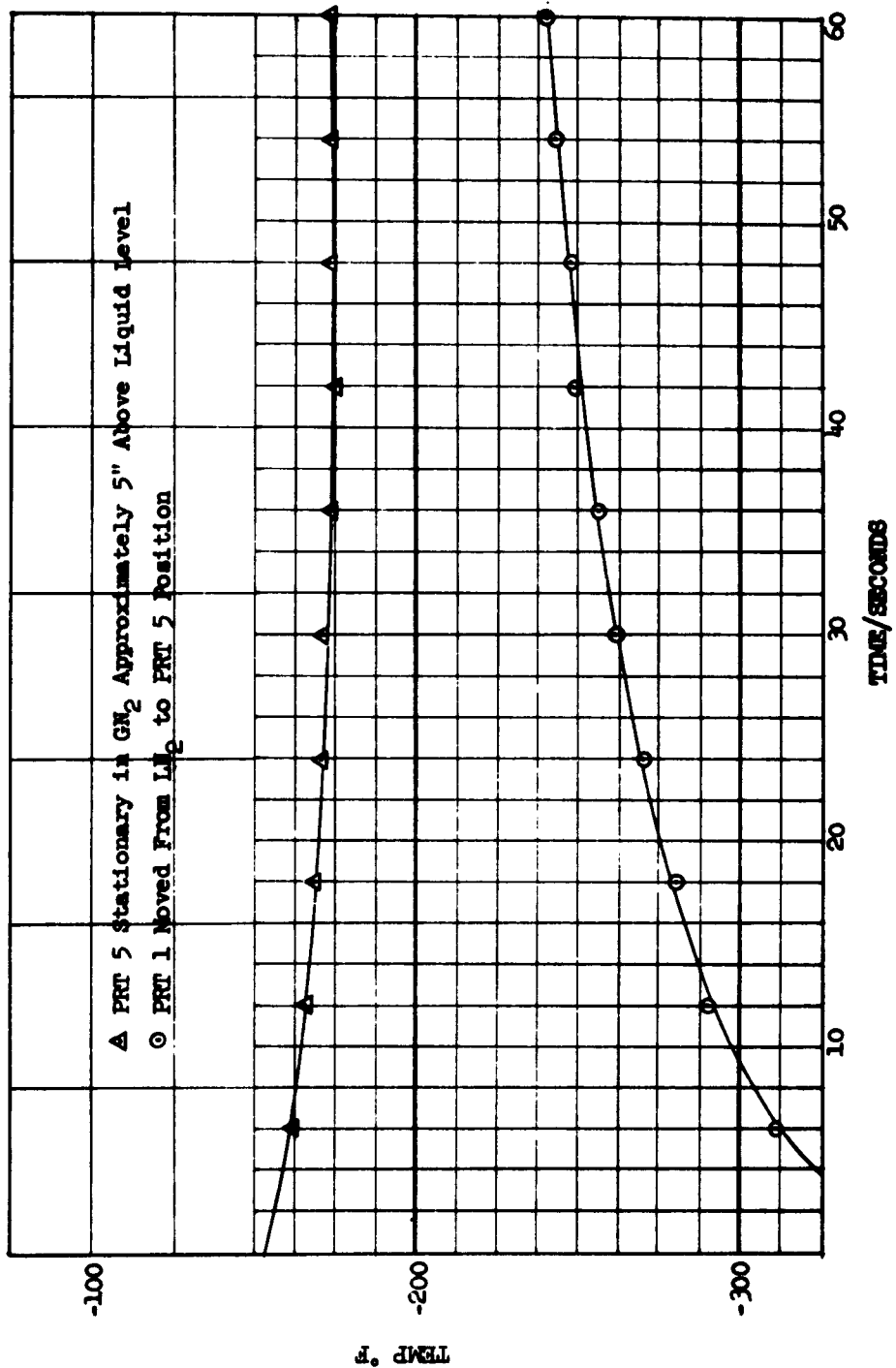
FIGURE 64
RESPONSE TEST 2
RUGE PLATINUM RESISTANCE THERMOMETER
ICE POINT 200 Ohms

▲ PRT 5 Stationary In GH₂ Approximately 5" Above Liquid Level
⊙ PRT 1 Moved From LH₂ To PRT 5 Position

TIME/SECONDS

TEMP °F
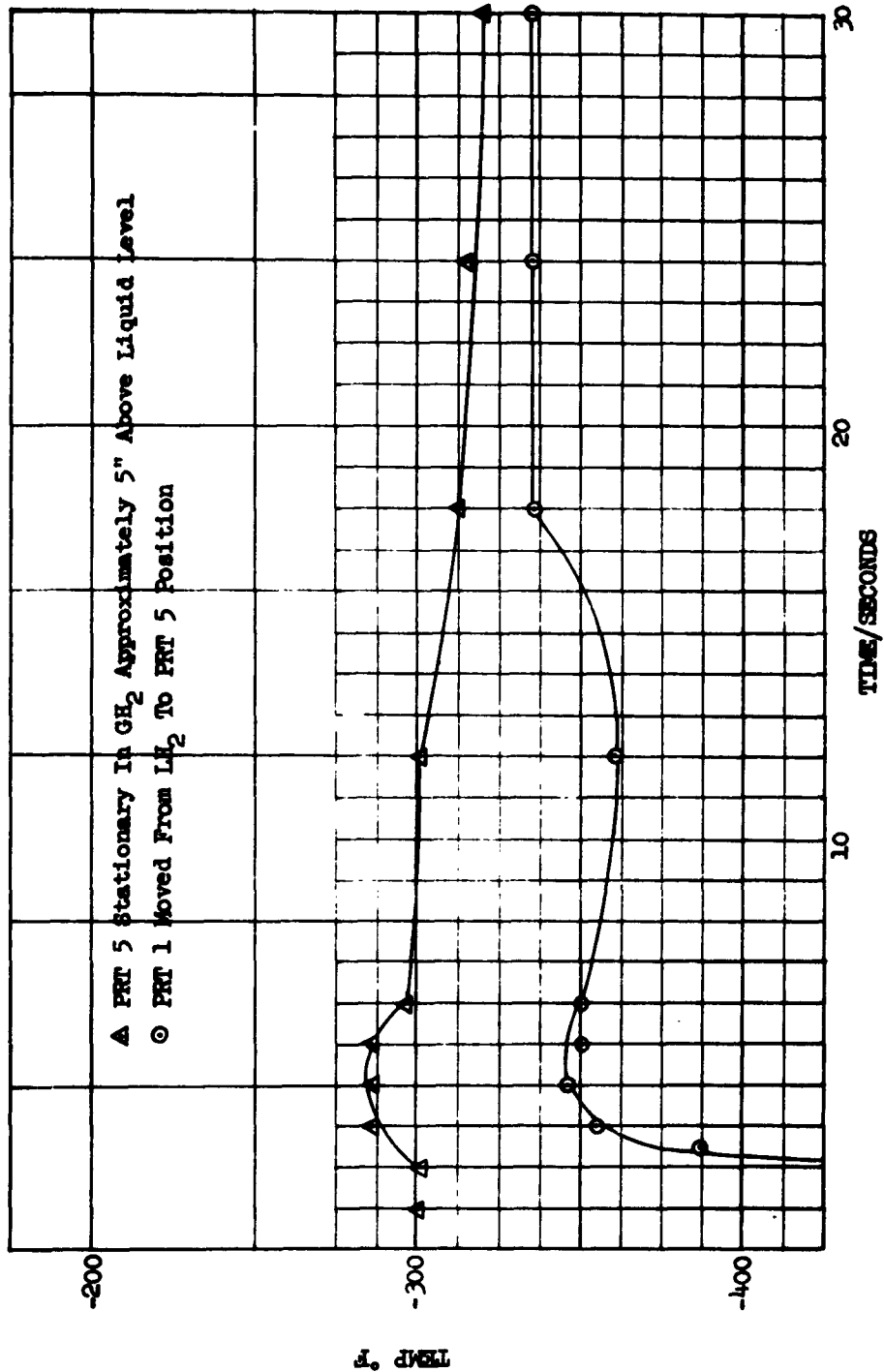
FIGURE 65
RESPONSE TEST 2
RUGE PLATINUM RESISTANCE THERMOMETER
ICE POINT 200 Ohms
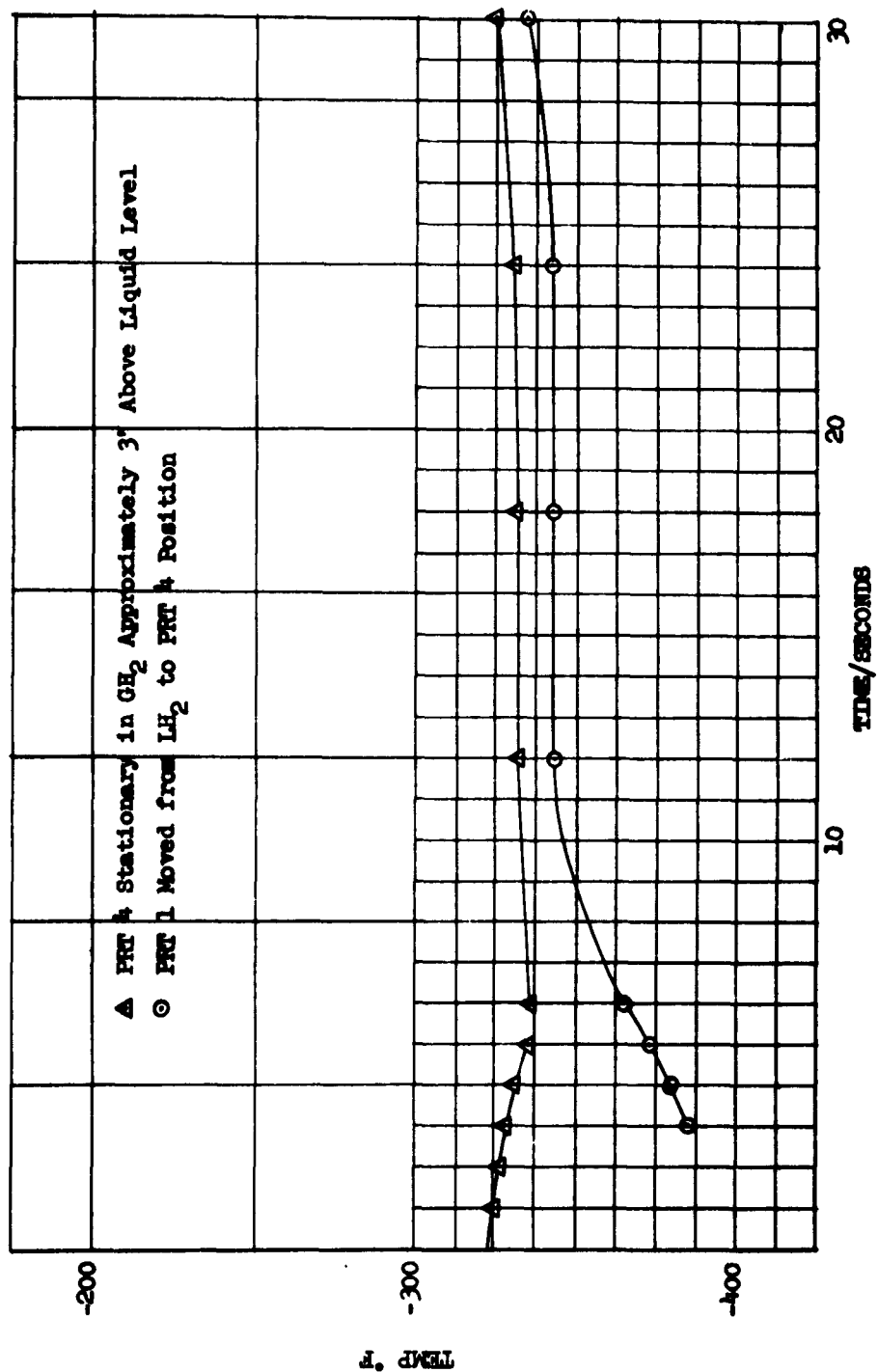
FIGURE 6(
RESPONSE TEST 2
RUGE PLATINUM RESISTANCE THERMOMETER
ICE POINT 200 Ohms
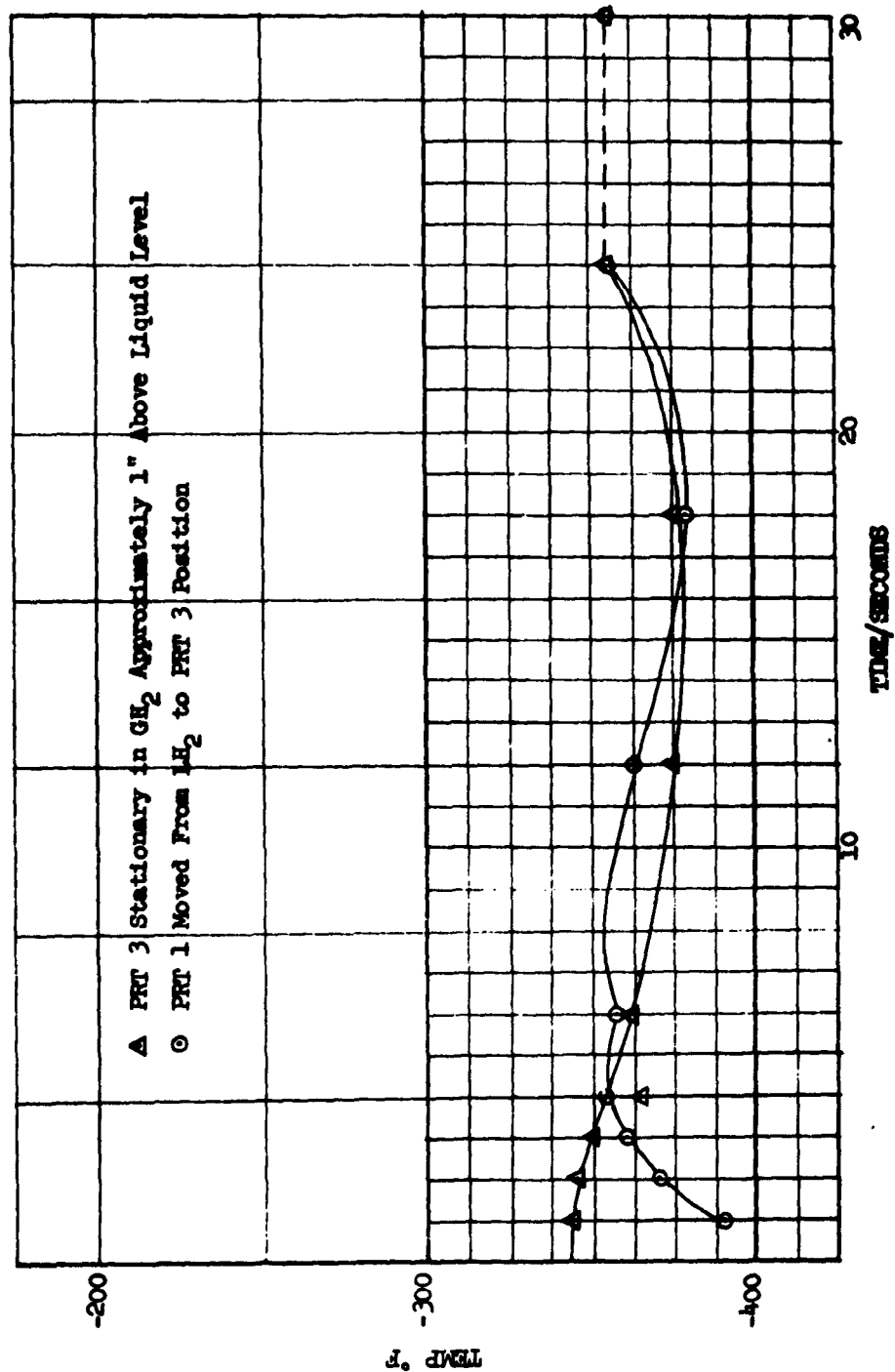
FIGURE 67
RESPONSE TEST 3
RUGE PLATINUM RESISTANCE THERMOMETER
ICE POINT 200 Ohms

△ PRT β Stationary in GH₂ Approximately 1" above Liquid Level
⊙ PRT 1 Moved From LH₂ to PRT β Position

FIGURE 38
RESPONSE TEST 3
RUGE PLATINUM RESISTANCE THERMOMETER
ICE POINT 200 Ohms

▲ PRT 4 Stationary In GH₂ Approximately 3" Above Liquid Level
⊙ PRT 1 Moved from LH₂ to PRT 4 Position

TEMP °F

TIME/SECONDS

FIGURE 66
RESPONSE TEST 3
RUGE PLATINUM RESISTANCE THERMOMETER
ICE POINT 200 Ohms

▲ PRT 5 Stationary in GH₂ Approximately 5" Above Liquid Level
⊙ PRT 1 Moved From LH₂ to PRT 5 Position

TIME/SECONDS

TEMP °F
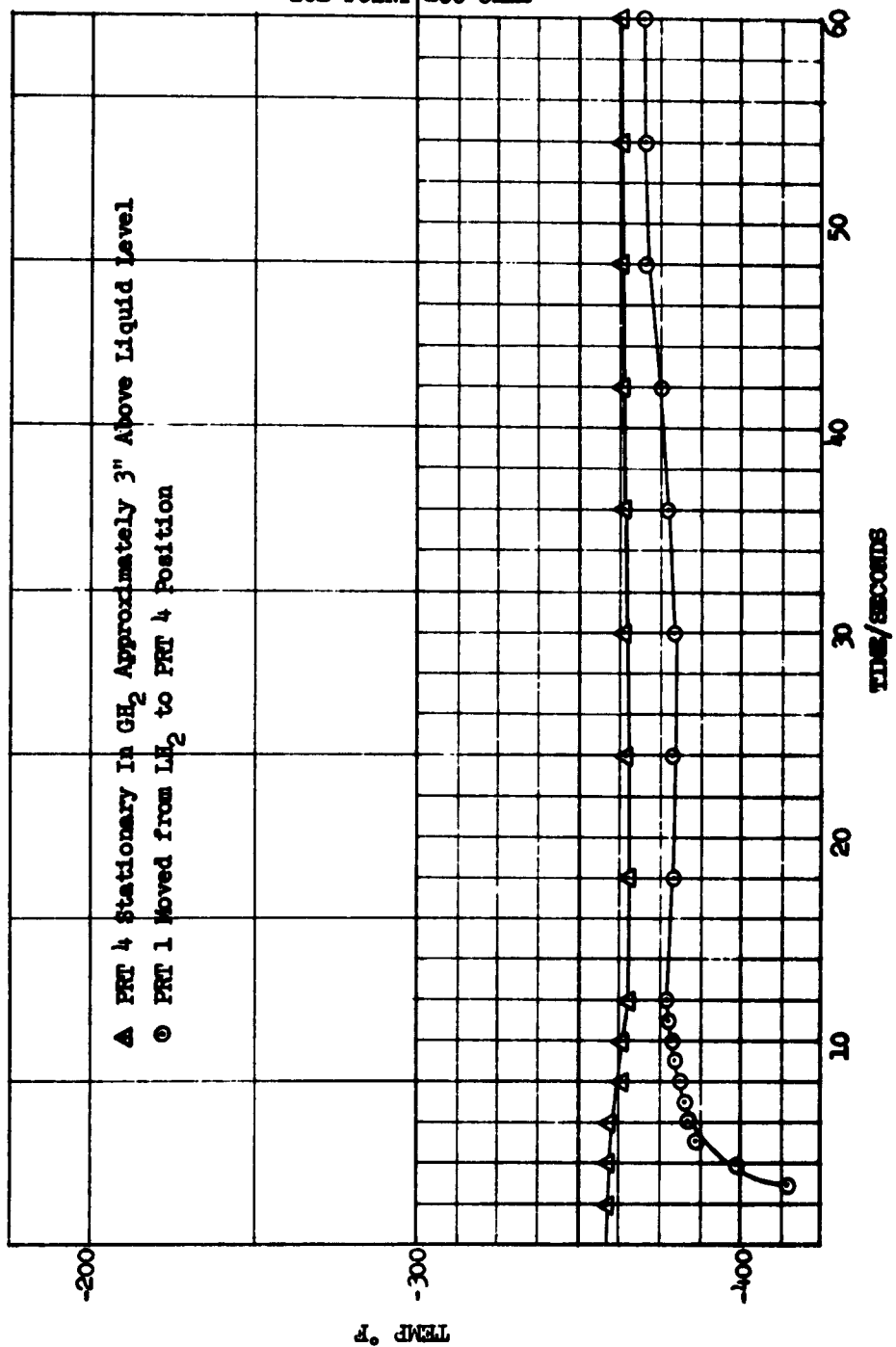
FIGURE 7C
RESPONSE TEST 4
COPPER CONSTANTAN THERMOCOUPLE

△ T/C 3 Stationary in GH₂ Approximately 1" Above Liquid Level

⊙ T/C 1 and 2 Moved from LH₂ to T/C 3 Position

TIME/SECONDS

TEMP °F
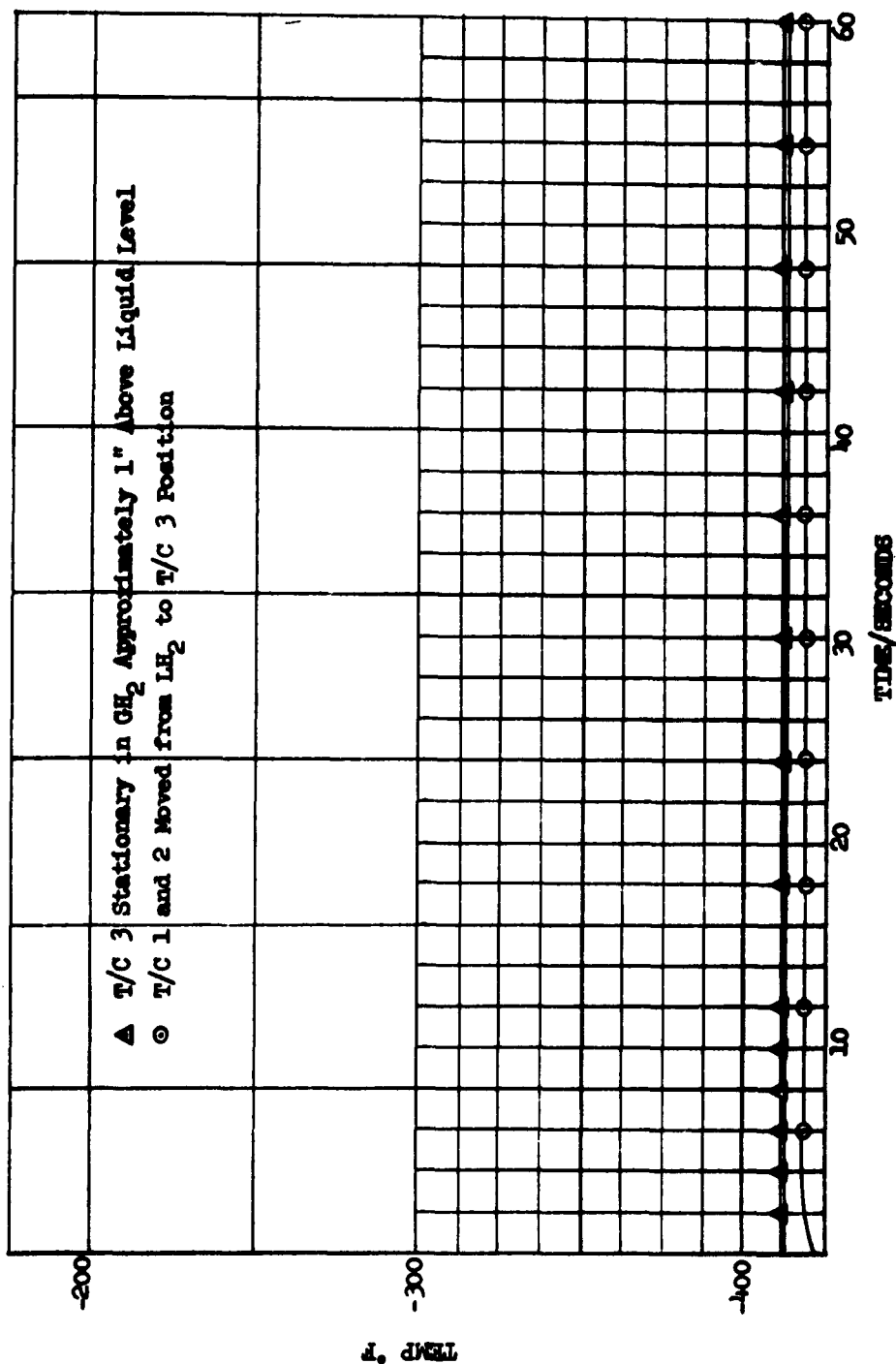
FIGURE 71
RESPONSE TEST 4
COPPER CONSTANTAN THERMOCOUPLE
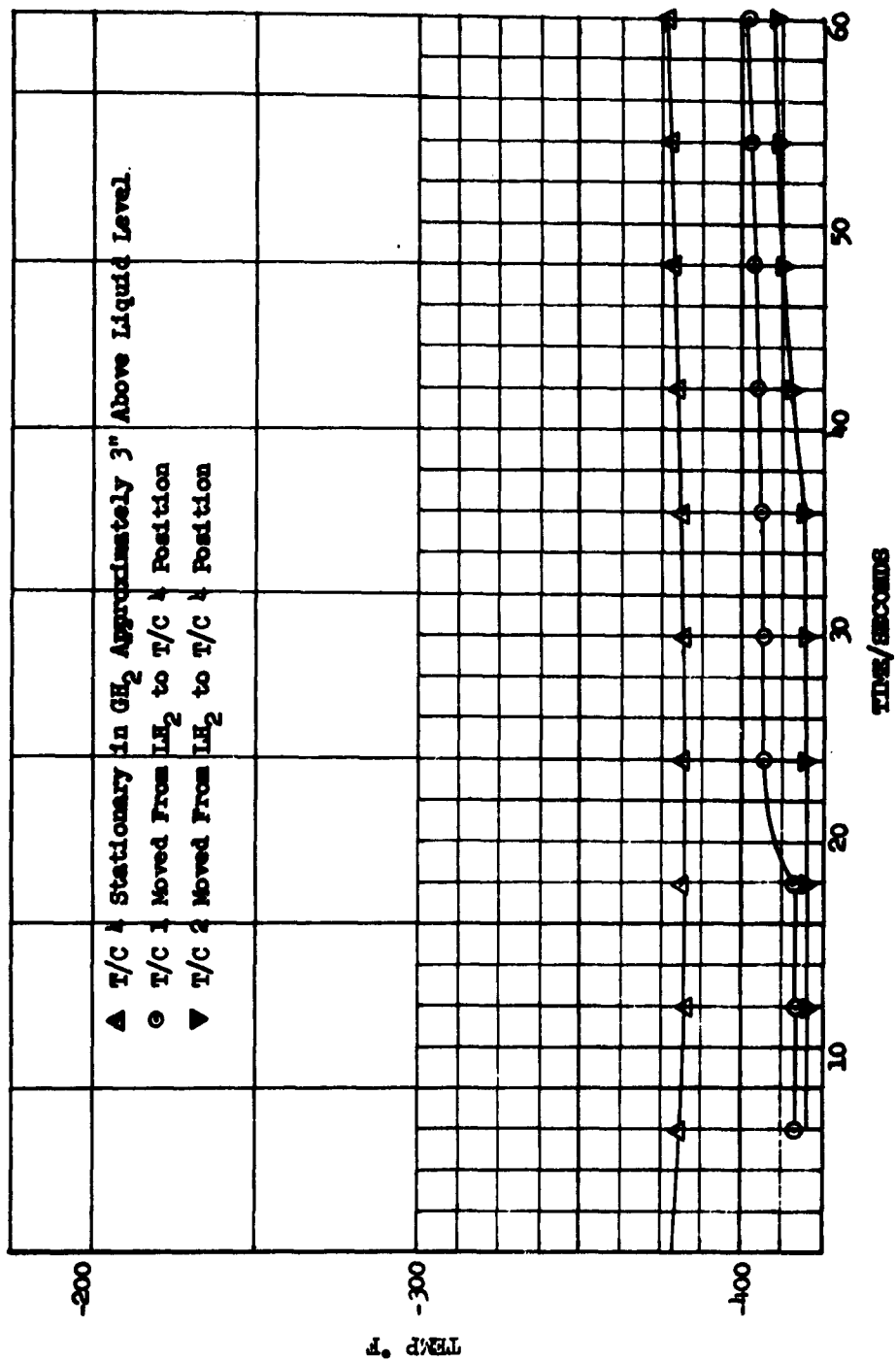
FIGURE 7.
RESPONSE TEST 4
COPPER CONSTANTAN THERMOCOUPLE

Stationary in GH$_2$ Approximately 5" Above Liquid Level

▲ T/C 5 Stationary in GH$_2$ Approximately 5" Above Liquid Level

● T/C 1 Moved From IH$_2$ to T/C 5 Position

▼ T/C 2 Moved From IH$_2$ to T/C 5 Position

TIME/SECONDS

TEMP °F

-200

-300

-400

10   20   30   40   50   60
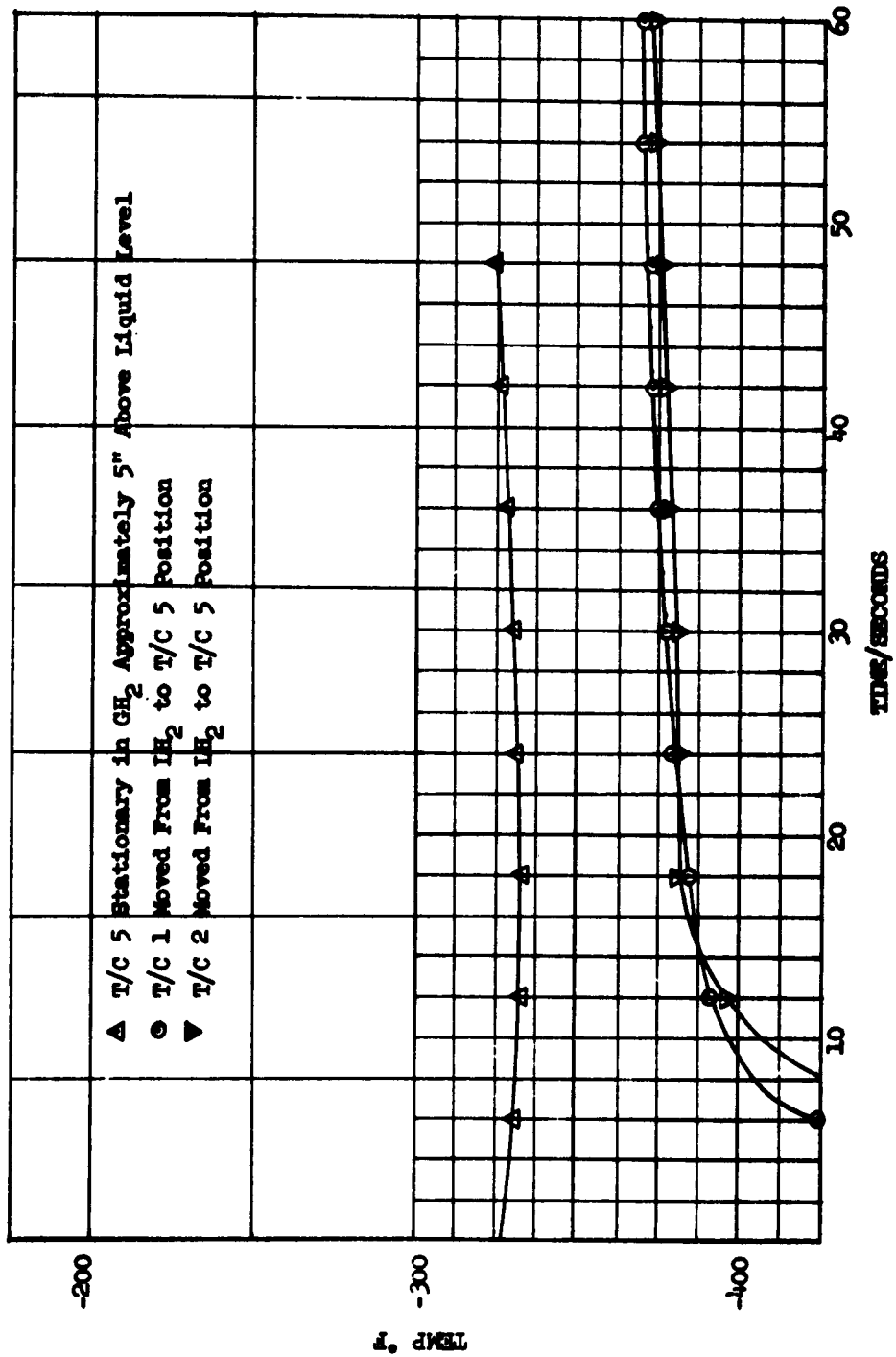
In Test No. 2 (LH$_2$ as the fluid), the response time was greatly reduced from that when LN$_2$ was used. Apparently, the probes were much more sensitive at the lower LH$_2$ temperatures. However, the curves (Figures 64, 65, and 66) show marked fluctuations in that both stationary and movable probe temperatures wander considerably. This was attributed to air liquefying in the cold H$_2$ gas in the open mouth dewar and migrating downward and into the liquid. For this reason and in the interest of safety, the remaining tests were conducted in a closed system by installing a cap on the dewar (reference Figure 60).

Test No. 3 was run in the closed dewar, giving more favorable operating conditions. Run No. 1 (Figure 67) actually shows the test and stationary probes inverted as compared to all other curves. A total response time of between 16 and 20 seconds is indicated.

Run No. 2 (Figure 68) indicates a response time of approximately 12 seconds, considerably less than the time indicated for the first run. Perhaps the increased resistance of platinum at this higher temperature would account for this apparent inconsistency. Run No. 3 (Figure 69) is fairly consistent with Run No. 2. It might be well to note the difference in readings between the stationary and movable probes and ask the question as to why they do not read out closer since all probes were first balanced in LH$_2$, and should read consistently.

Test No. 4 (LH$_2$ as the fluid) was run to show a comparison between thermocouples and platinum probes. In this test, the stationary rake with four thermocouples attached was used. In the first run (Figure 70), it was noted the entire temperature change experienced by the two movable probes was accomplished in something under six seconds. Inconsistent with this, runs No. 2 and 3 (Figures 71 and 72) indicated no temperature increase on the probe until between 8 and 20 seconds after removal from the liquid. This would indicate the greater the ΔT, the poorer the response time. This is inconsistent in itself. Therefore, we must consider that one set of data is insufficient to judge overall merit.

3.4.2.5 Conclusions

From results obtained in the tests, it would appear that the platinum probes have a shorter response time than the thermocouples, and will give a more consistent performance. However, further investigation in the field of transient temperature measurement should be made to answer the following questions:

(1) Why is there such an inconsistency between temperature reading between thermometers sensing the same temperature?

(2) What effect and how much does gas velocity have on response time? This may account for the shorter response time reported with LH$_2$ since more H$_2$ gas is given off with the same heat input.

(3) Another factor affecting response time is internal ohmic heating within the probe itself. How important is this characteristic in the overall performance?

3.5 Reporting Period November 1, 1961, to January 31, 1962

3.5.1 Hydrostatic Test Preparations

Prior to filling the tank with water for testing, various preparations were necessary. These preparations are discussed in the following subsections.

3.5.1.1 Handling and Transporting

Prior to moving the tank to the test area, all openings were sealed and the tank was pressurized to 3 psig with helium gas. A leak check was then performed covering all weld seams and cover plates. No leakage was indicated by the helium mass spectrometer used.

The tank was left pressurized for the moving operation. The handling fixture designed for use in transporting the stainless steel test tank previously was also used for the titanium tank. As a part of preparations, the annulus of each end of the tank formed by the skirt and head was to be filled with a urethane foam-in-place plastic. To accomplish this, the tank had to be suspended with each end in the upright position. Figure 73 shows the area to be filled with foam.

During the handling operation while still in the shop area, a crack was discovered in the weld joint joining the forward skirt to the splice band. This area had been repaired once before when a similar crack, caused by a failure of argon gas through the welding tip, developed. Approximately 1-1/2" of weld was made before the gas failure was discovered. The resulting crack in the weld was made before the gas failure was discovered. The resulting crack in the weld was cleaned of contamination and repaired with apparent success. However, when the tank was subjected to vibrations and stresses during handling the crack reoccurred. It was decided that further repair would not be successful and that the crack would be stop drilled to contain the damaged area and prevent the crack from growing. This operation worked very well.

Since the skirt is primarily for support during hydrostatic testing and does not form a part of the tank itself, it was decided to hydrostat the tank in one position only, using the good skirt for suspension. This would eliminate the possibility of a skirt failure while supporting the tank full of water, which would destroy the tank itself. The tank was first suspended with the forward head in the upright position. The annulus was then filled with the urethane foam. The position of the tank was reversed with the aft head in the upright position and the annulus filled with urethane foam. The tank was then in the desired position for the hydrostatic test, the weight of the filled tank being supported by the skirt with 100% good weld attachment. (See Figure 74)

FIGURE 73
CROSS SECTION OF HEAD SHOWING
AREA FILLED WITH FOAM

Tank Head

Skirt

Foamed Area
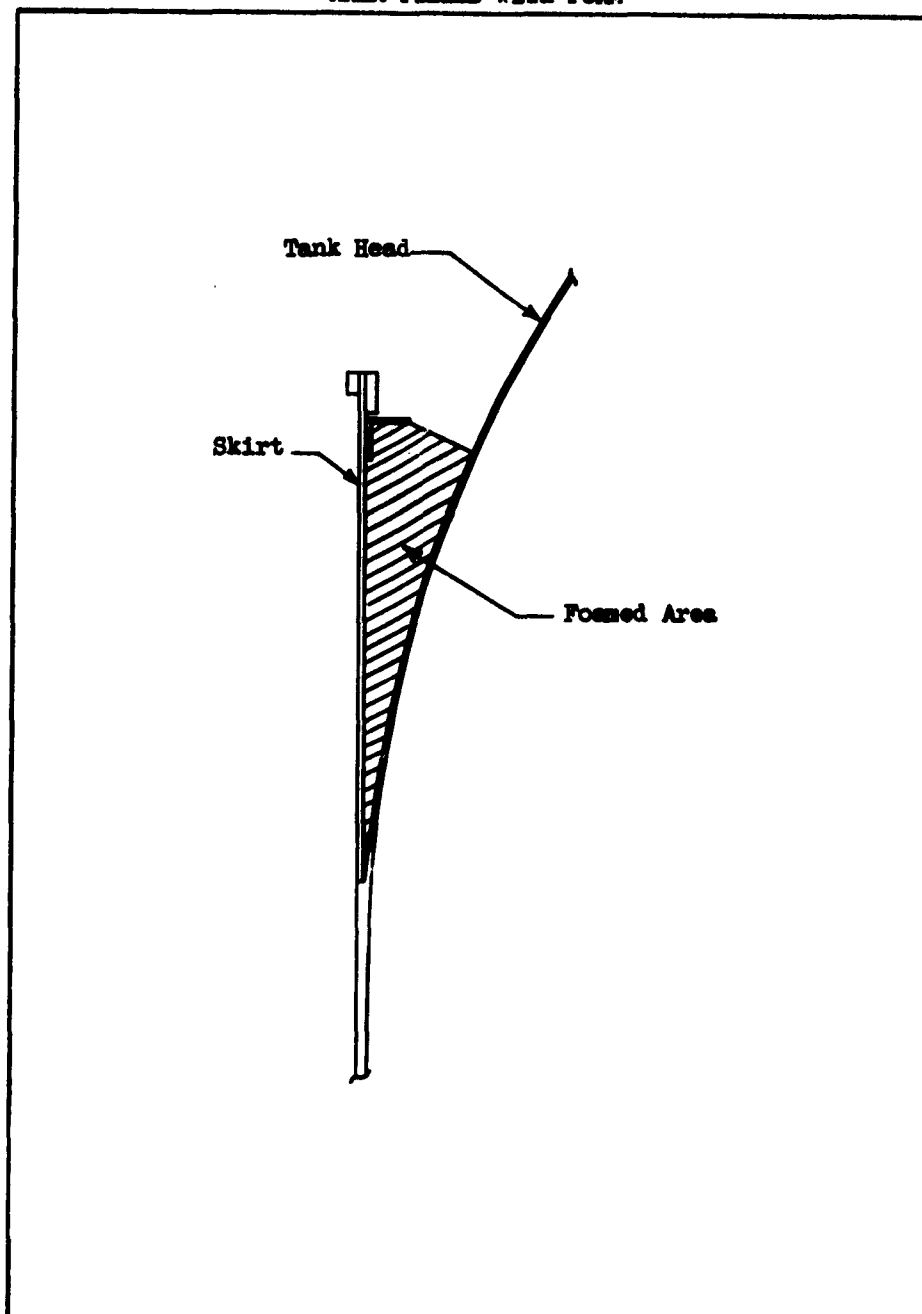
FIGURE 74
PHOTOGRAPH SHOWING TANK IN POSITION FOR HYDROSTATIC TEST
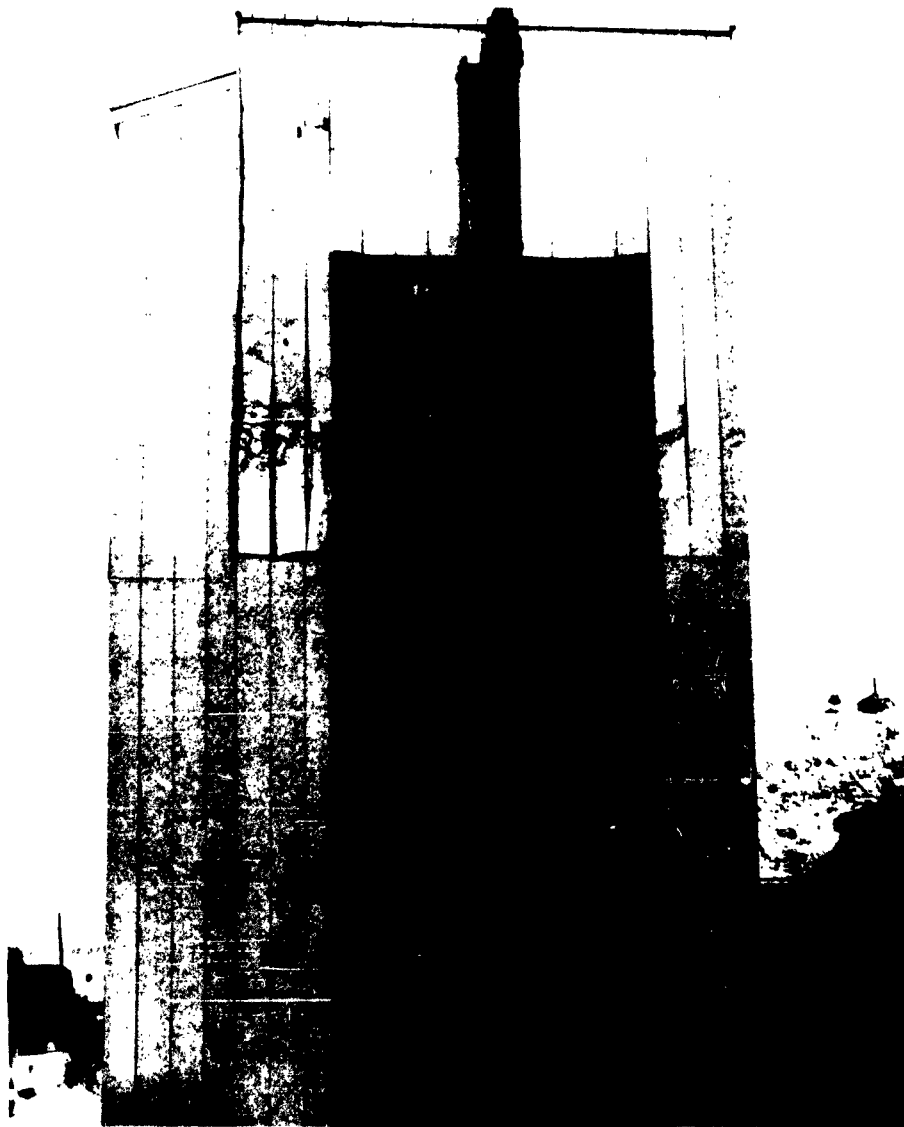
3.5.1.2 Instrumentation

To record the strain experienced by various parts of the tank shell, strain gauges were installed at those points calculated to be most critical. A total of 50 gauges were installed, 41 on the outer surface and 19 on the inner surface.

A series of thermocouples, distributed in a vertical line from the lower head to the upper head, was installed to record any changes of temperature while the test was in progress. All strain gauges and thermocouples were then connected into a harness leading to the recording instruments located in a remote area. The instrumentation was completed by adding a fill warning system at the top of the tank to sound a buzzer when the water level would be within 12" of the top. Figure 75 shows the location of strain gauge points and the thermocouples for skin temperatures. Fifty strain gauges were read directly from an SR-4 balance type strain indicator. Ten of the gauges (F-1, F-9, F-36, P-13, F-17, P-8, F-39, F-12, F-2, F-38) were connected to 10 channels of a Minneapolis-Honeywell Vistacorder for a continuous record of the test. Also connected to the Vistacorder were the six temperature thermocouples and the pressure at the top and bottom of the tank.

3.5.1.3 Plumbing

Figure 76 shows a schematic of the plumbing for filling and pressurization during the hydrostatic test. The pressurization and vent valves were controlled from a remote point. The hook-up provided for automatic venting to prevent over pressurization of the tank during filling and testing. The rate of fill was monitored by a turbine meter and the total accumulative gallon continuously indicated.

3.5.2 Thermal Test Preparations

During November, 1961, a series of fill and drain operations were performed in checking out the test tank, plumbing, data acquisition system, etc. During one of these check-out runs, the heat lamps were turned on. When the heat lamp switch was operated, all the circuit breakers on the facility were opened.

The trouble was found to be the aluminum foil cover on the tank itself. The cover had split open from top to bottom on two sides, allowing the foil to lay over against the lamp terminals, thereby causing the short circuit. The splitting action was apparently due to an anormal amount of contraction of the silicone rubber used to bond the aluminum foil wraps composing the cover.

The damaged cover was removed and the tank was rewrapped with a single layer of aluminum foil. The seams were sealed with an aluminum foil pressure sensitive tape. To prevent the aluminum foil from contacting the heat lamps should the cover split again, the tank was wrapped with aluminum screen wire. Figure 77 shows the tank with the new cover and screen installed.

FIGURE 75
LOCATION OF STRAIN GAUGES
DURING HYDROSTATIC TEST
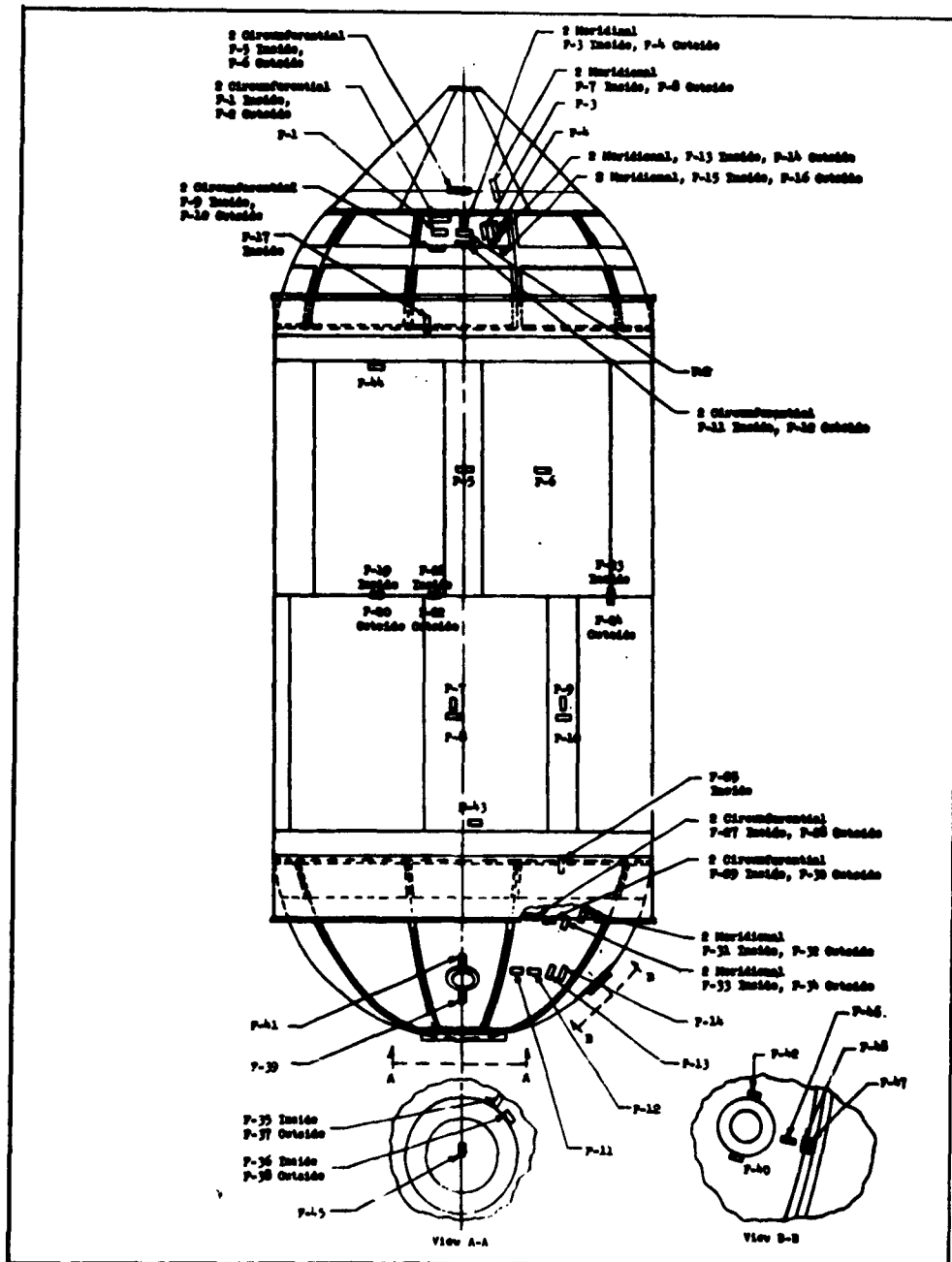
FIGURE 76

PLUMBING SCHEMATIC FOR HYDROSTATIC TEST
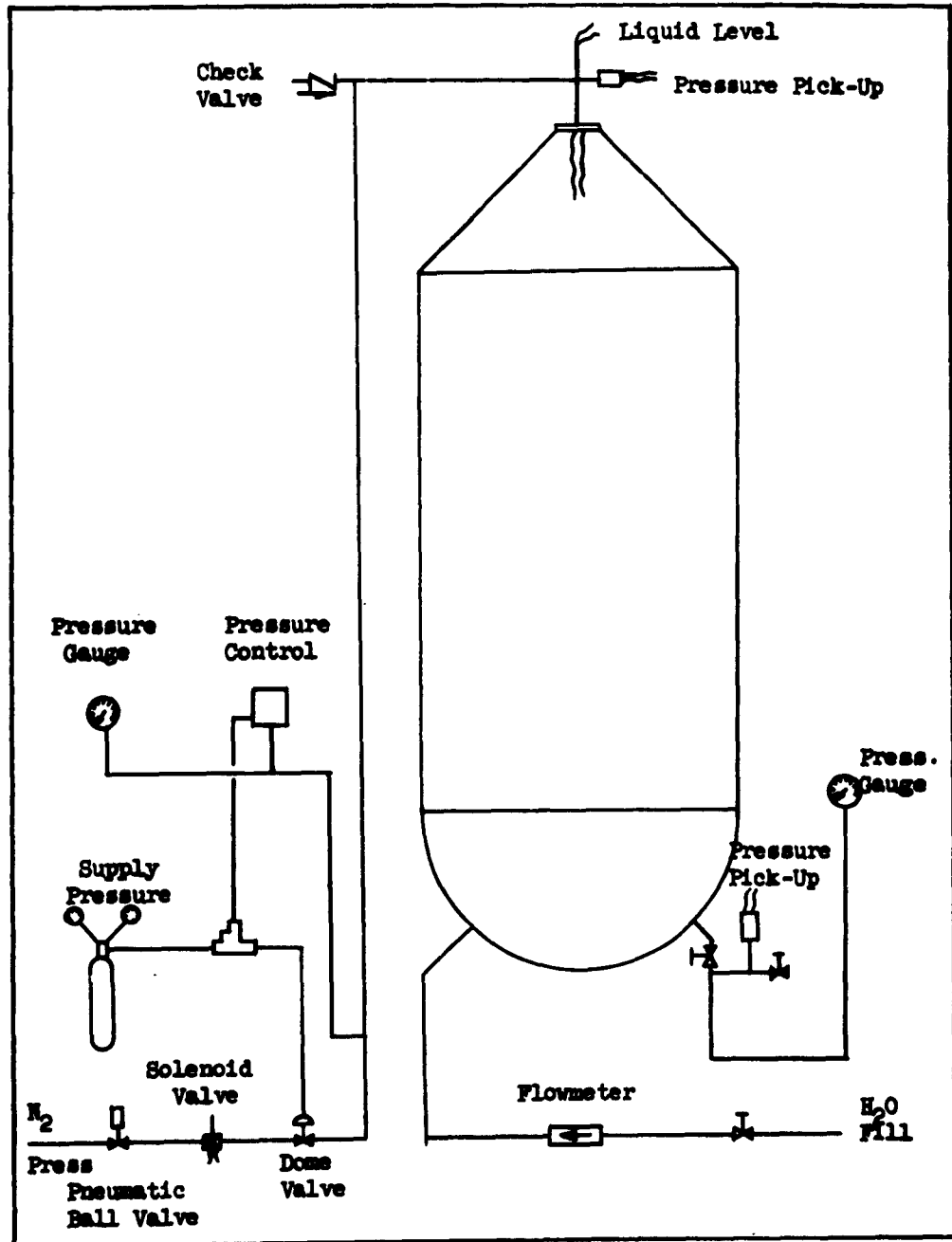
Check-out runs were resumed after the tank covering was completed. On December 5 damage was experienced by the test tank itself. During a fill cycle, the transition cone at the bottom of the tank buckled and split open, allowing several hundred gallons of LH_2 to run out into the first work level area. No fire resulted from this rupture. Examination of the damage revealed the cone had failed completely, buckling around the entire perimeter. Figures 78 and 79 are photographs of the damaged area. It would appear that the fill and drain line had moved upward and buckled the cone.

The funnel was removed from the tank and the flanges salvaged. A new cone was welded to the old flanges and the new assembly installed on the tank. Leak checks revealed no leaks and testing was resumed.

When the damaged cone was removed, the interior was found to be covered with a fine, white powder. Further examination revealed this fine powder in the tank and in the plumbing. It was determined the powder was insulation material of the type used in the insulation of the fill and drain valves for test tank and each storage dewar. These valves are enclosed in an aluminum can which is filled with the powder insulation. Each can was opened and a bad leak was found in the fill valve to the test tank. A Teflon gasket had failed which allowed the powder insulation to be drawn into the fill line and distributed throughout the plumbing system. The valve was repaired and the plumbing cleaned of insulation powder.

Three possibilities exist that could have caused the failure of the transition cone:

    (a) Overpressurization of the fill line
    (b) Explosion in fill line
    (c) Excess insulation plugging filter

Check-out of the thermal facility was resumed and was found to be operational.

During the latter part of November, a meeting was held with Edwards Air Force Base personnel, and it was agreed that the major emphasis of the thermal test program would be the study of stratification phenomena. To accomplish this, a special temperature probe was installed to study the stratification phenomena in the upper or lower region of the test tank.

Thermal testing began in December, 1961. Several preliminary runs were made (without recording data) for a final check on the entire system. On several occasions when the run button was pushed, the system would short circuit and stop. It was first though that the insulation may have opened up again and had made contact with the lamps again even though they were protected by the screen wire covering. A check of the tank revealed that the cover was intact and was not causing the trouble. The cause was then suspected to be corona discharges taking place within the evacuated bell chamber.

Earlier in the program the possibility of corona effect was discussed with DGRPT, and at their request, contact was made with the Martin Company, Denver, Colorado, for information on this subject. The information from Martin-Denver

FIGURE 78
PHOTOGRAPH OF DAMAGED TRANSITION CONE (1)
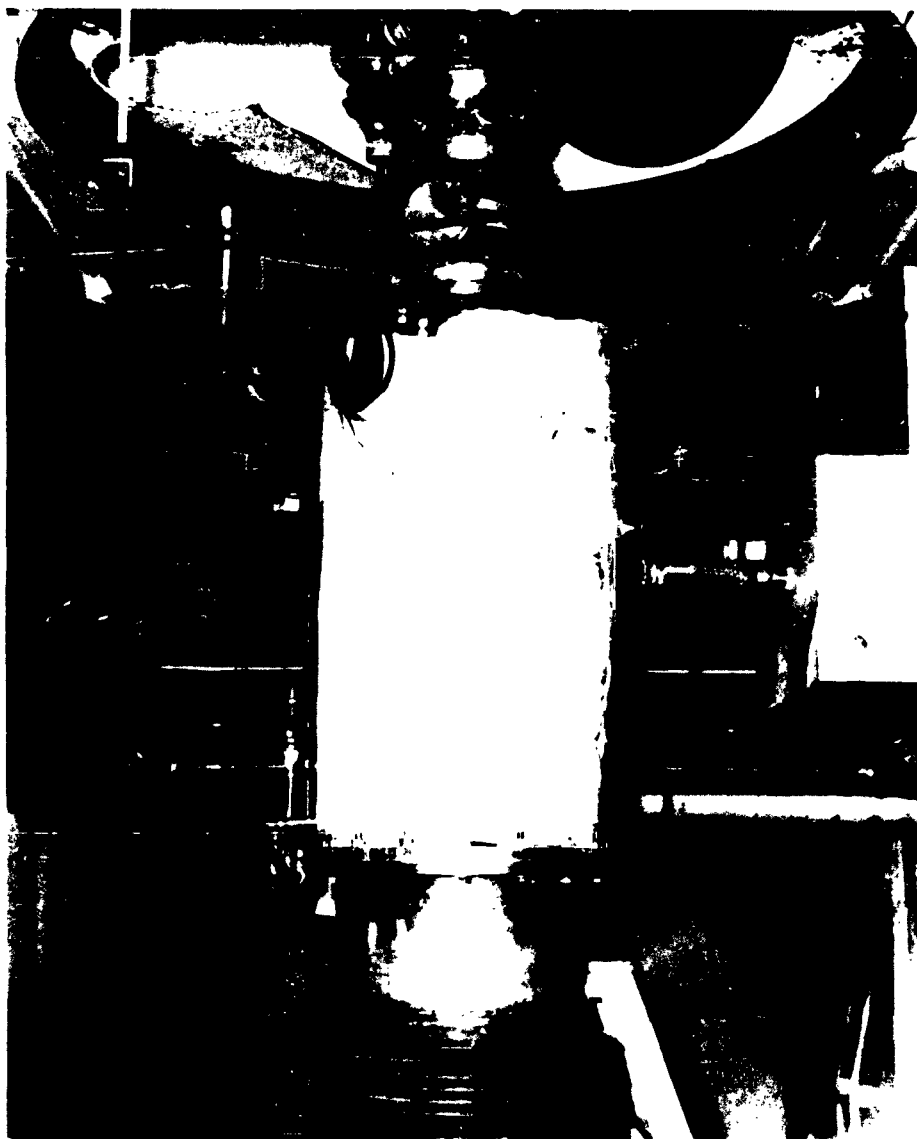
FIGURE 79
PHOTOGRAPH OF DAMAGED TRANSITION CONE (2)

was limited and inconclusive. Therefore, a test procedure was devised to check the possiblity of corona in the vacuum bell. A stainless steel test cylinder was installed and the bell sealed. The vacuum bell was evacuated to 20 mmHg and then increased in .5 mm increments. At each pressure the lamps were turned up to full voltage and then back to off. At no time did corona occur.

During the time that Beech was conducting these tests, the supplier of the heat lamp system (Research, Inc.) also conducted a series of tests and forwarded their data for consideration. This information indicated that corona discharges could be obtained on a 480 volt system operating in a pressure range of approximately 1.7×10^{-2} mmHg up to 1.1 mmHg. The possiblity of a discharge was reduced as the pressure increased above 1.1 mmHg. Tests also were conducted by Research, Inc. on a 240 volt system with no discharge obtained.

At the time the system was designed, it was known this phenomenon was possible with a 480 volt system and that a 240 volt system would materially reduce this possibility if not entirely eliminate it. However, at the time a 240 volt system was not available from Government sources and a 480 volt system was. Therefore, the 480 volt substation was installed.

After considering the data submitted by Research, Inc., which apparently bears out the results of the tests conducted in the heat tower by Beech, it was decided that for each thermal test, a pressure would be established where corona discharge did not occur and the test would be conducted at that pressure. The only difference in conditions existing between the corona tests and the actual thermal run is the temperature. The corona tests were made at ambient temperature. What effect this might have is not known.

3.5.3   Electrical and Data Acquisition

During the four thermal test runs, it was believed that the data acquisition system performed satisfactorily. While each test was in progress, the system was checked by a monitor scope. No discrepancies were noted during the runs and it was assumed that data was being accurately recorded since the system was balanced   prior to each run. In addition, the eight channels of the system which are recorded on strip charts, as well as magnetic tape, indicated the system was performing satisfactorily. A total of 96 channels were used, with the data being taken on magnetic tape.

After the tests were concluded, the magnetic tapes were processed and data from them examined as to quality. It was found the data was widely scattered and eratic.

It is believed the difficulty was caused by the corona discharges experienced just prior to the actual run in finding the pressure the system would tolerate. This caused a loss of synchronization in the multiplex system involving the commutator and the analog to digital converter that provides the data for the magnetic tapes. Contributing to this problem was dynamic resistance in the commutator itself. These combined difficulties apparently caused a shift of data on the tape. Investigation revealed that reduction with any real meaning was impractical.

3.5.4 Recommendations

Testing of the stainless steel tank has revealed serious problems in the control of the vacuum bell pressure and in the performance of the data acquisition system. It is felt, at this time, consideration should be given to certain desired changes before testing of the titanium test tank is scheduled. The changes are recommended as follows:

(a) Fabricate and install end closures on the vacuum bell to provide a closed vacuum system not dependent on large inflatable seals.

(b) Rework the data acquisition system to eliminate those problem areas known to exist and modification to provide a more reliable system.

(c) Convert the 480 volt power supply to 240 volt to eliminate corona discharge.

It is believed that if these changes are made, the system will then be capable of taking accurate and reliable data that will be usable to a large segment of the industry.

4.0 TESTING

4.1 Thermal Testing

On December 14, 1960, five programmed flow control tests were conducted without any difficulty. After these tests were completed, a 4-level heat rate thermal test was performed on the stainless steel experimental test tank. A description of the tests and the results is as follows:

A pertinent tank description is that of a 7,000 gallon capacity, liquid hydrogen fill,1/8" min-K insulated, stainless steel, pressure stiffened tank. The pressurization was provided by hydrogen gas boil-off maintained at 10 psig.

After filling, the outer surface of the tank was exposed to ambient conditions for a period of ten minutes. The resulting equilibrium temperature of the outer surface was 380°R, which was in good agreement with that of the theoretical analysis for 1/8" evacuated Min-K 504.

Three constant rate radiant heating intensities were imposed upon the tank. These rates were approximately .125, .250, and .375 Btu/ft^2-sec. The rates were only approximate, since a considerable amount of uncontrolled convective heat transfer resulted from exposure to a nitrogen gas environment during heating. As a result, the outer surface temperature varied considerably with tank height during the heating tests. The first two levels of intensity were maintained for a period of five minutes or more; the latter level was maintained for approximately one minute. Figure 80 shows the temperature distribution throughout the tank during heating at the approximate level of .375 Btu/ft^2/sec. The outer surface temperature varied from 415°R at the lower end of the cylindrical section to 833°R near the upper end of the cylindrical section. The inner surface temperature remained at 35.2°R + 1°R, the same as the temperature throughout the liquid. Temperatures of the liquid were taken at various distances from the tank wall ranging from .1 inch to 4 feet. Liquid temperatures were also taken at various heights in the tank. No temperature change occurred at any point in the liquid during these tests. It is interesting to note that the bulk temperature of the liquid in the tank after 20 minutes at 10 psig, 35.2°R, was the same as the equilibrium temperature of the hydrogen at 0 psig prior to leaving the storage dewar.

The above test data is presented for reference only and is not to be used as a criteria for calculations or design. This is due to the response time of internal temperature probes not being fast enough to record the actual changes of temperature versus time. Therefore, there is an inherent time error that cannot be compensated for in this series of tests. This problem must be investigated further to determine a method of accurate measurement of rapid temperature changes at LH$_2$ temperatures.

4.2 Hydrostatic Testing

The hydrostatic test procedure that was followed during this program is

FIGURE 80
TEMPERATURE DISTRIBUTION
STAINLESS STEEL TANK THERMAL TEST
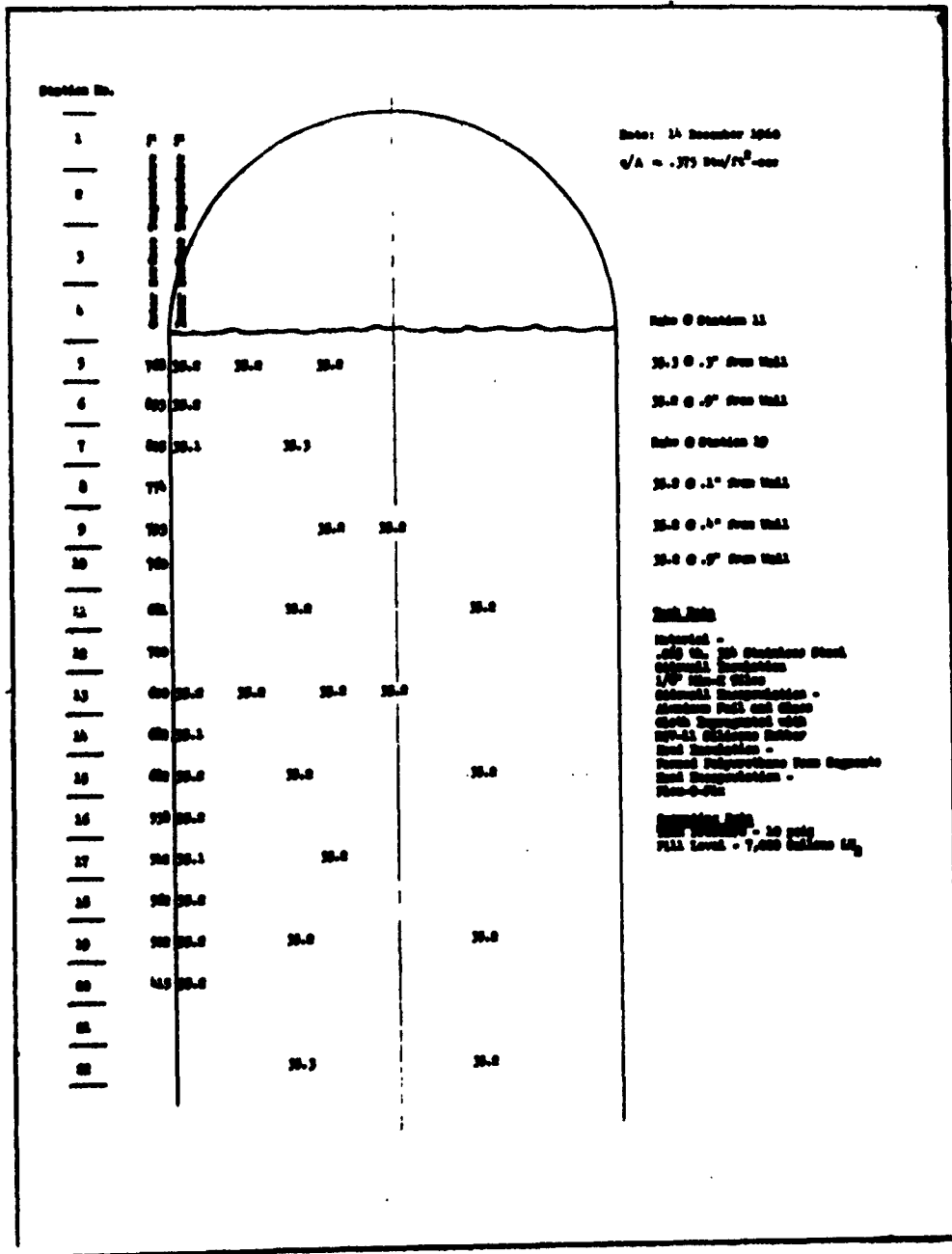
outlined in Engineering Test Request No. 4446. The results of testing and the conclusions drawn are discussed in the following paragraphs. The weight of the titanium tank as shown in Figure 85 was 460 lbs.

Figure 81 is a curve showing the total pressure applied versus strain. The pressure values shown do not include the hydrostatic head which had a value of 10 lbs/in^2 gage. The barometric pressure was 12 lbs/in^2.

Figures 82 and 83 are curves showing the actual and theoretical stresses at various points on the tank. The tank is divided into 14 stations to aid in locating the area of stresses discussed. Station 1 is located at the man-hole cover plate of the forward head.

4.2.1 Comparison of Actual and Theoretical Stresses

In comparing actual and theoretical stresses, it is seen that in almost every case the actual stresses are less than those predicted by theory. This is largely a result of the fact that a conservative analysis was made in determining the theoretical stresses. In areas of pure membrane stress, the minimum skin gage was chosen in computing stresses. The worst possible conditions were chosen at discontinuities. Since these conditions did not exist in the test tank, the measured stresses normally were less than the theoretical values.

There are other more specific factors which affect the differences in stress. These factors will be discussed for each station as follows:

Station 1 (Center of Man-hole Cover)

The actual and theoretical stresses were found to be nearly equal at this location. The strain gage was far enough from any discontinuity to be unaffected by any concentrations. In addition, the skin gage must have been nearly equal to that used in the theoretical calculation.

Station 2 and 12 (Hemisphere or Knuckle)

Excellent pressure strain curves were obtained in this area and since no discontinuities were near the gages, it must be concluded that stress differences are due to a variation in skin thickness. The theoretical stress was determined using a skin gage of .017 inches and resulted in a stress of 57,000 lbs/in^2. If a skin gage of .021 is assumed, the theoretical stress is found to be 47,200 lbs/in^2, which is only 2,400 lbs/in^2 greater than the measured stress. This difference may easily be accounted for by experimental error, differences in Poisson's ratio, modulus of elasticity, or other similar factors.

Station 3 and 11 (Hemisphere-Foam Juncture)

In the theoretical analysis, complete fixity was assumed at these stations because of the foam filler between the skirt and tank. Because of this, the only stress in the circumferential direction is from Poisson's effect

FIGURE 81
TOTAL PRESSURE LESS HYDROSTATIC PRESSURE
Vs.
STRAIN
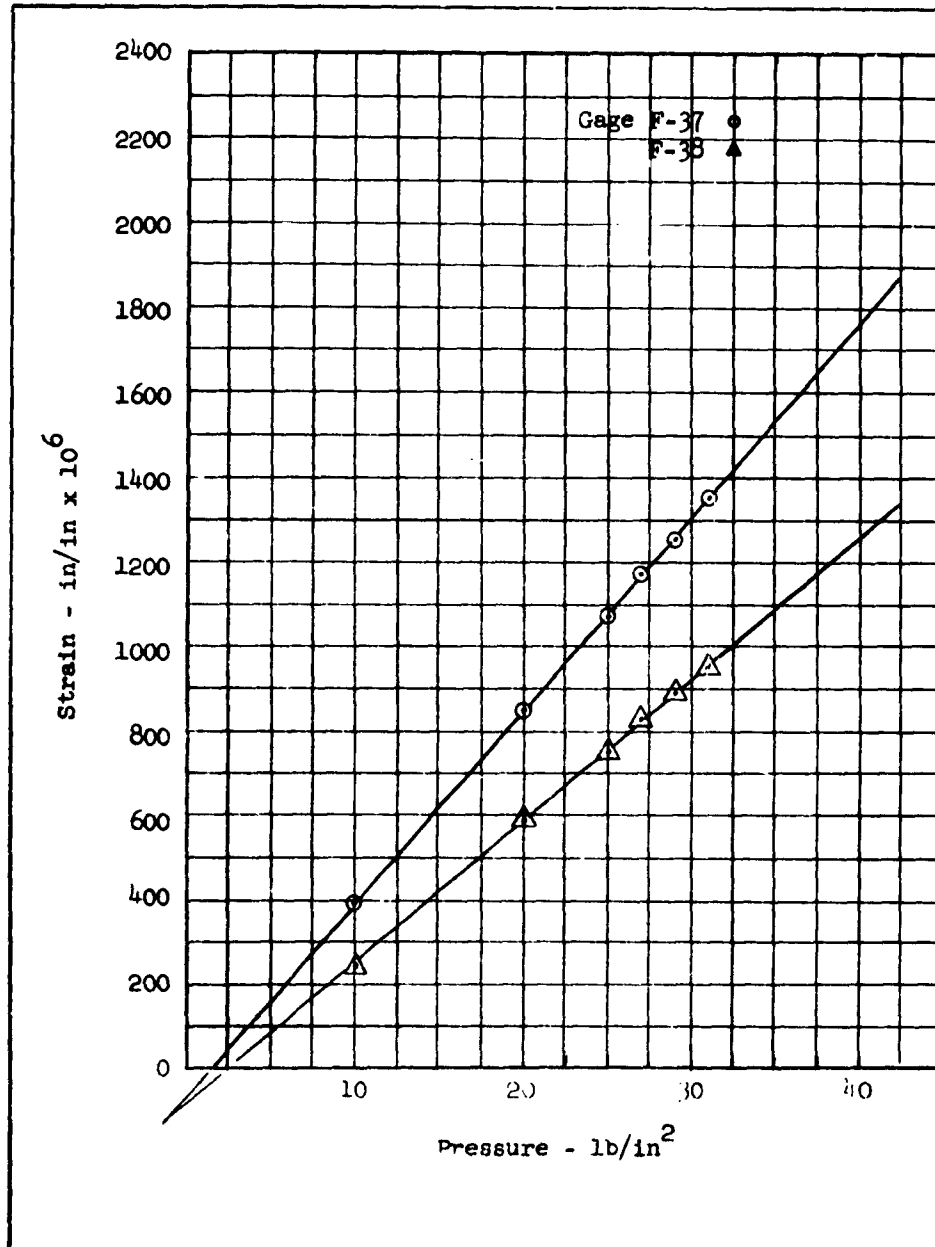
FIGURE 81
TOTAL PRESSURE LESS HYDROSTATIC PRESSURE
Vs.
STRAIN
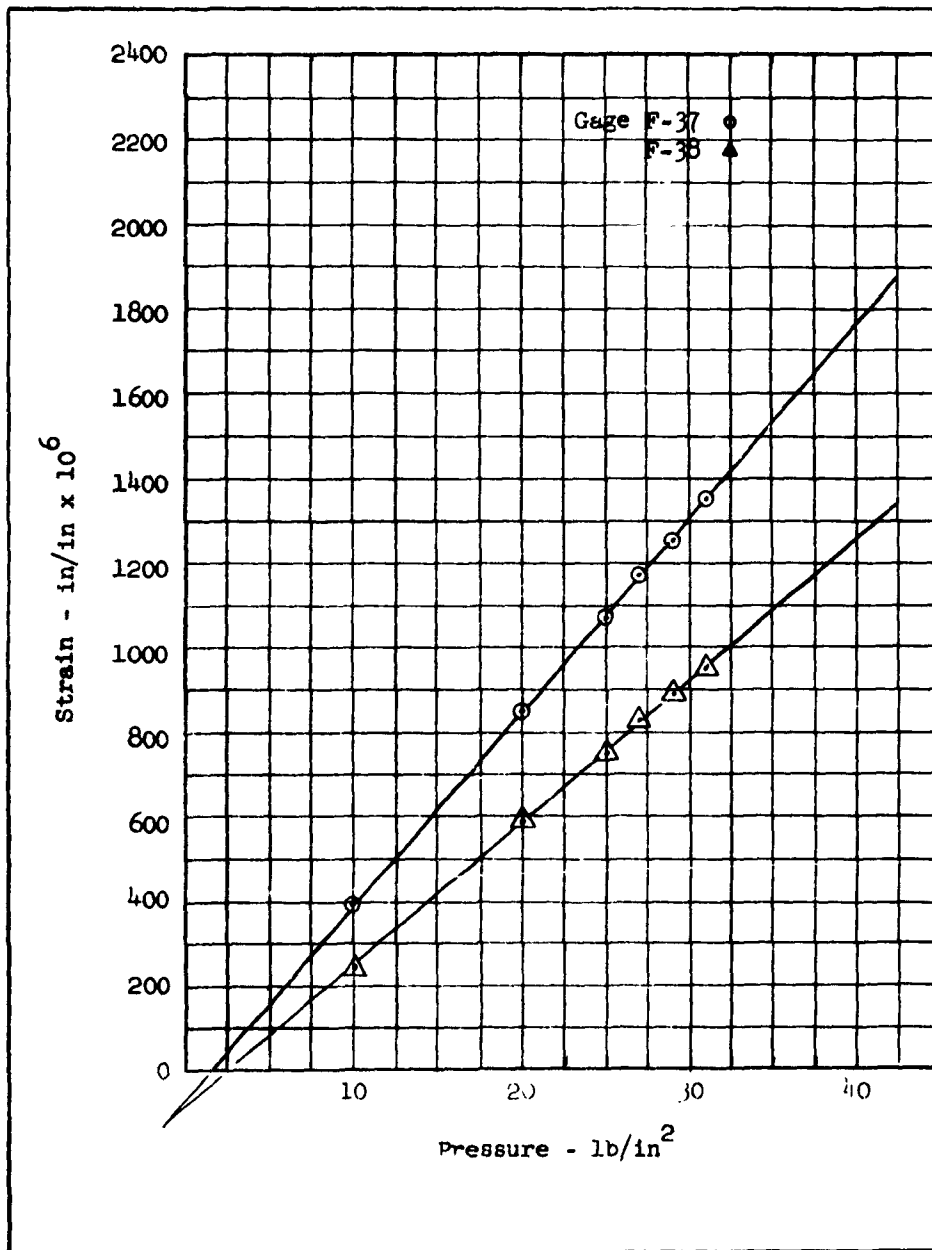
FIGURE 82
MERIDIONAL STRESS
7,000 GALLON TITANIUM TEST TANK
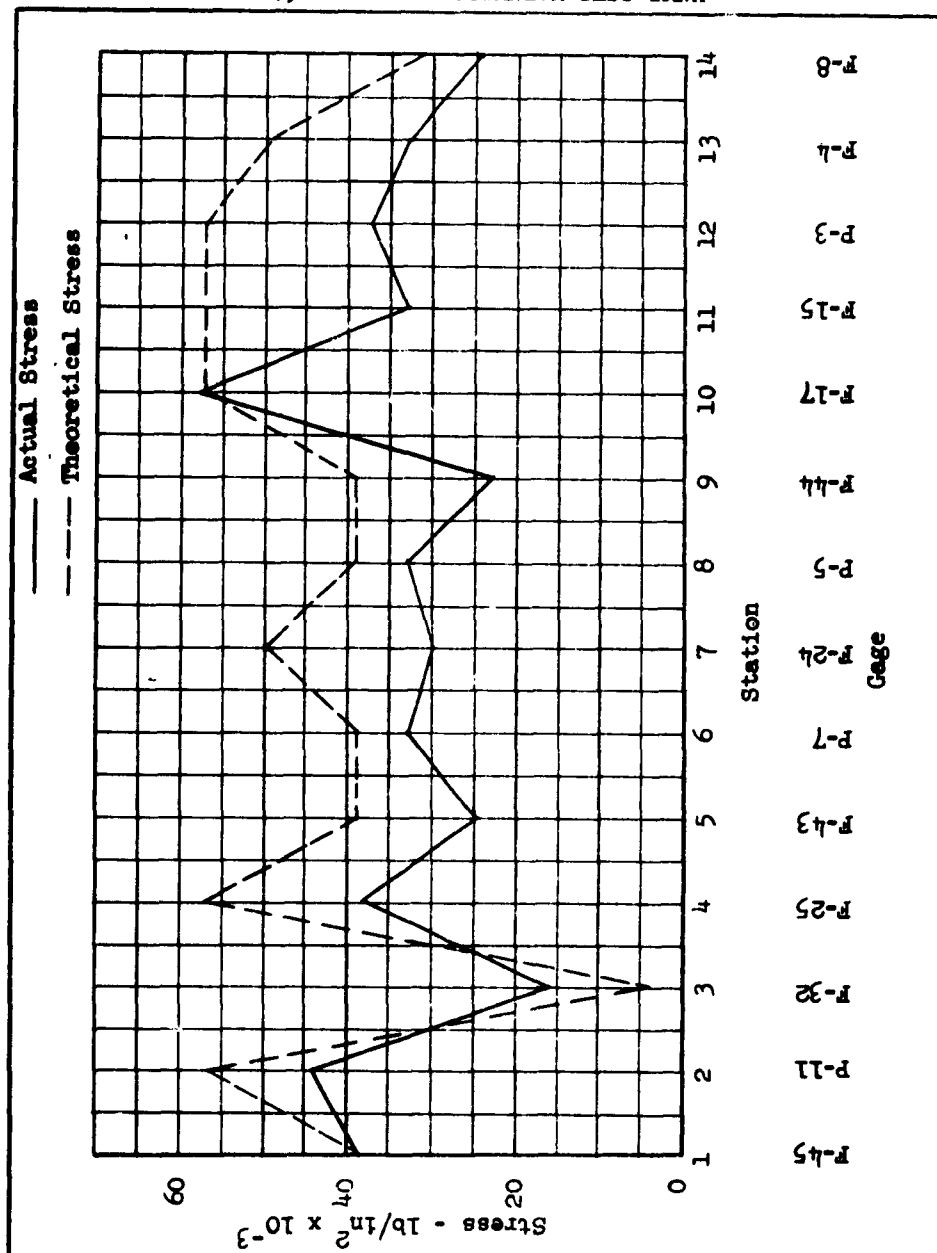
FIGURE 83
CIRCUMFERENTIAL STRESS
7,000 GALLON TITANIUM TEST TANK
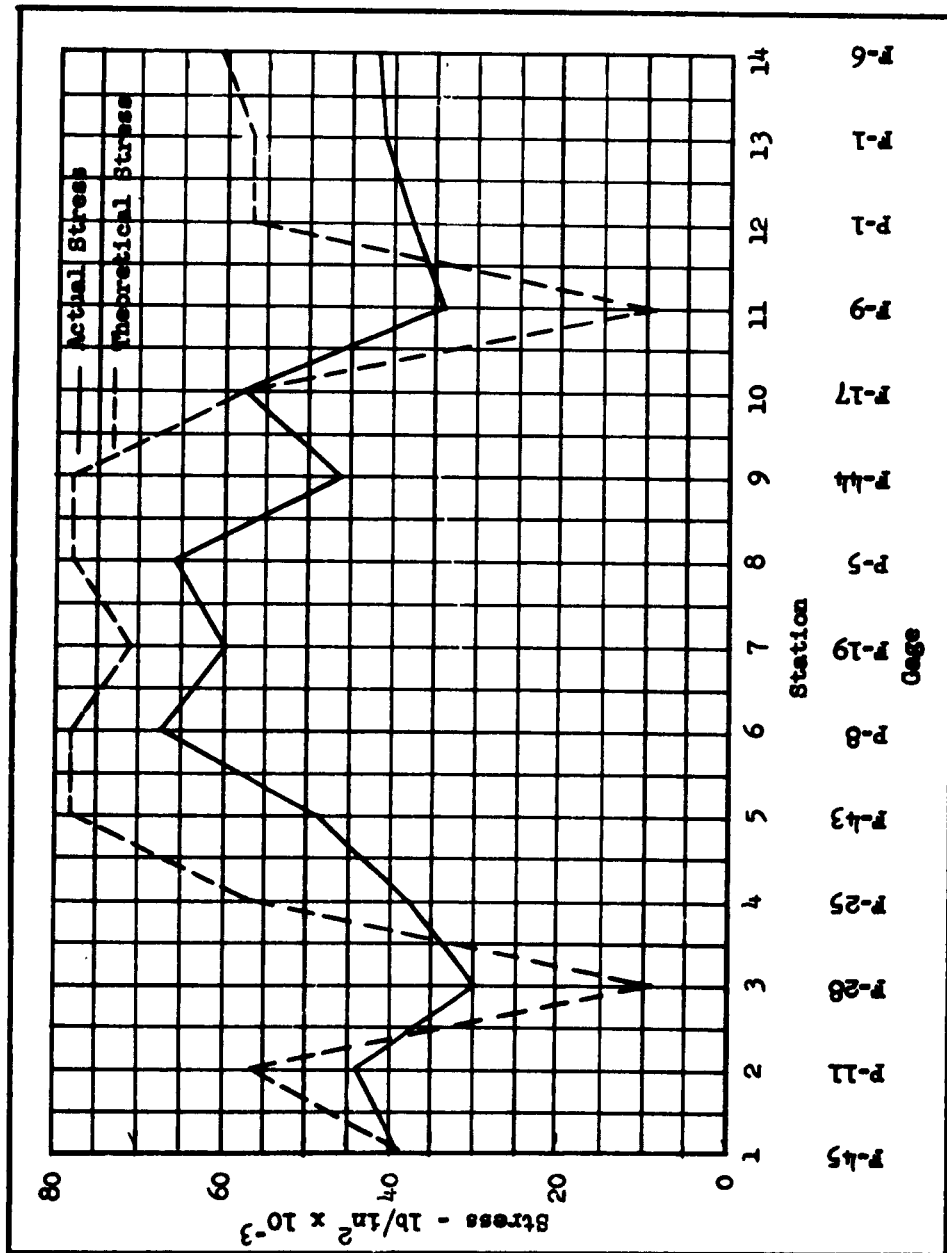
FIGURE 65

Photograph Showing Titanium Tank
After Successful Hydrostatic Test

FIGURE 85
PHOTOGRAPH SHOWING FOUR-MAN LIFT
OF 7,000 GALLON TITANIUM TANK

caused by bending in the meridional direction. The curves show the circumferential stress to be much larger than that predicted by theory. This must be caused by an expansion in the circumferential direction which indicates that the foam did not produce fixed ended conditions. The result of this effect on the meridional stresses is shown by the curve. Gage F-32, which is on the outside of the tank, indicates a stress which is higher than that predicted by theory. This is to be expected since the assumed fixed end condition would produce a higher bending moment than would result from an elastic condition of the foam filler. The reverse effect of the decreased bending moment is shown by Gage F-15, which is on the inside of the tank.

Station 4 and 10 (Cylinder-Hemisphere Juncture)

Some experimental error is believed to exist at one or both of these points because of the large stress difference between Gages 17 and 25. These two gages should show nearly equal stresses, but Gage 17 indicated a much higher stress than Gage 25. Because of this condition, it is felt that the recorded data for these gages is unreliable.

Station 5, 7, and 9 (Cylinder Weld and Base Material)

Stresses at these stations demonstrate the effect of the increased modulus of elasticity of the weld in that there is a decrease in the circumferential stress from that experienced in the pure membrane areas. The effect is small and produces no serious design problems. It is unfortunate that the gages reading meridional strain did not respond properly; therefore, no indication of bending stress was obtained.

Station 6 and 8 (Cylinder)

Any difference in stresses at these points is probably due to variations in skin thickness or material properties. All gages in these areas showed good agreement; therefore, it must be concluded that little experimental error exists.

Station 13 and 14 (Cone and Knuckle)

Meridional stress values show fairly good agreement, but a large difference in circumferential stresses exists. A portion of this difference may be explained by variations in skin gages or material properties, but it is felt that other differences exist.

Station A and B (Rings)

A comparison of the actual and theoretical stresses was not made in Figures 82 and 83. The actual stresses were generally lower than the theoretical values. Again, a portion of this difference may be explained by differences in material properties or skin gage. This is particularly true with gages F-39 through F-42. But, at the man-hole ring where discontinuity stresses were quite high theoretically, the actual and theoretical stresses differed almost by a factor of two. The actual stresses were only slightly different

than those at the vent ring. These facts indicate that the stress concentrations at a discontinuity are not as serious as the theoretical analysis indicated.

4.2.2 Conclusions

In general, the actual stresses were less than the theoretical stresses. Figures 82 and 83 show that the two stresses followed the same trend. The major exception to this rule occurs at the foam-filled areas where the actual stresses were higher than the theoretical.

The data indicates that the stress concentrations at discontinuities are not as serious as would be expected from a theoretical analysis.

In the theoretical analysis, it was assumed that the foam-filler between the skirt and the tank shell produced a fixed condition in the shell material in contact with the foam. The strain gage readings indicate that better correlation is obtained if the effects of the filler are ignored.

The results show that a reasonably accurate analysis may be made in designing large titanium tanks. No problems exist in designing fittings of a sufficient strength at junctures. It is quite possible that the design of components at these discontinuities may be overly conservative.

Figure 84 shows the tank being removed from the test tower after successfully completing the hydrostatic test. Figure 85 shows a four-man lift of the tank to emphasize the lightweight construction.

Following the procedure of finding a pressure where corona discharge did not occur, two thermal test runs were performed on December 12, with qualified success. Two more thermal test runs were performed on December 16, with greater success. Of the latter two runs, one was made without heat applied to the side wall and the other with heat applied to the sidewall. Results of the tests will be given below, Figures 86 to 90

Scale: 1/2" = 1'

7,000 Gallon

6,760 Gallon

17"

#1 .

#2 .

6,300 Gallon

6,000 Gallon

Location of Two Temperature Probes in Tank
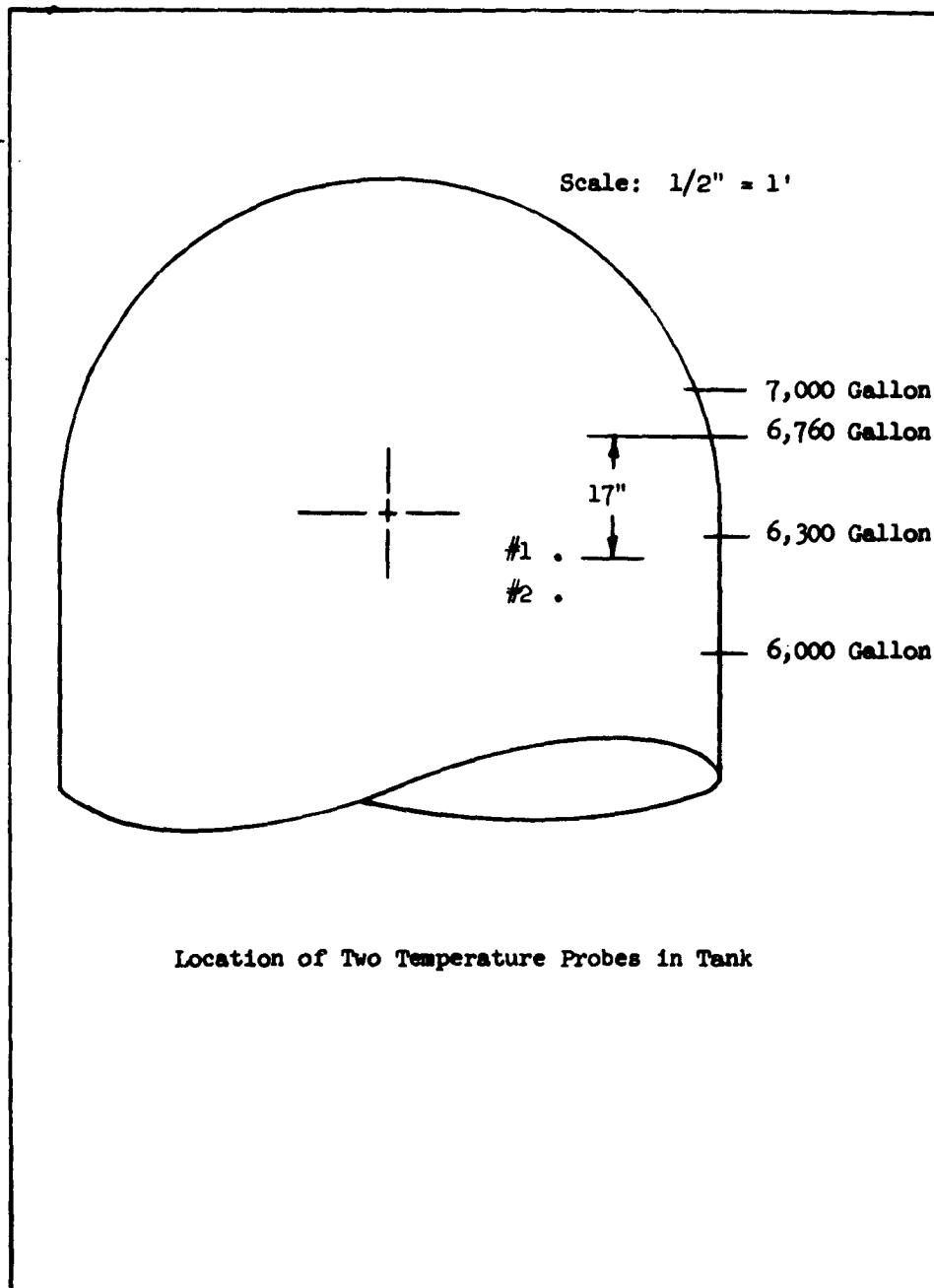
FIGURE 87
LH$_2$ IN TANK VS. TIME

Time - Seconds
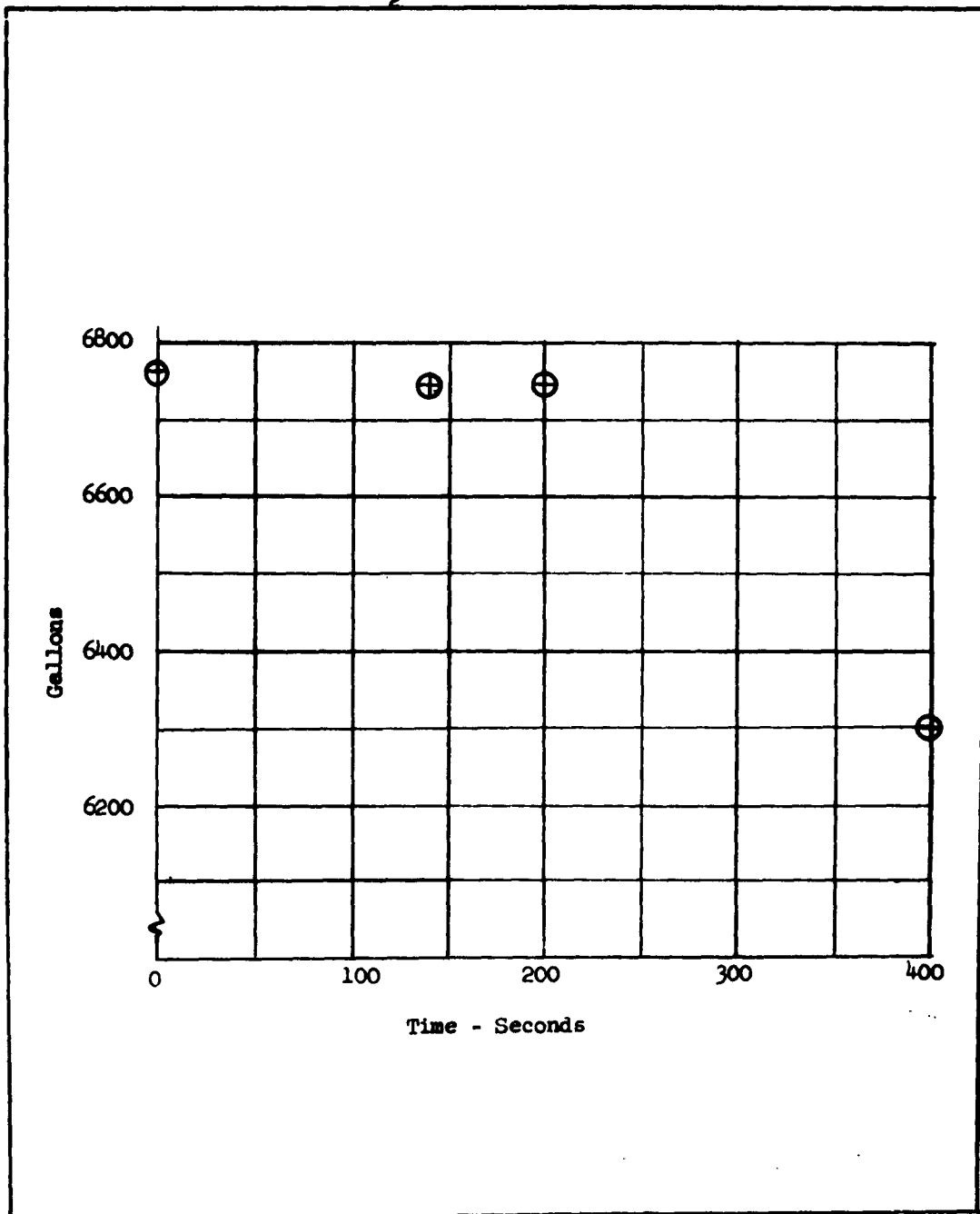
FIGURE ᘓᘓ
VENT FLOW RATE VS. TIME
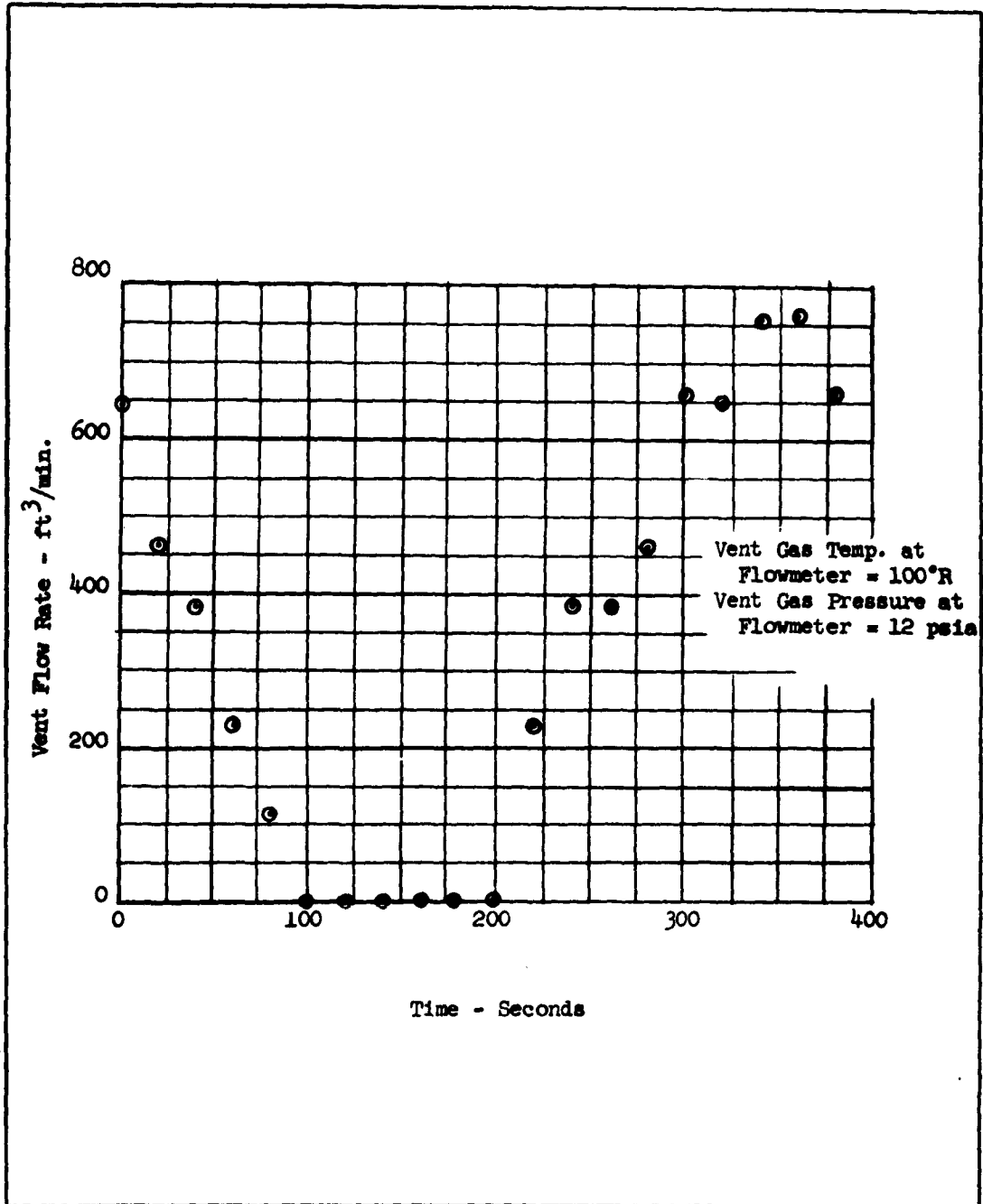
FIGURE 82
INTERNAL TEMPERATURE VS. TIME
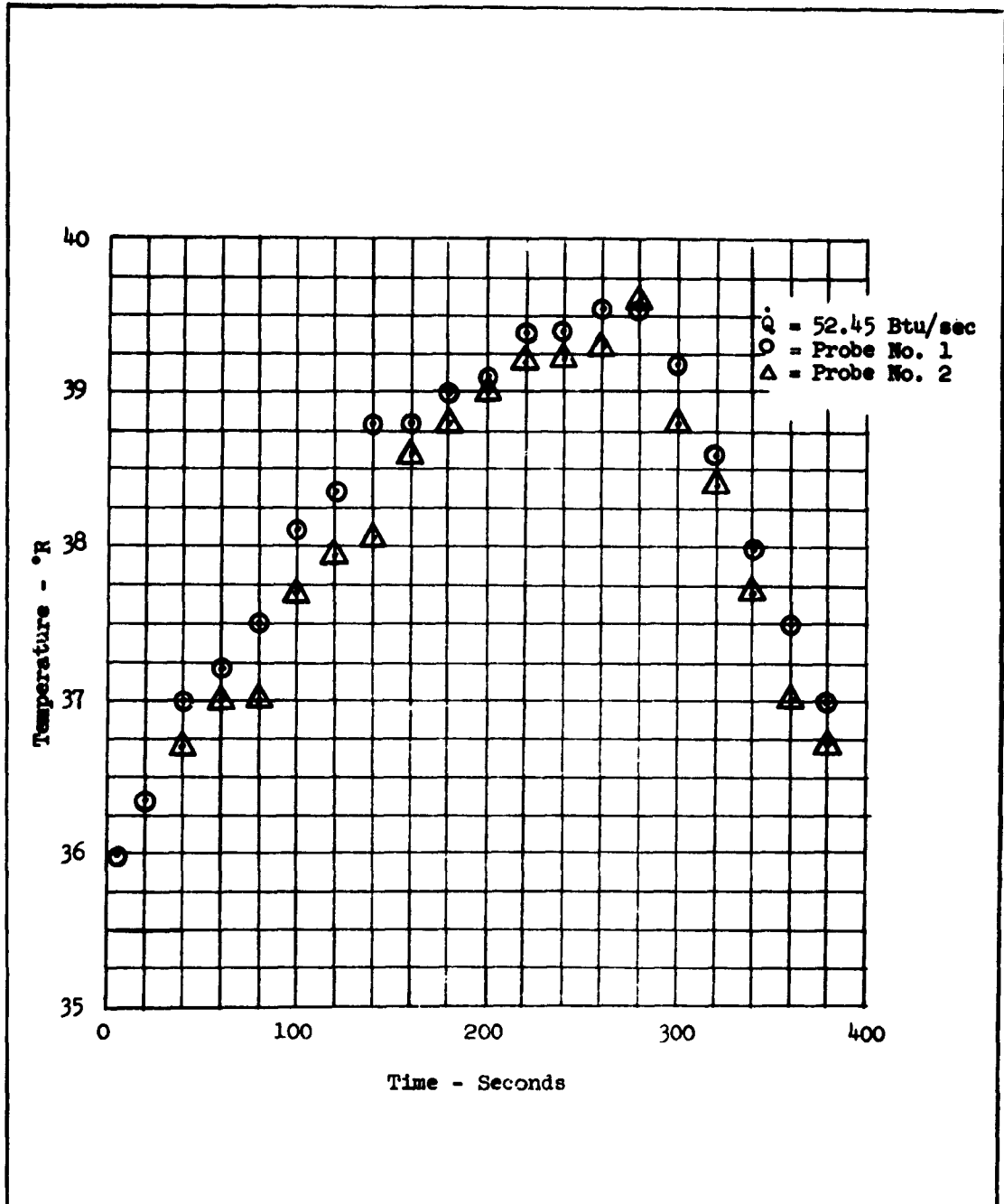
FIGURE 90
TANK PRESSURE vs. TIME
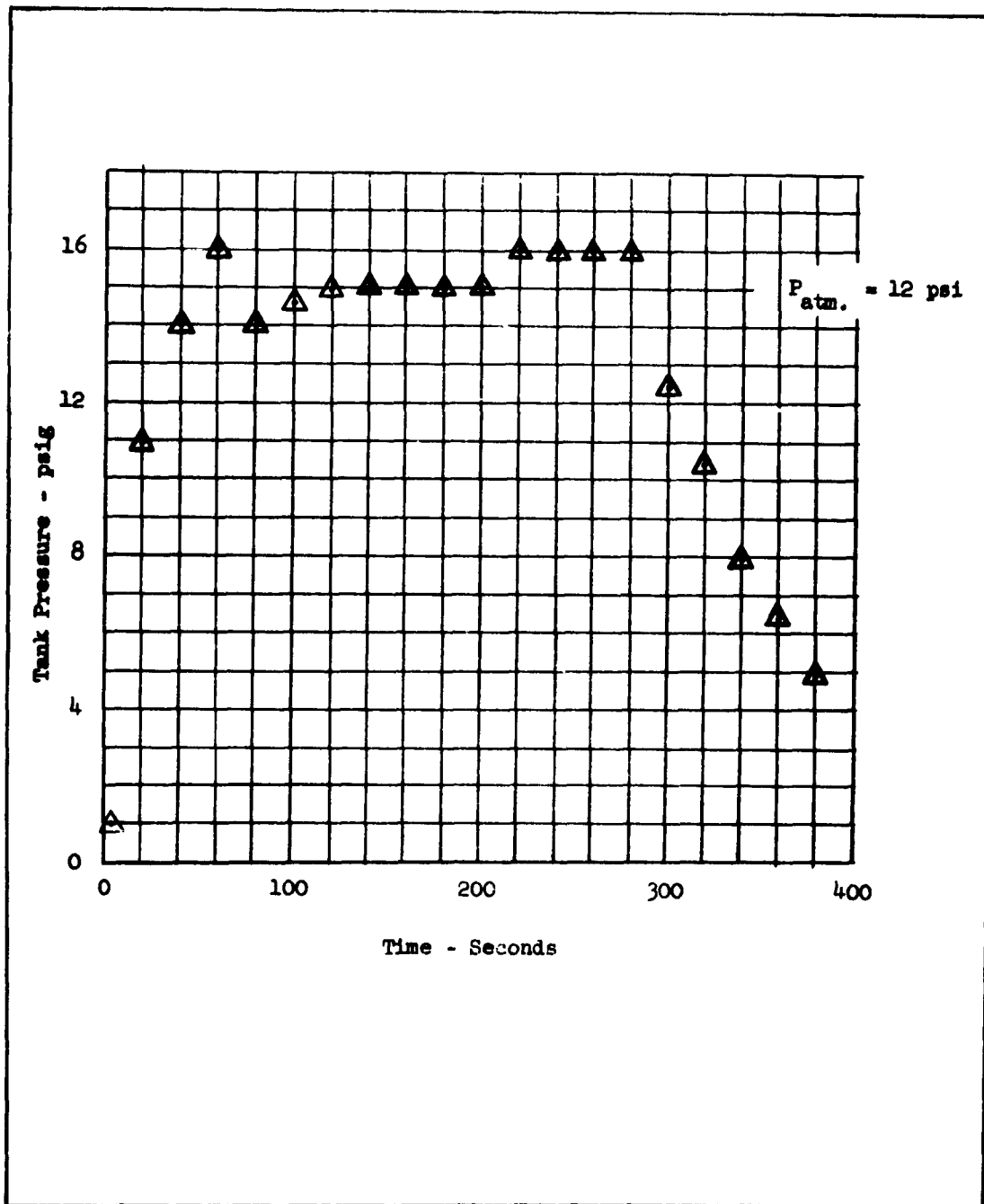
APPENDIX I

Trip Report - Surface Temperature Measurement Industry Survey
               13 August - 1 September 1961
               T. Bielawski and F. Major

McDonnell Aircraft, St. Louis, Missouri

The initial contact was made with Mr. Holland Hommes, who is in charge of the
high temperature thermocouple development program. No valuable information
was obtained due to the high temperature nature of the program which Mr. Hommes
supervises. However, through Mr. Hommes we contacted Mr. Russel Vogelsang.
Mr. Vogelsang, who is directly connected with surface temperature measurements
under radiant heat conditions, suggested the possibility of using Weldomatic
Model 1026 for welding the thermocouple directly to the aluminum foil. No
yardstick for backing up the temperature measurements by thermocouples was
available at this company.

Armour Research Foundation, Chicago, Illinois

The problem of surface temperature measurement was discussed with two research
engineers of the heat transfer laboratory: Messrs. Alexander Goldsmith and
James C. Hedge. Mr. Hedge suggested a total radiation pyrometer for checking
thermocouple readings between 100 and 600°F. The attachment method was dis-
cussed, and the only feasible method of attachment was suggested as welding
the thermocouples directly to the aluminum foil; however, in order to obtain
2% accuracy, Finn effects had large bearing on the readings. The shielding of
the thermocouple wires with the same material as the surface in order to have
the same absorptivity on both leads, was suggested. The calorimeter problem
was discussed with the above mentioned engineers and graphs of our test runs
were shown to them. The large scatter of temperature on the surface was ex-
plained to be due to the end effects. They suggested rebuilding the calorimeter
into a cylindrical shape in order to eliminate the end effects and have uniform
heating.

Lockheed Aircraft Corporation, Palo Alto, California

The method used by Lockheed to measure skin temperatures is to measure the
inner surface temperature then calculate the surface temperature. Thermo-
couples are used for surface temperature measurements which were initially
baked at 1000°F for a period of one month then calibrated against a platinum
resistance probe, which has an accuracy of .01% at any reading. The thermo-
couples are peened to the surface, leads are covered with the material of
the same absorptivity as the surface to eliminate the Finn effect. No yard-
stick is used besides the calibration but the accuracy desired is in the
order of 5%.

During the research program on the surface temperature measurement under the radiant heating condition, they discovered nonuniform heating. Later tests proved that the heat flux from the infrared lamps was not uniform. In order to measure the heat flux, they developed a heat flux calorimeter which is a cylinder of 1" diameter which is painted black to simulate black body conditions. The thermocouple is peened beneath the black body surface to measure the temperature. Their assumption is that all radiating heat will be absorbed by this calorimeter and give fairly good indications if the heat flux at this point. Problems of very small gauge thermocouple wires made into junctions were discussed, and they suggested the mercury pool with silicon oil.

The people contacted at Lockheed were:

> Dr. Steinberg
> Dr. Shapiro
> Dr. Crosby
> Mr. Gilligan, Jr.
> Mr. Ken Frame

University of Colorado, Boulder, Colorado

The person contacted was Tom Arnburg. Two methods of mounting the thermocouple were suggested. The first method was to apply another outer layer and the second was to apply a strip.

It was pointed out that the temperature drop through one layer of foil and silicon rubber would be very small and negligible compared to the temperature drop through the fiberglas. To insure that the surface temperature was being measured, the best method to attach the thermocouples mounted between the third and fourth layers. This method of mounting would insure that the surface of the tank would be uniform, the thermocouples would not come loose, and the thermocouples would most accurately measure surface temperatures.

The second method of mounting was to apply a strip of foil down the entire length of the tank with the thermocouples mounted behind the foil. Using this strip of foil instead of smaller patches, it would be possible to lay the thermocouple wires in a straight line and eliminate finned effects. In the case of smaller patches, it is necessary to spiral the thermocouple leads to eliminated finned effects. Laying the wire straight would also reduce the thermal mass near the sensing point and also help to insure that the surface near the thermocouple was uniform.

In both methods of mounting, it was pointed out that the sensing tip of the thermocouple be in good contact with the inner surface of the outer layer of foil.

An epoxy-aluminum powder mixture that has been used as a bonding agent at fairly high temperatures was suggested as a means of mounting the thermosouples. Information about this mexture could be obtained from the Physics Department at the University of Colorado. The exact temperature range was not known.

North American Aviation

Initial contact was established with Messrs. Bill Vance and Bill Martin. Referred to Mr. Mal Clancy. No binding agent was known that would work at both high and low temperatures. The use of ceramic cement was suggested, but the cement required a high cure temperature.

Teflon tape, 7000g glass tape and aluminum foil tape were discussed. The teflon and glass tapes were made by Mystic Tape and the aluminum tape by 3 M. All three tapes were used at temperatures between 500 and 600°F with good results. The teflon tape, although having good bonding power at room temperature, had a tendency to shrink and crack when heated. All three tapes were used to hold thermocouples in place. A sample of aluminum tape was obtained.

Optics Laboratory

The following personnel were contacts:

> Mr. Seymour Knopkin, Supervisor - Optics and Special Materials
> Mr. Bob Kelmm, Sr. Engineer
> Mr. Ed Miller
> Mr. Joe Partyke

A visit was made to the Optics Lab to determine what type of pyrometer was available to check the thermocouple readins. It was pointed out that temperatures below 600°F are quite difficult, but not too impossible to measure with a radiometer. Using a Barnes 4RF2 Radiometer, the temperatures near 600°F could be measured within 2°F. If a check on the thermocouple readings were desired, a bid could be obtained from the Optics Department.

Mr. M. A. Hegan of the special materials section gave a list of strain gage cements that had been used at extremes in temperature with some success:

> | | |
> |---|---|
> | Allen PBS | Most highly recommended. Sample obtained. |
> | CA9R | Manufactured by Englehard Industries |
> | SM-25 | Manufactured by Emerson Cummings |
> | Foster 30-43 | Manufactured by Benjamin Foster Co., Philadelphia, Pennsylvania |

Douglas Aircraft Corporation

The following personnel were contacted:

John B. Douglass   Transducer Group Engineer
Space Vehicle Electronics
A2-260

Earle V. McNeil
W. L. Cellio

A method of gold brazing a piece of stainless steel shim stock and then spot welding the aluminum to the gold was discussed as a possible means of measuring surface temperature. The thermocouple was then spot welded to the stainless steel. It was noted that this system may have some thermal lag.

Convair

Initial contact was established with Mr. Bill Mitchell by phone and was referred to Fred Herzberg and John Heckenburger. A demonstration of the Weldomatic 1026 welder was given. An attempt was made to weld a copper constantan thermocouple to a 1/32 inch thick sheet of aluminum. The constantan thermocouple lead was welded to the sheet of aluminum foil without much trouble, but the copper lead could not be welded due to the heat conduction rate of both the copper and aluminum.

Mr. Franklin of the instrumentation group suggested Allen PBX as a bonding agent. It was pointed out that the exposed portions of the PBX should be coated with a fluoro lub grease to prevent moisture from entering into the joint.

APPENDIX II

BEECH AIRCRAFT CORPORATION

ENGINEERING TEST REQUEST

No.4446

From: H. E. Sutton   Date: November 8, 1961

To: J. R. Mabbitt   CC: J. H. Rodgers

Engineering Data: Page 1 of 2

This request supersedes and cancels Test Request 4785.

TEST SETUP:

7,000-gallon, 6Al-4V test tank with strain gages per Drawing No. 6090-4037.

TEST RUN CONDITIONS:

1. Pour foam in annulus between skirt and dome at both ends of tank.

2. With tank in top-suspended, normal upright position in pretest tower at zero gage pressure record strains.

3. Pressurize tank to 5 psig and record strains.

4. Start filling tank with water maintaining 5 psig gas pressure until lower end of cylinder is wetted after which the tank may be completely filled at zero gas gage pressure.

5. Record strains and hydrostatic gage pressure on bottom of tank.

6. Increase gas pressure at top of tank; when tank is completely filled, increase gas pressure in the following increments: 10, 10, 5, 5, 2, 2 psig, recording strains and gage pressures at each increment. Do not exceed 45 psig pressure on bottom of tank.

7. Empty tank of water maintaining constant 5 psig.

8. With tank in top-suspended, inverted position in pretest tower at zero gage pressure, record strains.

9. Pressurize tank to 5 psig and record strains.

10. Fill tank with water. Record strains and hydrostatic pressure at the bottom of the tank.

TEST RUN CONDITIONS (Continued)

11. Increase gas pressure at top of tank; when tank is completely filled, increase gas pressure in the following increments: 10, 10, 5, 2, 2, 2 psig, recording strains and gage pressures at each increment. Do not exceed 44 psig pressure on bottom of tank.

12. Empty tank and remove strain gages per Specification 7601.

13. Final tank configuration: Prepare for insulation installation.

INSTRUMENTATION:

1. Strain gages operative per locations in Specification 7601.

2. Pressure gages to measure:

   a. Hydrostatic pressure at lowest point of tank
   b. Gas pressure on water in tank

DATA REQUIRED:

1. Strain gage record: 2 records per each of 56 gages.

2. Pressure readings: Hydrostatic and gas gage recorded on strain gage record.
                           Barometric pressure at start of each day's test.

3. Temperature: Ambient air.
                           Tank water.

APPENDIX III

The following report (No. 10572) is presented in its entirety and without
change. Therefore, the page numbers contained in the report are the
originals and do not affect the numbering of this report of which it be-
comes a part.

TEST REPORT
ON
METHODS OF MOUNTING THERMOCOUPLES
FOR MEASURING SURFACE TEMPERATURE

F. Major
J. Brondyke
BEECH AIRCRAFT CORPORATION
Report No. 10572

September, 1961

1.0 SCOPE

The tests described in this report were performed to determine the best method of attaching a thermocouple to a 1 mil thick aluminum foil surface, and to determine what type of thermocouple mounting will most accurately measure the surface temperature of the test tank. The following tests were also conducted to check what effect position had upon the thermocouple readings.

2.0 TESTS PERFORMED WITH TEST FIXTURE NO. 1

The test fixture for this test was a 12" x 24" x 1/16" piece of 6061-T4QQ-A-327 aluminum metal. Eleven thermocouples were located on the specimen as shown in Figure 1.

```
  .          .          .          .
  1          2          3          4

        .          .          .
        5          6          7

  .          .          .          .
  8          9          10         11
```
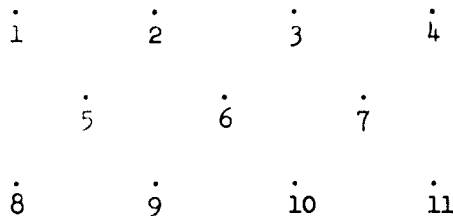
Figure I - Mounting Points of Eleven Thermocouples

The TC's were mounted on the aluminum sheet by drilling two 1/64 inch holes approximately 1/8 inch apart and inserting the thermocouple leads into the holes. The aluminum metal around each hole was then peened until the thermocouple lead was tight in the hole. The junction was then formed from the copper to the aluminum and from the aluminum to the constantan.

The first test was to check the output of each thermocouple on a Leeds and Northrup pot box. With the specimen at room temperature, all thermocouple outputs indicated within 1.4°F of each other. The second test was to place the specimen inside an oven at 317°F for 1.5 hours and read the outputs on the same Leeds and Northrup pot box. All thermocouples indicated within 3.6°F of each other; and excluding the two thermocouples in the lower right hand corner, readings were within 1.2°F of each other.

On 8 August 1961, two tests were conducted on the specimen using the radiant heating system. The first test was conducted with the test fixture in a vertical position. At the end of the four-minute test, Thermocouple No. 8 indicated the lowest temperature at 118°F. In general, the higher indicating thermocouples were on the upper level near the center and the lower indicating thermocouples were on the lower levels near the outer edges.

To test what effect position had upon the thermocouple readings, the test fixture was placed in a horizontal position. At the end of the 4-minute test,

E-270 - 1

TESTS PERFORMED WITH TEST FIXTURE NO. 1 (Cont'd)

the thermocouples near the center of the specimen read approximately equal and somewhat higher than those near the outer edges. The highest indicated temperature in the center of the specimen was 120°F and the lowest on the outer edge was 107°F. Power input on both tests was approximately 1.01 KW (0.5 btu/sec/ft^2).

3.0 TESTS PERFORMED WITH TEST FIXTURE NO. 2

The test fixture for this test was a 12" x 24" x 1/16" sheet of 6061-T4QQ-A-327 aluminum metal primed with GE XS-4004 silicone primer. A coat of GE RTV-11 silicone rubber was then applied to the primed side of the aluminum sheet. While the RTV-11 silicone rubber was pliable, a 1 mil thick sheet of aluminum foil, primed on both surfaces with the GE XS-4004 primer, was bonded to the sheet of aluminum. A second sheet of 1 mil foil, primed on the dull side with the silicone primer, was bonded to the first sheet of foil with another layer of RTV-11 rubber. The RTV-11 silicone rubber was then cured in the sun for approximately 3 hours.

Five thermocouples were attached to the specimen, two on the first level, one on the second level and two on the third level. The two thermocouples on the first level were placed approximately 8 inches in from the sides, and four inches down from the top. The thermocouple on the second level was placed in the center of the specimen. The two thermocouples on the third level were placed approximately four inches up from the lower edge, and eight inches in from the sides.

All thermocouples were copper constantan with fiberglas insulation. The thermocouples were spiraled for approximately six inches with the junction in the center of the spiral. The thermocouples were mounted on the specimen using a mixture of 3M's EC-1648 A/B and EC 1290. The spiraled thermocouple was then covered with a foil patch approximately 2" x 2" square and bonded with the 3M adhesive mentioned above. After the 3M adhesive had cured a small weight was placed on each spiral so that good contact would be made between the thermocouple and adjoining layer of foil.

On 8 August 1961, two radiant heat tests were conducted on Test Fixture No. 2. Power input in both cases was approximately 1.02 KW (0.5 btu/sec/ft^2).

With the test fixture in a vertical position, at the end of the four minute test the thermocouple indicated that the temperature had increased from 68°F ambient to 139°F and 118°F on the highest and lowest indicating thermocouples respectively. The highest indicating thermocouple was on the left hand corner of the upper level, and the lowest indicating thermocouple was on the right hand corner of the lower level.

With the test fixture in a horizontal position, the temperature increased from 70°F to a high and low of 129.5°F and 117.5°F respectively. Two high indicating thermocouples were noted; one in the center and the other in the lower left hand corner. The low indicating thermocouple was in the lower right hand corner of the fixture.

E-270 -1

4.0 TESTS PERFORMED WITH TEST FIXTURE NO. 3

The test fixture for this test was a 12" x 24" x 1/16" sheet of 6061-T4QQ-A-327 aluminum metal. Five thermocouples were mounted in a 2" x 2" area near the center of the fixture. All thermocouples were copper constantan with fiberglas insulation. Two thermocouples were peened into the sheet in the manner described in Paragraph 2.0. The other three thermocouple leads were welded to copper constantan strips approximately 1/4 inch square. One thermocouple was attached to the fixture near the upper, peened thermocouple with the welded side down, using a 3M EC 1648-A/B and EC 1290 mixture. The other two thermocouples were joined together (welded sides together) and mounted on the fixture near the lower, peened thermocouple using the adhesive mentioned above. The exposed surface of the strip thermocouple and the area near the peened thermocouple were cleaned to a high gloss when the 3M adhesive had cured.

On 8 August 1961, a radiant heat test was conducted using Test Fixture No. 3. The power input for 210 seconds was 1.02 KW (0.5 btu/sec/ft^2). The upper, peened thermocouple indicated 162°F and the upper strip thermocouple indicated 170°F. The lower, peened thermocouple indicated 157°F and the outer and inner strip thermocouples indicated 168°F and 164°F respectively.

The results of these three tests show conclusively that the calorimeter produced uneven heating due to both stratification and end effects. The stratification was particularly noticeable when the fixture was in the vertical plane and a large ΔT existed between the upper level thermocouples, which indicated high; and the lower level thermocouples, which indicated low. The end effects were noticeable when the fixture was in either the vertical or horizontal position and the thermocouples near the center of the fixture read higher than those near the edges. These tests also show that the emissivity of the mounting surface of the thermocouple must approach the emissivity of the test fixture.

The following tests were made on 28 August 1961 on the 3M No. 425 pressure-sensitive aluminum foil tape. The purpose of these tests was to determine what affect thermo shock and high and low temperature had upon the adhesive. The aluminum foil was 3 mil thick and the adhesive was 2 mil thick. The initial sample of aluminum foil was obtained from North American Aviation in Los Angeles.

A 1" x 1" piece of foil was used to stick a thermocouple to a 2" x 2" piece of 1/8-inch thick aluminum shim. The sample was placed in an oven at approximately 300°F for 20 minutes and then the sample was dipped in LN$_2$, using the thermocouple lead as a means of suspension. An attempt was made to shake the thermocouple and tape from the shim. The entire cycle was repeated on the fixture several times, but the bond on the tape could not be broken.

Another shim sample was made using two 1-inch strips to cover the shim. The sample was then placed in an oven at approximately 600°F and after a 30-minute

TESTS PERFORMED WITH TEST FIXTURE NO. 3 (Cont'd)

stabilizing period, the sample was dropped in LN_2. This cycle was repeated several times, but the bond could not be broken between the foil and the shim. The only change that the foil tape experienced was that the foil, once it had pulled loose from the shim, would not adhere again.

5.0   TESTS PERFORMED WITH TEST FIXTURE NO. 4

This test fixture was the same as Test Fixture No. 2, except the mounting of the temperature sensing units was changed. Three spiraled thermocouples and two platinum resistance probes were mounted in approximately a 5.5 square inch area. The five sensors were then covered with one common sheet of foil. The platinum resistance probes are type P/N 3007. A bridge balance circuit was designed to signal condition the information from the probe.

On August 15, 1961, a radiant heat test was conducted on Test Fixture No. 4. Power input for four minutes was 1.016 KW (0.5 $btu/ft^2/sec$) from an ambient temperature of 70°F. The two resistance probes indicated temperatures of 145°F and 155°F and the highest indicating thermocouple was 109°F.

6.0   TESTS PERFORMED WITH TEST FIXTURE NO. 5

This test fixture was the same as Test Fixture No. 2 except for the mounting of the thermocouples.

The following tests were run using the radiant heat system, and the foil tape. Six thermocouples were placed on the fixture in close proximity of each other, near the center of the 12" x 24" plate. All thermocouples were within an area of 3-1/2" x 1-1/2". On the fixture were two spiraled, 2 straight, and 2 thermocouples placed between the outer layer of foil and the second layer of foil, bonded in place with the GE RTV-11 silicone rubber. The two straight thermocouples were covered for approximately 1-1/2" with foil tape. On both the straight and spiraled thermocouples the outer layer of fiberglas insulation was removed within 1/4" of the end of the foil tape. The leads were then twisted and a welded junction was made.

Three tests were performed with the power input set at approximately 0.5 btu/ft^2 for 4 minutes. Ambient temperature at the beginning of the tests was approximately 68°F and at the end of the 4 minute runs, temperatures indicated by all six thermocouples were within 3°F of each other on all three tests. The highest end temperatures at the end of the first, second and third tests, were 105.5°F, 100.5°F, and 109.6°F, respectively.

A Unitek Power Supply, 1032 Welding Head and HP-2000 Tweezer Handpiece were obtained on loan from Vinson Associates of Englewood, Colorado. This model welder was recommended by Russ Vogelsang of McDonnell Aircraft and also by Fred Herzberg of Convair.

Much time and effort was spent attempting to weld a 36 gauge copper constantan lead to the 1 mil aluminum foil without success. The HP-2000 Handpiece

E-270 -1

TESTS PERFORMED WITH TEST FIXTURE NO. 5 (Cont'd)

Tweezer was used with molybdenum-alloy-tipped electrodes. The 1032 Welding Head was then used with good results to weld the metals. The head was equipped with copper-cadmium-alloy electrodes.

On 30 August, a sample of 1 mil foil and copper constantan lead wire was sent to Unitek so a weld evaluation could be performed. (The evaluation would give the best possible pressure settings, power input and electrode type to obtain a weld between the copper constantan lead wire and the aluminum foil.) The Weld Evaluation Report was returned 12 September 1961.

7.0 TESTS PERFORMED WITH TEST FIXTURE NO. 6

The fixture for this test was the same as Test Fixture No. 5 with the following changes. One of the straight foil-covered thermocouples was placed on the back side of the 1/16-inch aluminum sheet to measure the Δ temperature from the top of the foil to the bottom of the sheet. Three other thermocouples were added to the fixture. One thermocouple was a copper constantan wire welded to the aluminum foil tape; the second was a copper constantan strip welded to the foil at the junction of the copper constantan. Leads were then welded to the strip. The third thermocouple was a Baldwin-Lima-Hamilton miniature copper constantan thermocouple, encased in a bakelite strip. This thermocouple was mounted using the foil tape.

On 7 September 1961, a radiant heat test was conducted on the fixture using a programmed temperature versus time curve. A Research Inc. computer was used as the control, with the welded strip thermocouple as the feedback loop. The thermocouple curve increased in 25 degree steps from 75°F to 175°F in 20 minutes. The greatest Δ temperature between thermocouples was 7°F which occurred at the end of the test. The welded thermocouples and the Baldwin-Lima-Hamilton miniature thermocouple were within 3°F of each other at all times, including the period when the temperature was increasing (Lamp function was used during temperature increase between step) from one temperature to the next. During this time, the other thermocouples were reading lower by as much as 10°F. This test was repeated 3 times with approximately the same results.

8.0 CONCLUSIONS

From the results of the previous tests, the best method for mounting the thermocouple and the thermocouple type that would most accurately measure surface temperature are as follows:

> The thermocouple leads welded to the aluminum foil tape appears to be the best method. This type thermocouple has high thermo response, low thermo mass and will take the expected temperatures.

DISTRIBUTION LIST

		No. of Copies

1. Commander   1
   Air research and Development Command
   ATTN: RDZND
   Andrews AFB
   Washington 25, D. C.

2. Commandant   1
   Air Command and Staff College
   ATTN: Director, Weapons Course
   Maxwell AFR Alabama

3. Commander   1
   Air Force Ballistic Missile Division
   Air Research and Development Command
   5760 Arbor Vitae Avenue
   Inglewood, California

4. Commander   1
   Air Technical Intelligence Center
   ATTN: AFOIN-4E3, A. Voedisch
   Wright Patterson AFB, Ohio

5. U. S. Atomic Energy Commission   1
   Albuquerque Operations Office
   ATTN: Asst. Mgr. for Advance Planning
   P. O. Box 5400
   Albuquerque, New Mexico

6. National Aeronautics and Space Administration   1
   Lewis Flight Propulsion Laboratory
   Cleveland Airport
   Cleveland, Ohio

7. Air Force Plant Representative   2
   Douglas Aircraft Company, Inc.
   ATTN: Mr. Charles S. Glasgow, Chief Engineer
   Long Beach Division
   Long Beach, California

8. Assistant Air Force Plant Representative   3
   Rocketdyne Division, North American Aviation
   ATTN: Mr. George P. Sutton
   6633 Canoga Avenue
   Canoga Park, California

DISTRIBUTION LIST
(Continued)

No. of Copies

9. Assistant Air Force Plant Representative   3
    North American Aviation, Inc.
    Missile Development Division
    ATTN: Mr. William S. Reid, Jr.
    12214 Lakewood Boulevard
    Downey, California

10. Commander   1
    Field Command, AFSWP
    ATTN: Capt. Edwin R. Turner SWTG
           Technical Library
    Albuquerque, New Mexico

11. Bureau of Aeronautics Representative   3
    Aerojet General Corporation
    P. O. Box 296
    Azusa, California

12. Commanding Officer   1
    Jet Propulsion Laboratory
    ATTN: Messrs. W. H. Pickering/I. E. Newlan
    Pasadena, California

13. Office of Naval Research   1
    ATTN: E. E. Sullivan
    Department of the Navy - Code 735
    Washington 25, D. C.

14. Air Force Plant Representative   3
    Boeing Airplane Company
    ATTN: Mr. John H. Zipp, Jr.
    Oklahoma City Air Material Area
    Seattle 24, Washington

15. Air Force Plant Representative   3
    Convair Division, General Dynamics Corporation
      (Astronautics)
    ATTN: Mr. Louis Canter
    P. O. Box 1950
    3165 Pacific Highway
    San Diego 12, California

AFFTC TR 60-43(IV)   -145-

DISTRIBUTION LIST
(Continued)

		No. of Copies
16.	Assistant Air Force Plant Representative Missile Systems Division ATTN: Mr. Frank Clark Hoyt Lockheed Aircraft Corporation Sunnyvale, California	3
17.	Air Force Plant Representative The Martin Marietta Corporation ATTN: Mr. George E. Halpern, Chief, Libraries Baltimore 3, Maryland	3
18.	AiResearch Manufacturing Company Division Garrett Corporation 9851 Sepulveda Boulevard Los Angeles 45, California	3
19.	Chandler-Evans Corporation Charter Oak Boulevard West Hartford 1, Connecticut	2
20.	National Bureau of Standards Boulder, Colorado	1
21.	The Glenn L. Martin Company Missile Division Denver, Colorado	3
22.	Boeing Airplane Company ATTN: Mr. C. M. Long Wichita, Kansas	1
23.	Arthur D. Little, Inc. 30 Memorial Drive Acorn Park Cambridge 40, Massachusetts	1
24.	National Aeronautics and Space Administration 1520 H Street Northwest Washington 25, D. C.	6
25.	Commander Air Force Flight Test Center ATTN: FTRDI Edwards AFB, California	7

DISTRIBUTION LIST
(Continued)

26. Air Force Plant Representative   1
    Douglas Aircraft Company
    3000 Ocean Park Boulevard
    Santa Monica, California

27. Air Force Ballistic Missile Division   1
    Headquarters, Air Research and Development Command
    Los Angeles 45, California

28. Headquarters   27
    Armed Services Technical Information Agency
    Arlington Hall Station
    Arlington 12, Virginia

29. The Marquardt Corporation   1
    ATTN: Mary Burdett
    16555 Saticoy Street
    Van Nuys, California

30. Liquid Propellant Information Agency   3
    Applied Physics Laboratory
    The John Hopkins University
    Silver Springs, Maryland

31. Arnold Engineering Development Center   1
    Air Force Systems Command
    ATTN: AEOIM
    United States Air Force
    Arnold Air Force Station, Tennessee

32. George C. Marshall Space Flight Center   1
    ATTN: Mr. W. Y. Jordan, Jr., M-S and M-FE
    Huntsville, Alabama

33. Office of the Chief of Staff, USAF   1
    Scientific Advisory Board
    Energy Conversion Committee
    Washington 25, D. C.

34. Air Force Flight Test Center   10
    Edwards Air Force Base, California
    ATTN: FTOOT